A MECHANISM FOR STORM RUNOFF GENERATION DURING LARGE RAINFALL EVENTS

by

ROBERT JOSEPH MCKINNON

(Under the Direction of John F. Dowd)

ABSTRACT

A series of subsurface gutter experiments, situated on the mid-slope of a Piedmont catchment, were conducted to investigate a potential mechanism for the rapid mobilization of storm runoff from the unsaturated zone. Covered gutters were 1.45 m long and installed approximately 10 cm below the ground surface. Nearly a year of natural and artificial rainfall monitoring data showed a close relationship between rainfall intensity and runoff in the subsurface gutters. The gutter response closely followed the onset of intense rainfall and "switched off" with the cessation of storm events. This behavior is not indicative of a saturated subsurface flow mechanism. Deuterium analysis of runoff samples demonstrated that stormflow was comprised primarily of pre-event soil water. The data suggest that runoff from large storm events occurs when high intensity rainfall generates pressure waves that rapidly travel through the soil and produce pre-event water.

INDEX WORDS: kinematic, pressure wave, runoff, stormflow

A MECHANISM FOR STORM RUNOFF GENERATION DURING LARGE RAINFALL EVENTS

by

ROBERT JOSEPH MCKINNON

B.S., Clemson University, 2002

A Thesis Submitted to the Graduate Faculty of The University of Georgia in Partial Fulfillment of the Requirements for the Degree

MASTER OF SCIENCE

ATHENS, GEORGIA

2006

A MECHANISM FOR STORM RUNOFF GENERATION DURING LARGE RAINFALL EVENTS

by

ROBERT JOSEPH MCKINNON

Major Professor:	John F. Dowd
Committee:	Dinku M. Endale
	David B. Wenner

Electronic Version Approved:

Maureen Grasso
Dean of the Graduate School
The University of Georgia
December 2006

ACKNOWLEDGEMENTS

First and foremost, I would like to express my deepest gratitude to my major professor, Dr. John Dowd. This research would not have been possible without his knowledge, nor would I have been able to complete it without his patience, guidance, and support. The sense of humor and "hanging out" in the office chatting almost daily certainly didn't hurt either (except when discussing politics). I look forward to implementing the knowledge I have gained from him in my career.

I sincerely thank my committee members, Dr. Dinku Endale and Dr. David Wenner, for their wisdom and support. I am also very appreciative of consulting professors, Dr. Todd Rasmussen and Dr. Andrew Williams.

Additional thanks goes to everyone at the USDA-ARS J. Phil Campbell Sr. Natural Resource Conservation Center, and Stephen Norris in particular, for providing me with my field site, equipment, and expertise. Also in this respect, thanks go to Dr. Larry Morris, Dr. David Radcliffe, Dawit Yifru, Julia Cox, Kimberly Coke, Jim Muckler (thanks roomie), and the UGA Department of Geology.

Last, although certainly not least, I would like to extend my sincerest gratitude to my family, Robert L. and Bobbie McKinnon. Their love and support have been unwavering and I am more thankful than they will ever know. I look forward to using all that I have learned on this journey to have a positive impact on the world around me.

TABLE OF CONTENTS

Page

LIST OF TABLES

Page

LIST OF FIGURES

Page

INTRODUCTION

Large rainfall events cause large runoff events and a rapid mobilization of water in the shallow subsurface. During these events, there are many flow paths that can link hillslopes to headwater streams. Although there is considerable literature regarding flow paths, there is little understanding of what drives runoff delivery to the rapid flow paths during large precipation events. Traditional explanations of stormflow are often applicable only for small storm events, are often site specific, or use hydrologic inconsistencies when applied to large storm events.

Residence times of catchment soil water are important in inferring storm runoff during large storm events. Incoming precipitation, or "new" water, causes a rapid runoff response in a catchment. However, studies have shown that new water is not a substantial contributor to the discharge appearing in headwater streams. Isotopic studies using environmental tracers have demonstrated that subsurface storm runoff is dominated by "old" water, or pre-rainfall event water that was present in the catchment prior to the rainfall/runoff episode. The mechanism by which pre-event water is introduced into ephemeral rapid flow path networks during large precipitation events has not been clearly defined. A laboratory core experiment by Rasmussen *et al*. (2000) suggests a kinematic pressure wave phenomena in the subsurface could be the mechanism.

A study monitoring rainfall and runoff on a hillslope was conducted to demonstrate pressure wave generated runoff under natural field conditions. Subsurface gutter collection systems were installed on a hillslope in a small, humid, vegetated catchment to collect subsurface stormflow during rainstorms. The timing, intensity, and volume of rainfall and runoff data for the site were analyzed. An isotopic study was conducted to establish residence times and

origins of event runoff. Artificial rainfall simulations were also conducted to determine how the hillslope responded under various scenarios when rainfall conditions could be directly manipulated. The efficiency of the gutter design was also determined.

Understanding the runoff generation mechanism will enable researchers to identify the areas of the watershed and conditions that cause runoff. This will be useful in many catchment management applications, such as agricultural runoff studies. Determining whether pesticides will be held in storage or transported to streams given certain conditions is an example. Land usage affects watershed behavior and can be planned for accordingly. The prediction and abatement of contaminant transport in the shallow subsurface, and the policy affecting it could be improved and refined through studies of storm runoff pathways.

LITERATURE REVIEW

The chemical composition of streams and usable groundwater is heavily dependent upon the interaction between soils and water. Non-point source pollution moves over land and through soil as runoff causing uptake of natural and anthropogenic pollutants and delivery to various sensitive environments, such as streams, wetlands, and groundwater. Non-point source pollution runoff is the leading cause of water quality problems (EPA-841-F-94-005, 1994). As water quality and environmental health become increasingly important to the public, runoff studies explaining the delivery of runoff can be useful in determining how to better manage the quality of water entering streams.

During storm events, runoff is discharged from the contributing watershed to the stream. The size and intensity of a storm are two factors that determine the amount of discharge response. Small storms do not generally result in large runoff events and the variable source area concept explains the discharge observed in streams during these storms (Beldring *et al*., 2000). During large storm events, however, there is a rapid, high-volume response where the contributing watershed source area can exceed sixty-five percent (for example, Meyles *et al*., 2003).

During rainfall events, runoff is quickly generated and flows to streams via a number of possible flowpaths, such as shown in Figure 1. They can include Hortonian overland flow, saturation overland flow, return flow, macropore flow, saturated lateral flow, unsaturated lateral flow, and baseflow. Storm hydrographs are a common tool used in describing storm runoff. Although storm hydrographs quantify the volume of discharge into streams, they do not describe the sources, i.e. flowpaths, or how water enters the flowpaths (Nutter, 1973). Many

studies give an explanation of the mechanism of flow during runoff events, although, most explanations for large storm events fail to correlate the rapid mobilization of runoff with environmental tracer studies of stream discharge. The following review examines traditional explanations of storm runoff and current research.

Variable Source Area

Rejecting the Hortonian model, Hewlitt and Hibbert (1967) helped to shift the paradigm concerning the lateral transport of water on hillslopes with a study located in small catchments at the Coweeta Hydrologic Laboratory in Otto, NC. The study helped to establish the concept of the variable source area—the dynamic area adjacent to the stream that expands and contracts with temporal variation and intensity of storms and produces runoff. In addition Hewlitt and Hibbert concluded, excluding some seasonal response factors, that soil properties are a main limiting factor in stormflow generation while watershed size has little effect.

Dunne and Black (1970a, 1970b) used interception drains and trenches in a Vermont watershed to analyze subsurface contribution of runoff to streams. They found that a small portion of the catchment contributed to the stream, and this area varied in aerial extent depending on the size of the storm event, which varies seasonally. Furthermore, they found little evidence of overland flow, and Darcian subsurface flow was too slow to produce the observed rapid discharge. Dunne and Black hypothesized that runoff production took place near-stream in the variable source area.

Meyles *et al*. (2003) conducted a runoff generation study in the Holne Moor experimental watershed located in Dartmoor National Park, UK. Rainfall and resulting stream discharge, timing, and volume were recorded. The percentage of upslope area that contributed runoff to the stream was calculated. Runoff was produced from increasingly larger upland areas during the

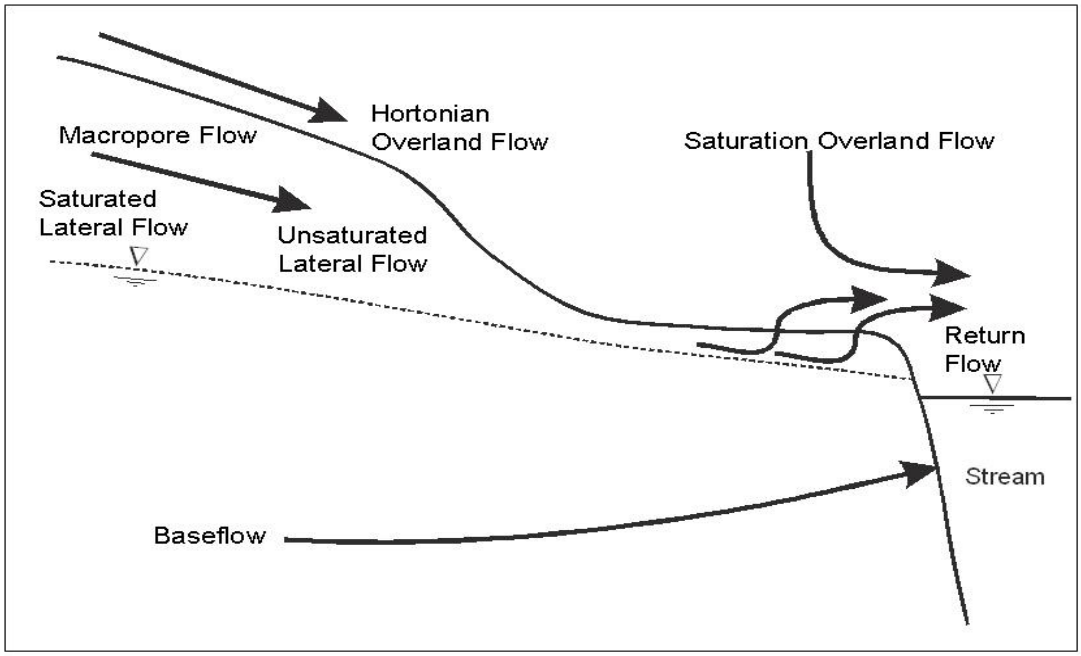

Figure 1: Runoff flowpaths

larger storm events. Smaller storms yielded runoff from 10% of the watershed, or the near-stream area, while larger storms generated water from nearly 70% of the watershed. Yet the lag to peak time was similar for small and large storms. The rapid response of stream discharge suggests that small and large storm events require differing mechanisms for runoff generation. The variable source area model appears to fit the discharge response exhibited by small storms, but not large storm events.

Environmental Tracer Studies

Accumulating evidence from environmental tracer studies is causing a re-conceptualization of the subsurface transmission of water from the hillslope to the stream (Stanley *et al.*, 2002). Kirchner (2003) details a "double paradox" that exists within catchment hydrology: water in small, humid, vegetated catchments is quickly translated to the stream

network during large runoff events, however, the water is not "new." Furthermore, stormflow and baseflow both consist primarily of pre-event "old" water, although, they have differing chemical signatures (Kirchner, 2003). Counter to traditional thought, pre-rainfall event water dominates streamflow at peak discharge (Buttle, 1994). Stable isotopic analyses of stream water samples indicate storm runoff discharge into streams, excluding direct precipitation, is largely "old" water, which is water that has been residing in a watershed prior to a rainfall event. The isotopic signature of precipitation (new water) can vary temporally and spatially, depending on climatic conditions (Clark and Fritz, 1997). Old water, however, is derived from infiltrated water residing in the unsaturated zone (Buttle, 1998). Old water consists of an isotopic mixture of previous rainfall events because the subsurface prevents the fractionation that occurs at the surface and in the atmosphere due to evaporation.

The rapid mobilization of vadose zone old water during storm flow events supports the concept that most runoff is quick subsurface flow, as suggested by Hursh (1944). Previous environmental tracer studies have attempted to rectify the "double paradox." However, they are often forced to rely on hydrologic inconsistencies or site-specific conditions to satisfy both the observed rapid mobilization of water and the unseemingly related old water criteria. Pearce *et al*. (1986a), for example, conducted one of the first studies examining the old water/new water concept. Eight small forested catchments at the Maimai study area were outfitted with throughflow pits (Pearce et. al, 1986b) and studied over several years to determine whether old water or new water is the dominant contributor of discharge to the stream hydrograph following a rainfall event. A comprehensive set of volumetric, solute chemistry, and stable isotope analysis was conducted on precipitation, stream flow, and groundwater samples. Old water was found to be the primary contributor to discharge to the stream during large or intense storms and

the response was very rapid. New water contributed approximately 3% to the hydrograph volume during the study, which can be attributed to direct precipitation. Given the duration of the study, the old water component was found to have a four month mean residence time in the catchment. Kubota and Tsuboyama (2002) observed that larger or more intense storms produced greater proportions of old water in stream samples.

Pearce *et al*., (1986a, 1986b) were among the first to challenge new water subsurface flow mechanisms. The authors offered groundwater ridging as an influential mechanism, where the water table, consisting of old water, rises near-stream and feeds the adjacent variable source area. McDonnell (1990) used groundwater ridging as a mechanism to correlate the rapid response of hillslopes to rainfall with the old water phenomenon. The study was conducted at the same New Zealand study areas (Maimai) as in Pearce *et al*., (1986a, 1986b). McDonnell suggested new water mixes with the rising water table following infiltration and enters rapid flow pathways, such as macropore networks. The study recognized that Darcian flow is too slow to produce observed peak discharges. However, groundwater ridging still does not produce enough flow to account for peak discharge commonly observed during large storm events. Also, new water doesn't rapidly mix at the water table, instead it would behave much like saturated overland flow. As a mechanism of flow, groundwater ridging would result in new water on a short time scale.

Overland flow

Hortonian overland flow has often been invoked as the primary explanation for storm runoff. Water ponds at the surface when rainfall rates exceed the infiltration capacity of a soil and runs over the surface as overland flow (Horton, 1933). Although Hortonian overland flow is seen in urban environments, it is rarely visually observed in vegetated, humid catchments.

Nutter (1973) conducted rainfall simulation experiments on covered physical hillslope models to establish the importance of soil water in the hydrologic behavior of basins. He found that most of the event water was retained in the system, emitted by unsaturated zone subsurface flow, or emitted from delayed subsurface flow. Hortonian overland flow was not found to be a significant contributor of flow. Although the Hortonian overland flow model of hillslope flow does provide a rapid response and adequate volume for large storm event discharge, environmental tracer studies have shown that this process is a "new" water process, which does not agree with environmental tracer studies that observe "old" water producing processes (Williams *et al*., 2002).

Macropore Flow

Macropores are large conduits in soil, created by soil fauna, roots, cracks, etc., that move water quickly through the subsurface. These rapid flow routes have been thought to be an important component of flow (Jones, 1971). Beven and Germann (1982) describe macropore flow in detail and define macropores as pores that permit nonequilibrium channeling of flow down a preferential pathway. Beven and Germann estimate that the rainfall intensity needed to incite infiltration is 1-10 mm h^{-1}. Infiltration is facilitated by macropores, which inhibits ponding and overland flow. Macropores can account for rapid discharge of lateral downslope flow that Darcian subsurface flow is simply too slow to permit through the soil matrix, although they must be well-connected to do so (Williams *et al*., 2002).

Although macropore flow transmits water very quickly, traditional macropore flow, which is often invoked to explain rapid storm runoff, is a new water process that conducts event infiltration. Dowd *et al*., 2005, suggests that stored old water could be found in macropore networks if there is a mechanism for delivering soil water to them.

Lateral Flow

Catchments store old water in the soil matrix pores of the vadose zone. Contrary to traditional overland and macropore flow mechanisms, lateral downslope flow can produce old water. However, these pathways transmit water too slowly to match the timing of storm runoff response. Lateral flow in the soil matrix of the unsaturated zone is largely Darcian, and therefore not a rapid pathway (Gaskin *et al*., 1989).

Baseflow

Baseflow, or recharge by groundwater, contributes old water from the saturated zone to stream discharge. However, baseflow doesn't generally respond to individual storm events, as demonstrated in a typical storm hydrograph depicted in Figure 2.

Pressure Wave Translatory Flow

Translatory flow, as presented by Hewlett and Hibbert (1967), is where old water in soil pores is displaced into channels with the input of precipitation. Translatory flow moves a short distance (cm or m per day), however, it responds very quickly to rainfall (Buttle, 1998). Baldwin (1997) demonstrated a different type of flow where old water was displaced by pressure waves.

Rasmussen *et al*. (2000) and Williams *et al*. (2002) discuss a laboratory soil core tracer experiment conducted by Baldwin (1997) that indicates a kinematic process of flow through the core. Baldwin's experiment utilized three intact saprolite columns taken from Comer, GA. The columns (see Figure 3) were irrigated by misting 0.3 mm of water, calcium chloride tracer, and flush water at various intervals in a repeating cycle. The columns were kept wet by the misting nozzles, but never saturated. The cores were 30 cm in diameter and 38 cm in length and were outfitted with micro-tensiometers at various depths to measure soil moisture tension at one

minute intervals. Tube lysimeters were installed horizontally, feeding collected samples to a spectrophotometer for chloride analysis.

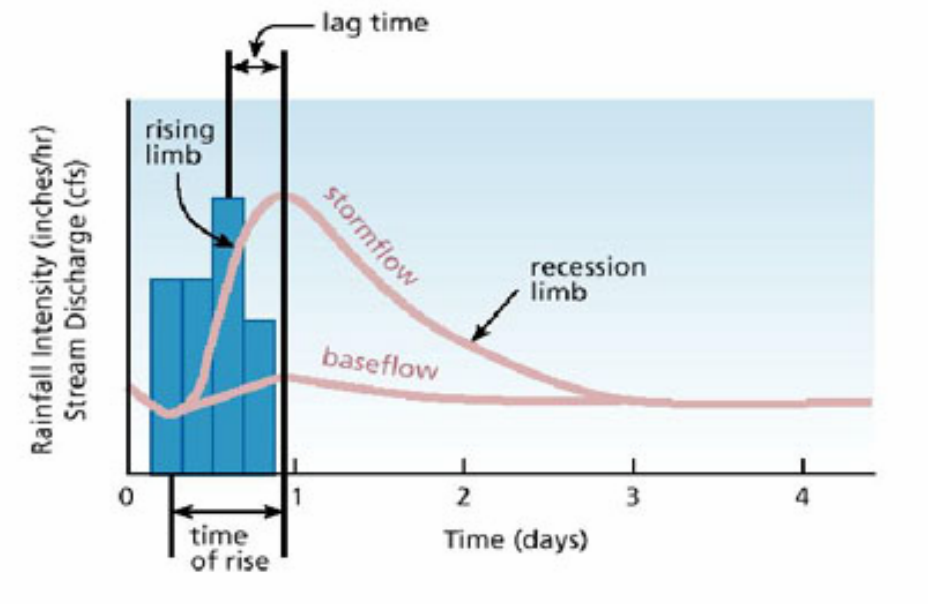

Figure 2: Baseflow component of a typical storm hydrograph (www.epa.gov/watertrain/stream/s10.jpg)

The tracer velocity through the saprolite cores was consistent with preferential flow and took approximately two days for the peak concentration to appear in the uppermost lysimeter. Within minutes of mist application, however, some water was ejected out of the core bottom. Figure 4 shows abrupt pressure changes that are immediately induced in the core with each spray interval. Baldwin found that soil water celerity was ~1000x greater than pore water velocity. The jagged chloride response, shown in Figure 4, is due to the tracer moving in and out of pores due to fluctuating changes in pressure. Although it took days for water to travel through the core, the soil water tensions were significantly larger than the head that was applied to the cores and water was pushed out of the cores due to the "waves" of pressure changes (Williams *et al*., 2002).

Torres (2002) discusses a study where tracer data from an irrigation experiment showed no spike increases in fluid pressure throughout the system. Therefore, it is likely that the tension response that indicates pressure wave translatory flow is related primarily to perturbation by rainfall, as demonstrated in Baldwin's spray experiment. There is a pressure gradient between surrounding soils and macropores that keeps water from sitting in the rapid flow routes. A decrease in the pressure to near-zero leads to enhanced drainage and a release of water into the macropores (Torres and Alexander, 2002). Changes in gradient cause a redistribution of energy in the soil pores around macropores. Thus, a possible mechanism of runoff generation involves the perturbation of rain that causes pressure waves that continually push pre-event catchment water into rapid flow paths, i.e. macropores, and provide the observed celerity of runoff discharge—until the precipitation event decreases below an intensity threshold that generates pressure waves.

Kinematic Stormflow Network

Meyles *et al.* (2003) conducted a hillslope field experiment that clearly illustrates the mobilization of storm runoff that is old water dominated. The study took place in the Holne Moor watershed, located in Dartmoor National Park, UK. Site characteristics are presented in Appendix A. A perennial stream exists in the watershed and can be quick-flowing during storm events, as show in Figure 5. The old water/new water paradox (Kirchner, 2003) was apparent at the Holne Moor watershed, as shown in Figure 6. Stream discharge and soil water samples taken from lysimeters have similar $\delta^{18}O$ values. Rainfall samples, however, are more variable and visibly differ from the soil water and stream discharge baseline. The "House" sample was collected at a location approximately forty miles from Holne Moor while the rest were collected on the watershed, illustrating the spatial variation of stable oxygen in rainfall. The Holne Moor

data contain small and large storm and runoff events (Figure 7). There are several storm events depicted in Figure 7 of comparable size, however, discharge into the stream is highly varied. Even with rainfall events of similar volume, runoff volume can be very different. Thus, the runoff response to rain is a complicated relationship (Meyles, 2003).

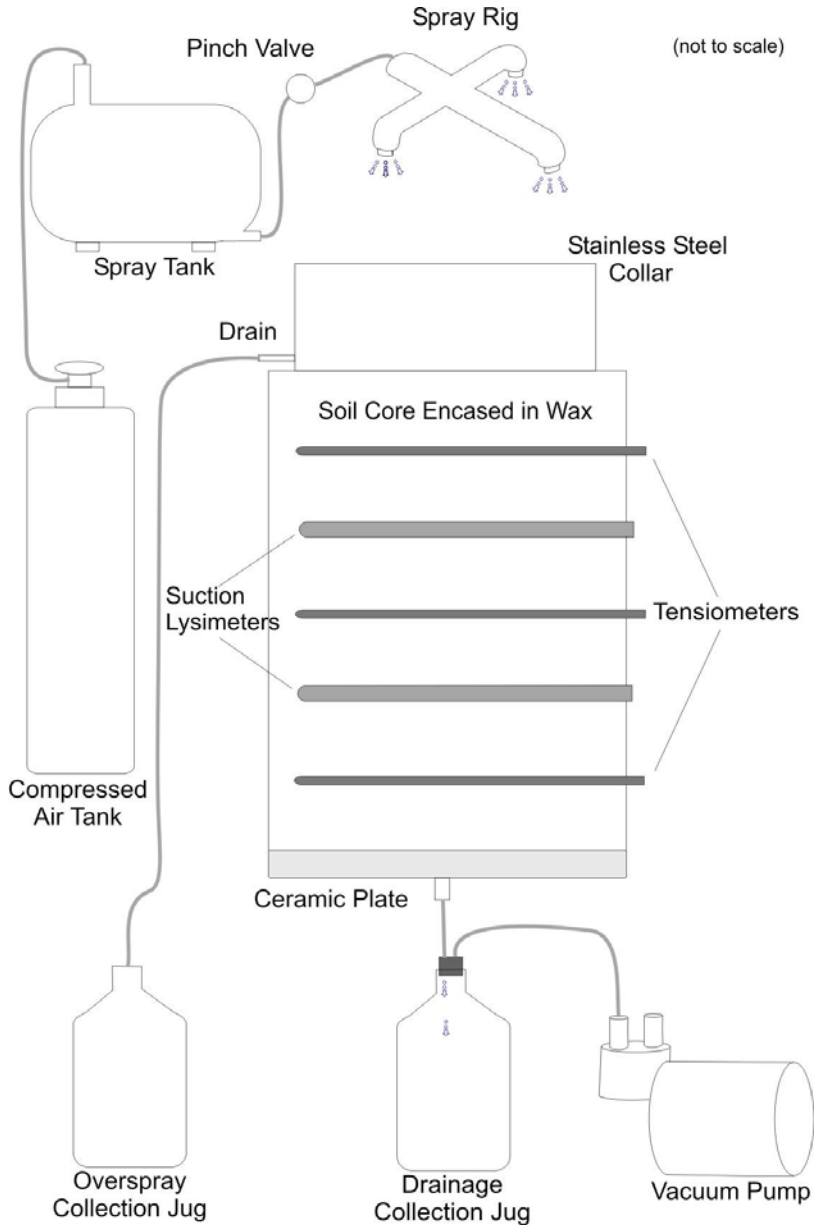

Figure 3: Comer, GA, intact saprolite core and tracer spray system (Baldwin, 1997)

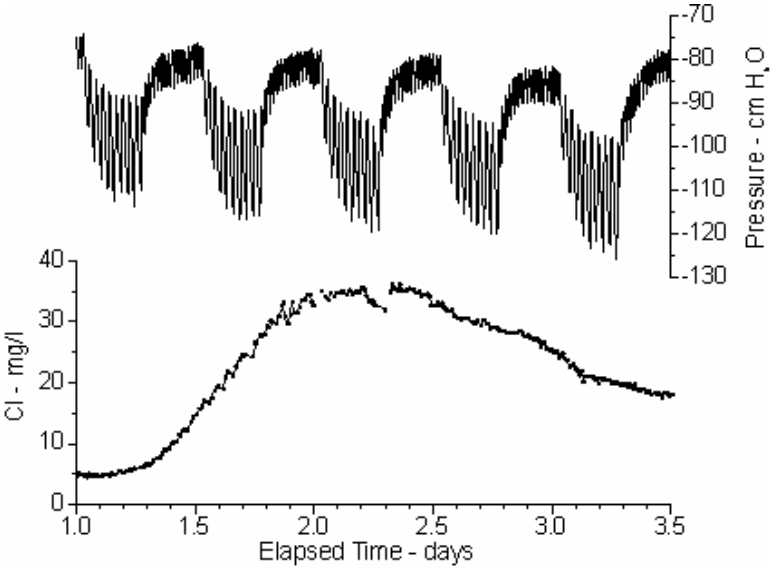

Figure 4: Core experiment results illustrating pressure waves (Rasmussen *et al*., 2002)

Figure 5: Holne Moor ephemeral stream during the recession of a storm event

The percentage of runoff contributing upslope area of the Holne Moor watershed was calculated (Figure 8). The larger storms contribute runoff from increasingly larger upland areas. While many smaller storms contribute runoff from roughly ten percent of the watershed, the larger storms produce runoff from up to nearly sixty-five percent. However, the lag-to-peak time is similar for large and small events (on the order of minutes to hours), and there is a rapid response of runoff to rainfall (Meyles *et al*., 2003). Figure 9 depicts the contributing upslope area spatially over the watershed. The larger storms expand the contributing area to the lighter-green shaded regions. The variable source is outlined, and represents the traditional explanation of runoff for smaller events.

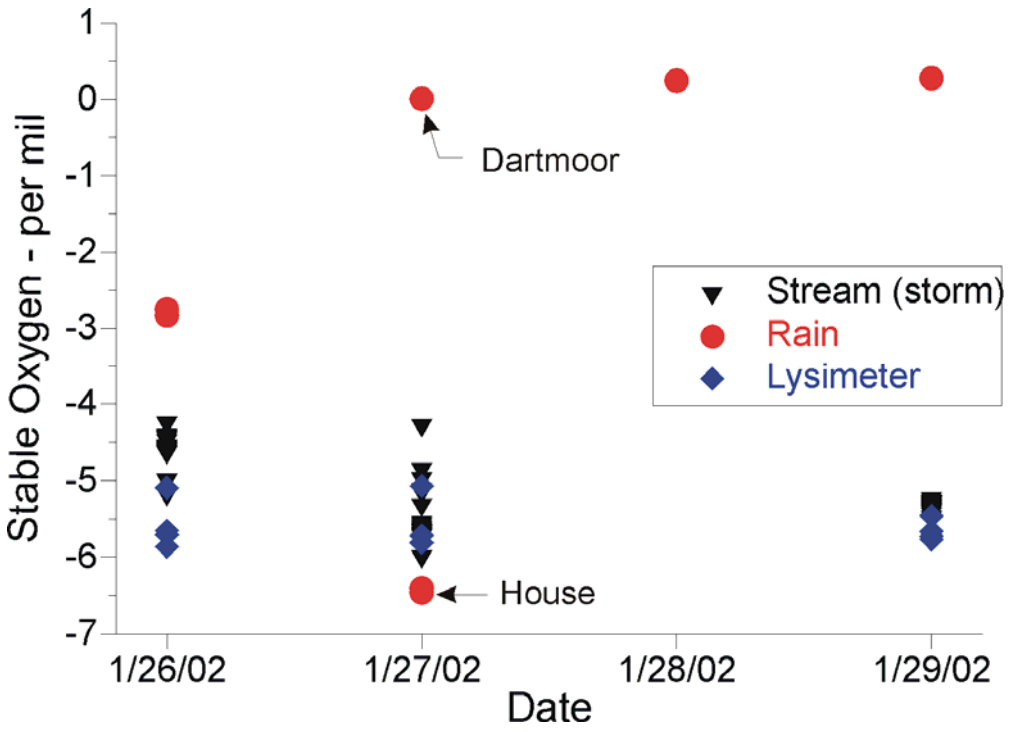

Figure 6: $\delta^{18}O$ results—Holne Moor watershed

Meyles *et al.* (2003) demonstrated at the Holne Moor watershed the mobilization of pre-event water during large events where a rapid flow network built upslope intra-storm. These

findings highlight the aspects of storm runoff where the mechanism that delivers old water is largely unexplained.

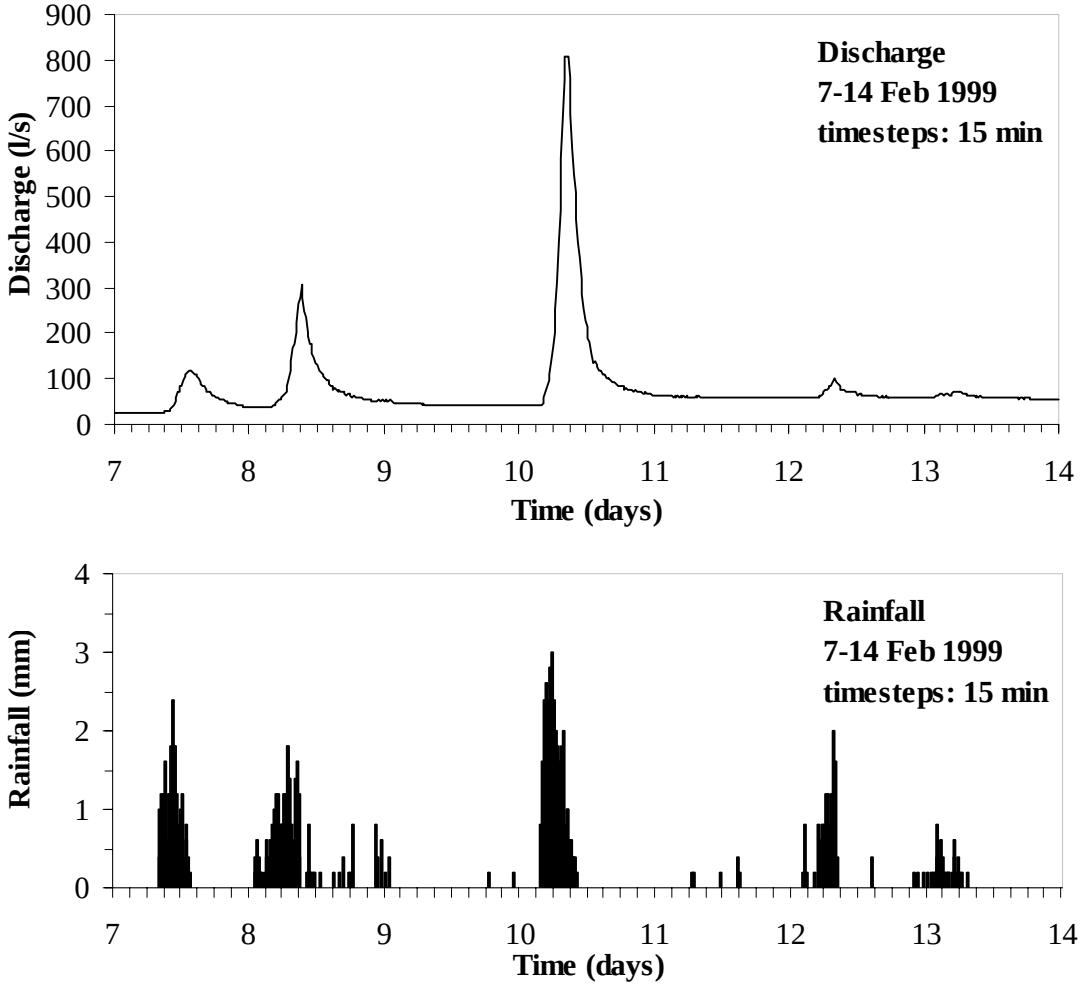

Figure 7: Holne Moor storm hydrograph (Meyles *et al.*, 2003)

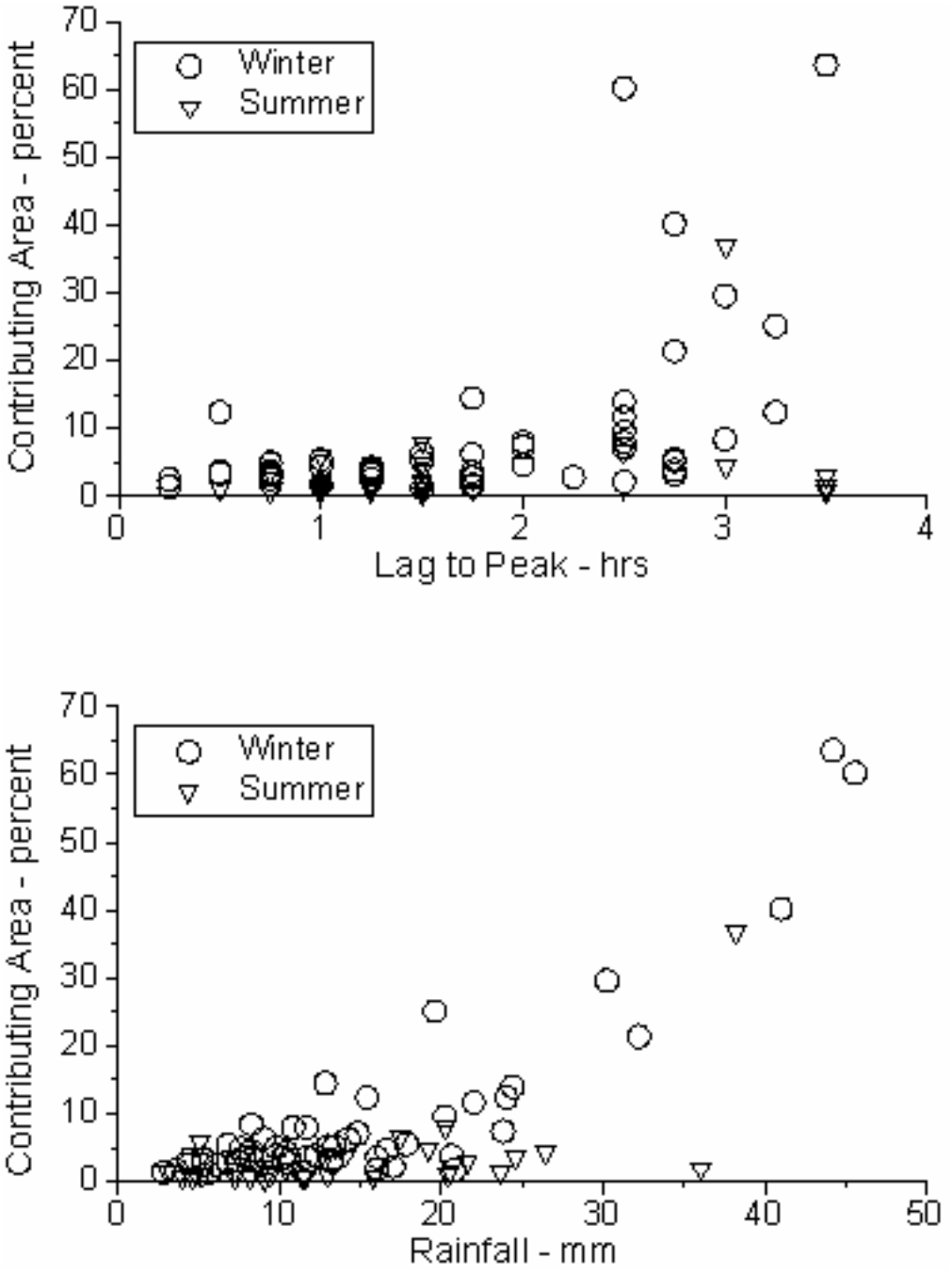

Figure 8: Contributing upslope area (percentage) of Holne Moor (Meyles *et al*., 2003)

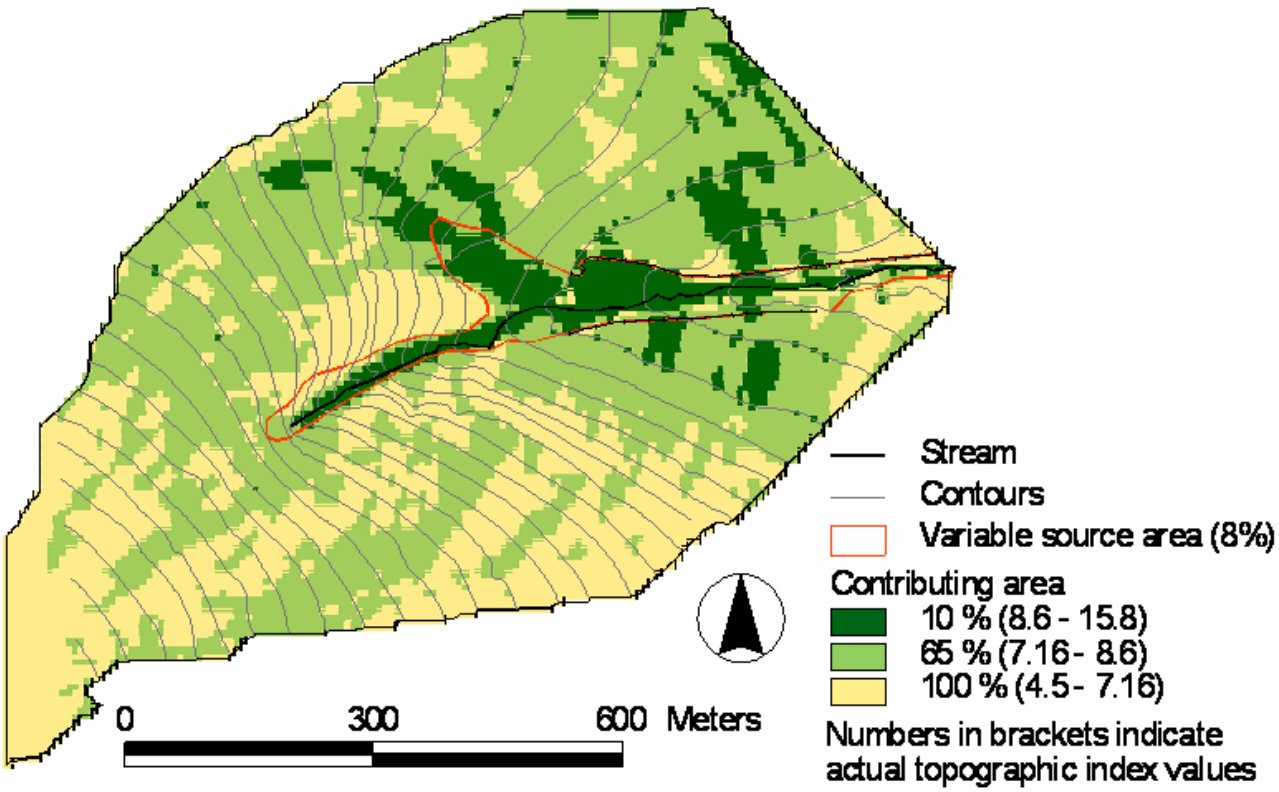

Figure 9: Holne Moor watershed contributing area (Meyles *et al.*, 2003)

SITE DESCRIPTION

The study area (Figure 10), as described by Endale *et al*. (2002), is a humid, vegetated watershed in the Southern Piedmont Physiographic Province. The experimental watershed is located at the J. Phil Campbell, Senior, Natural Resource Conservation Center, a part of the Agricultural Research Service agency of the United States Department of Agriculture, in Watkinsville, GA, about 12km south of Athens, GA (83^{o}24' W and 33^{o}54' N).

A sloped agricultural research pasture, designated 1E of the East Unit of the USDA-ARS property, was chosen for the rainfall/runoff investigation (Figure 11). A 13 m X 10 m plot was enclosed on the hillslope for the installation of a gutter collection system to collect rain and runoff samples. The pasture is used primarily for the rotation of cattle at various times throughout the year. Vegetation in the study area is comprised mostly of fescue grasses.

Climate

The study area climate is typical of the humid, southeastern United States. Average rainfall at the research station is 1.24 m. Mean rainfall distribution does not vary greatly throughout the year; it is highest during the winter months (103-119 mm) and lowest during the fall months (76-88mm). Rainfall typically peaks in March with approximately 137 millimeters of precipitation. Average daily temperatures range from 4.4 to 7.2^{o} C during the winter months and from 23.9^{o} C to 26.7^{o} C during the summer months (Endale *et al*., 2002).

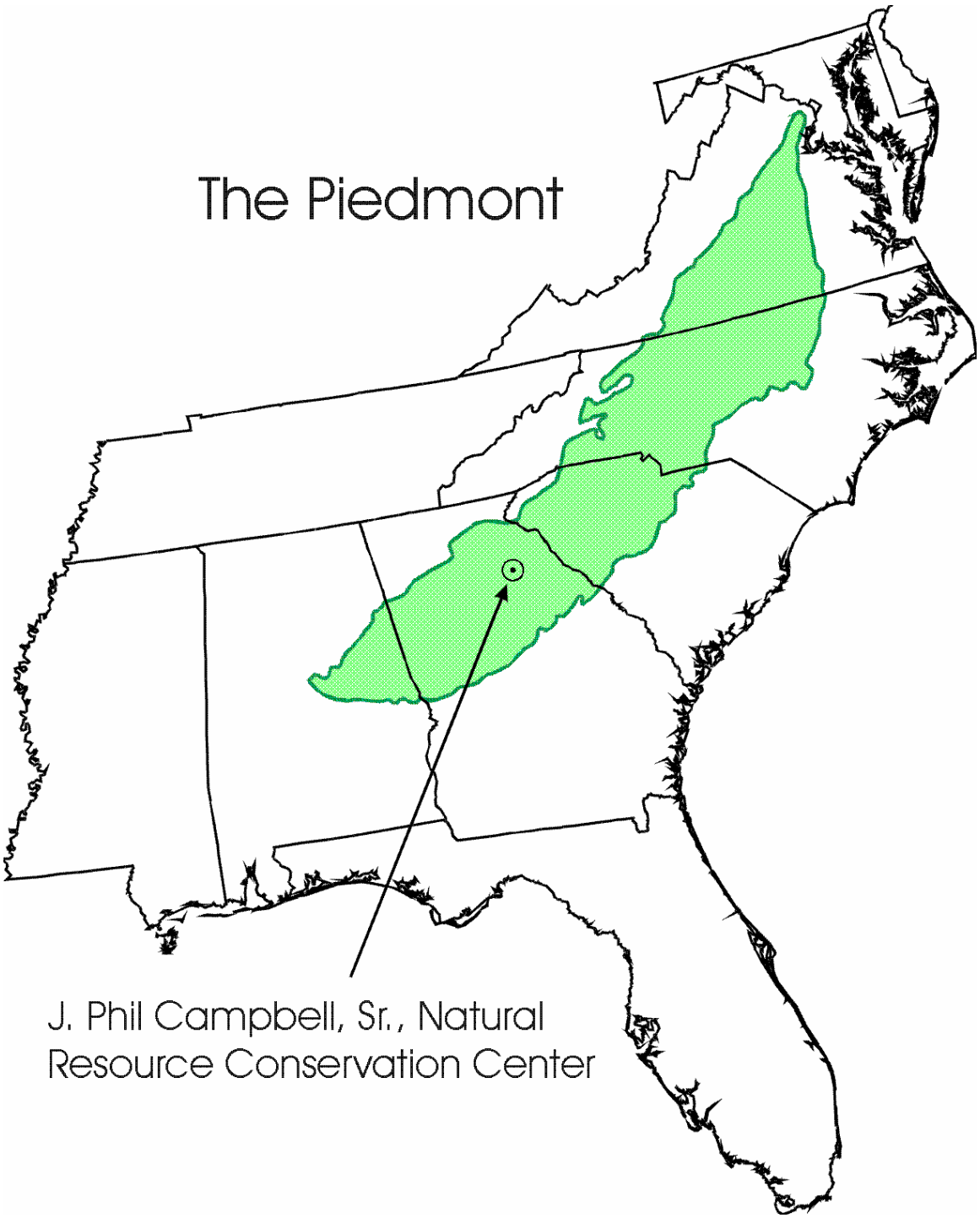

Figure 10: J. Phil Campbell, Sr., Natural Resource Conservation Center

Soils

The study area soil is a sandy loam of the Cecil soil series (fine, kaolinitic, thermic Typic Kanhapludult) (Endale *et al*., 2002). Cecil soils, described by Bruce *et al*. (1983) and Perkins (1987), are common on the ridges and hillslopes of the Piedmont region and are deep, well-drained, and moderately permeable. The Cecil soils are commonly formed by the weathering of metamorphic rock.

The soil profile at the field experimental site consists of the following (from surface to depth): the Ap horizon at the uppermost 20 cm, the Bt horizon (100 cm), and the BC horizon (30 cm). The C horizon, where the water table is located, consists of saprolite. The bedrock underlying the saprolite is Athens Gneiss (Railsback *et al*, 1996).

Figure 11: Watkinsville, GA field site.
A. Experimental pasture
B. Field experiment plot

MATERIALS AND METHODS

Runoff resulting from rain storm events was monitored during a field experiment that was conducted on a hillslope in a Watkinsville, GA, catchment. Rainfall and runoff collection systems were installed on the hillslope during January, 2005. The rainfall/runoff monitoring and sampling period took place from February, 2005, to January, 2006.

Study Plot

The rainfall and runoff collection systems were installed in a 13 X 10 m fenced plot on the hillslope. Within the plot were two repetitions of a subsurface runoff gutter collection systems. Repetition 1 (left) and Repetition 2 (right) are shown in Figure 12. The systems were placed approximately 2 m apart in the mid-slope region of the hillsloped catchment. The study plot was outfitted with various instruments to determine various hydrological parameters of the study area.

Rainfall/Runoff Collection Systems

Rainfall and runoff were sampled for nearly one year following rainstorms that yielded a measurable volume of runoff. Water samples were stored in sealed glass vials with no headspace. For rainfall sampling, natural precipitation was collected in a 5 gal Nalgene storage reservoir via a funnel that was mounted on an iron stand and connected by Tygon tubing. An ONSET tipping bucket rain gauge with a HOBO Event data logger was vertically mounted approximately 0.5 m above ground and used to record rainfall volume in real-time at 0.01 in intervals (Figure 14)

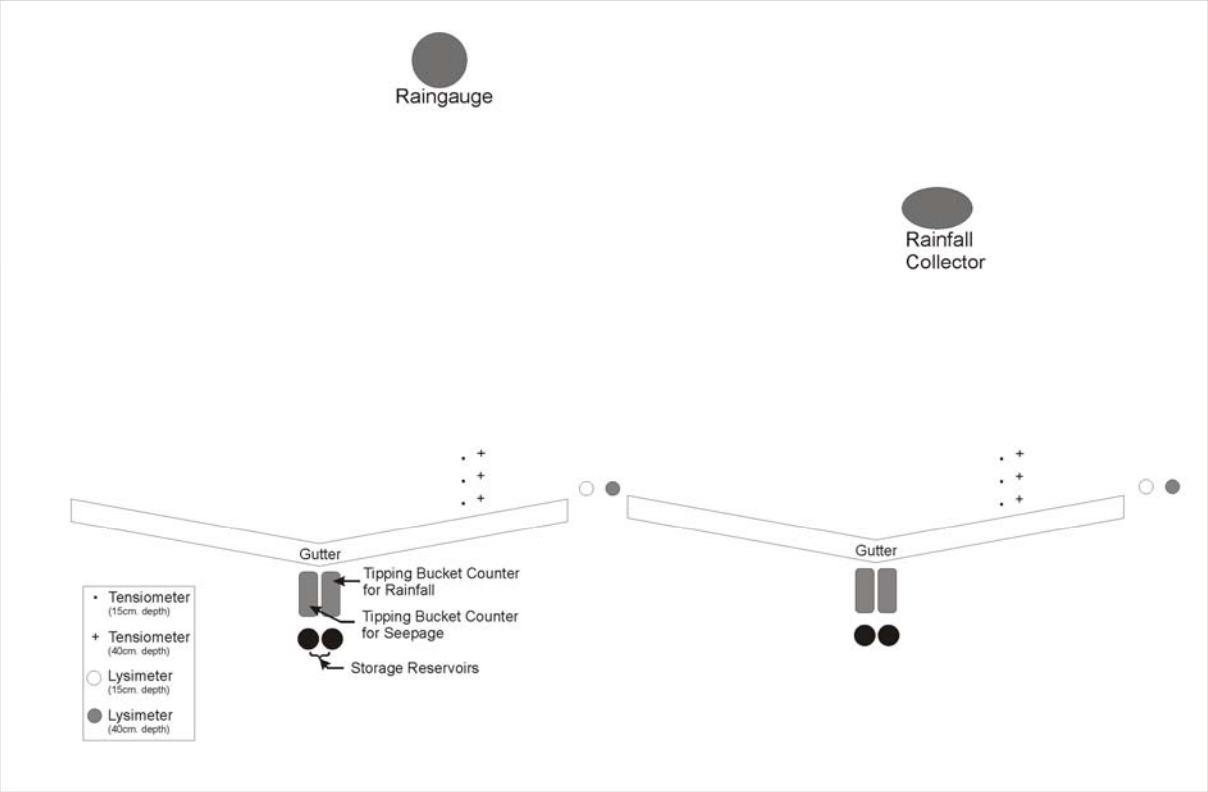

Figure 12: USDA-ARS Watkinsville study plot (map view)

The runoff gutter collection system design was improved over time to minimize sample contamination. The following description details the ultimate design of the gutter collection system, which was used for the majority of the sampling period.

Each runoff collection system consisted of two trenches in which 1.25 m long gutters were installed to collect subsurface stormflow. The two trenches were oriented in a slight V-shaped configuration to provide an incline so that water would flow down-gradient in the gutters and into storage reservoirs (Figure 16). Steel plates were driven at an angle and side-by-side in a line into the upslope soil face of the trenches to facilitate the seepage of subsurface runoff to drip into the gutters (Figure 15). The drip plates were installed in the soil face approximately 15 cm at depth just above the Bt horizon. The drip plates induce soil water conditions similar

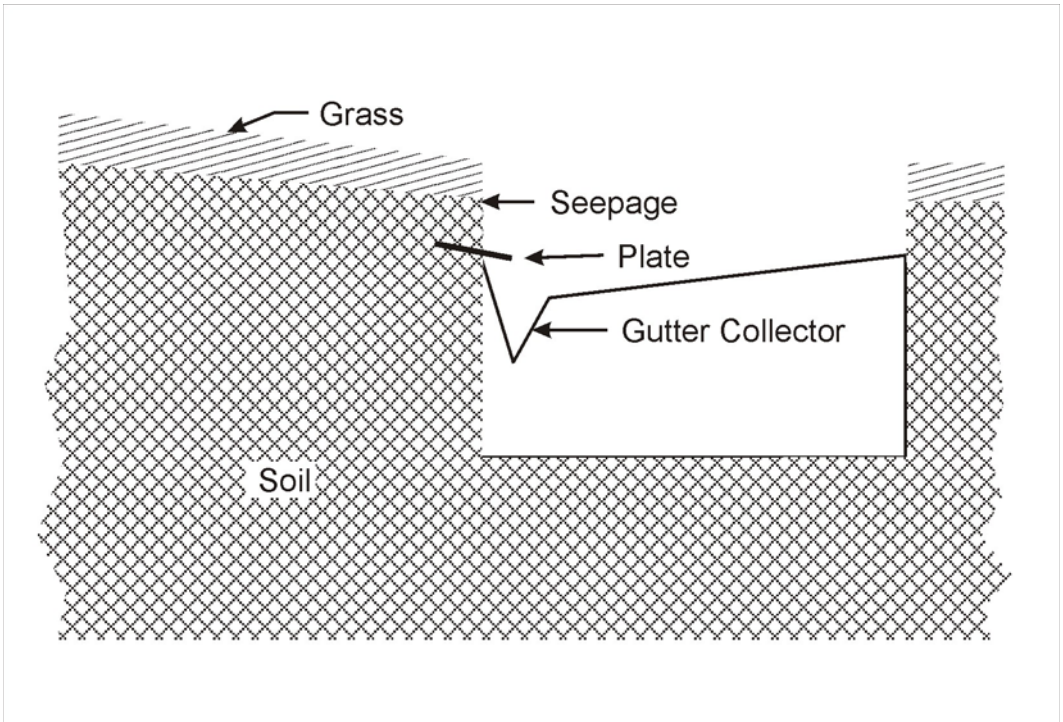

Figure 13: Gutter design

to incipient channels or pipe-flow. A (near) saturated wedge collects at the lip and transmits flow across the steel plate lip, which in turn drips into the gutters (Figure 13). The trenches were covered so that no direct precipitation could enter the subsurface gutters. Figure 16 shows the complete runoff collection system. Down-slope of the gutter trenches is an ONSET tipping bucket rain gauge with a HOBO Event data logger. Tygon tubing is connected to the discharge point of the gutter and directs flow into the tipping bucket rain gauge. Following each precipitation event, the event data was downloaded using the Boxcar Pro 4.3 computer program. The tipping bucket rain gauges were mounted on wooden boards and kept level. The tipping buckets have drains at the base where Tygon tubing is connected to divert the runoff to storage reservoirs. Following each rainstorm event that generated significant storm runoff, water samples were taken from the 19 L Nalgene storage reservoirs for subsequent isotopic analysis. Both the tipping bucket rain gauges and the storage reservoirs were set up in a pit downslope

from the gutter trenches and covered to prevent precipitation contamination of the tipping bucket data or water samples.

Figure 14: ONSET tipping bucket rain gauge

Artificial Macropore

An artificial macropore was constructed and installed into the soil face of a trench in Repetition 1 of the subsurface runoff collection systems. It was constructed out of a 2.54 cm diameter PVC pipe with five lines of small holes drilled 2 cm apart along the length of the approximately 30 cm pipe. The artificial macropore was installed into the soil face by drilling a hole upslope and ensuring that the macropore was tightly fit in the hole. The depth of installation was twelve centimeters. The ends of the macropore were sealed with rubber stoppers; one stopper being fitted with a tube for the discharge of runoff that the macropore collected. Tygon tubing was connected to the discharge tube to divert flow to a tipping bucket rain gauge and then to a storage reservoir.

Figure 15: Experimental soil face and gutter

Figure 16: Runoff collection system

Lysimeter Instrumentation

Suction lysimeters were placed in the vadose zone near each gutter repetition (Figure 17). The instruments induce pore water under negative pressure to enter the device through a porous ceramic cup where samples can be collected at the surface (Fetter, 2001). Unsaturated zone soil water samples were collected from the suction lysimeters after storm events for isotopic analysis. Deuterium analysis of background soil water provides a basis of comparison for the subsurface runoff water samples. Each runoff gutter collection system was outfitted with a shallow and a deep lysimeter (L1 and L2 for Repetition 1, L3 and L4 for Repetition 2)—15 cm and 40 cm deep respectively.

Figure 17: Suction lysimeters

Tensiometer Instrumentation

Tensiometers were installed in the immediate up-slope from the gutter trench repetitions (Figure 18) to measure soil water potential. The tensiometers consisted of 2.15 cm outer diameter plastic pipe with a 2.22 cm outer diameter ceramic porous cup at the lower end, and a 5

cm section of clear plastic pipe at the upper end that was sealed by a rubber stopper. De-gassed water was used to fill the tensiometer column. A tensimeter was used to measure the negative pressure that is created within the tube. Water is drawn from the tube, causing a negative pressure equaling the soil water tension (Dowd and Williams, 1989).

In each repetition, there was a line of three shallow tensiometers and three deeper tensiometers extending upslope at depths of 15 cm and 40 cm deep respectively. A pair of 15 cm and 40 cm depth tensiometers (place 10 cm apart) were placed at the following distances up-slope from the gutter at each repetition: 20 cm, 50 cm, and 100 cm. Figure 18 illustrates the arrangement of the two tensiometer fields in relation to the gutters. Matric potential readings were recorded after storm events during water sampling. Additional readings were taken at random to observe antecedent conditions. In addition to observing changes in matric potential, water content values of the study area soil were calculated from the tensiometer readings.

Figure 18: Tensiometer field

Bulk Density and Water Content

Soil samples were taken at an excavated soil pit at the study area field site. Three steel soil core rings (volume=340.47 cm^3) were driven into excavated faces, at different locations in the soil pit, of the uppermost 10 cm of soil, which is primarily the Ap horizon. The soil samples were placed into moisture cans to prevent evaporation. The wet weights of the samples were recorded, then the samples were heated in a 105 °C oven for one week and the dry weights recorded. Bulk density, gravimetric water content, volumetric water content, and relative water content were then calculated.

Particle Size Distribution

Particle size distribution is useful in describing many site parameters, including water content and groundwater movement. Three soil cores from an excavated soil pit near the gutter trenches were sent to the University of Georgia Soil Testing Laboratory to measure the percentages of the sand, silt, and clay constituents of each sample.

Hydraulic Conductivity

A laboratory experiment was conducted to determine the saturated hydraulic conductivity of soil cores taken from an excavated soil pit near the gutter trenches. The Ap horizon soil cores were soaked until saturated with 0.05N $CaCl_2$. The calcium chloride was used instead of de-ionized water to limit clay dispersion. A Mariotte bottle apparatus (Radcliffe, 2005) was constructed to siphon the solution into the soil cores in order to determine saturated hydraulic conductivity. A plastic cup was placed under the soil core to catch flow through the core. Sufficient time was allowed for the establishment of steady state flow through the core. The head of standing water in the apparatus was measured using a ruler. Once steady state flow conditions were reached in the soil core, the volume of water transmitted into the plastic cup was

measured on a balance at one minute time intervals. Five measurements of flow volume were recorded. The average of the closest three measurements were used to determine the flow rate through the core.

A field experiment was also conducted *in situ* to measure the field saturated hydraulic conductivity of the Ap horizon with a constant compact head permeameter (CCHP). A borehole was augered to 10 cm with a radius of 3.5 cm. Once the flow was at a constant rate, water level recordings in the flow measuring reservoir were taken at two minute intervals. Ammozegar (1989) describes the specific procedure used for the CCHP apparatus. The procedure was repeated for three boreholes at various points within the study plot.

Isotopic Analysis

Stable isotopic analysis for deuterium was conducted on the rainfall, runoff, and lysimeter samples that were collected following runoff generating storm events. Each two μl sample (except on November 1, 2005, when 0.5 μl samples were run) was prepared manually for deuterium analysis on a vacuum extraction line at the Department of Geology Stable Isotope Laboratory at the University of Georgia, in Athens, GA. Afterwards, the water samples were analyzed on a Finnigan Mat model Delta E mass spectrometer with a reference gas of known isotopic composition. During each analysis, ten water samples were analyzed for deuterium along with two standards—the Athens Tap Water standard (ATWS) and the Greenland Ice Sheet Project standard (GISP). Replicate samples were prepared for every sample for the purpose of precision and repeatability during the first several weeks of analysis. Later, replicates were run regularly for random water samples. All results underwent a two-point calibration to report the data isotopic composition of hydrogen versus Vienna Standard Mean Ocean Water (VSMOW).

Artificial Rainfall Simulations

Two rainfall simulations were conducted at the field site (Figure 19). The volume, timing, and rates of the simulated rainfall and subsurface runoff were measured by collection systems. An artificial macropore was constructed to measure runoff response as part of a rapid pathway network. A chloride tracer experiment was also conducted in conjunction with the simulated rainfall.

The single-spray nozzle rainfall simulator (Figure 20), a Tlaloc 3000 (Joern's Inc., West Lafayette, NC), was used for the application of simulated rain on the study plot. The artificial rainwater was pumped from a 500 gal tank located on a road above the pasture. The spray nozzle of the simulator was mounted approximately 3.7 m above ground. Because of the slope of the hill, the spray rig framework was leveled so that the nozzle sprayed directly down on the plot, and was adjusted to provide an even distribution of rain upslope from the gutter trenches. The simulator rained on a 2.5 m X 2.5 m area upslope of the gutter trenches. The spray nozzle was positioned so that there was direct precipitation on the trenches in order to produce rainfall infiltration directly in front of the experimental soil face where the gutters collect runoff. The trenches were covered by boards and plexiglass (for viewing and filming the seepage into the gutters) to prevent direct precipitation into the gutters. Berms were constructed above the excavated soil faces of the trenches to deflect grass drip into the gutters. Tarps were used as a wind shield and enclosed the simulator (Figure 20).

The subsurface runoff gutter collection system is described in Sampling Methods. During the rainfall simulation, the gutter flow was directed to an ONSET tipping bucket rain gauge with a HOBO Event data logger recording the volume and timing of the subsurface response to the simulated rain. Another data logging tipping bucket rain gauge was vertically

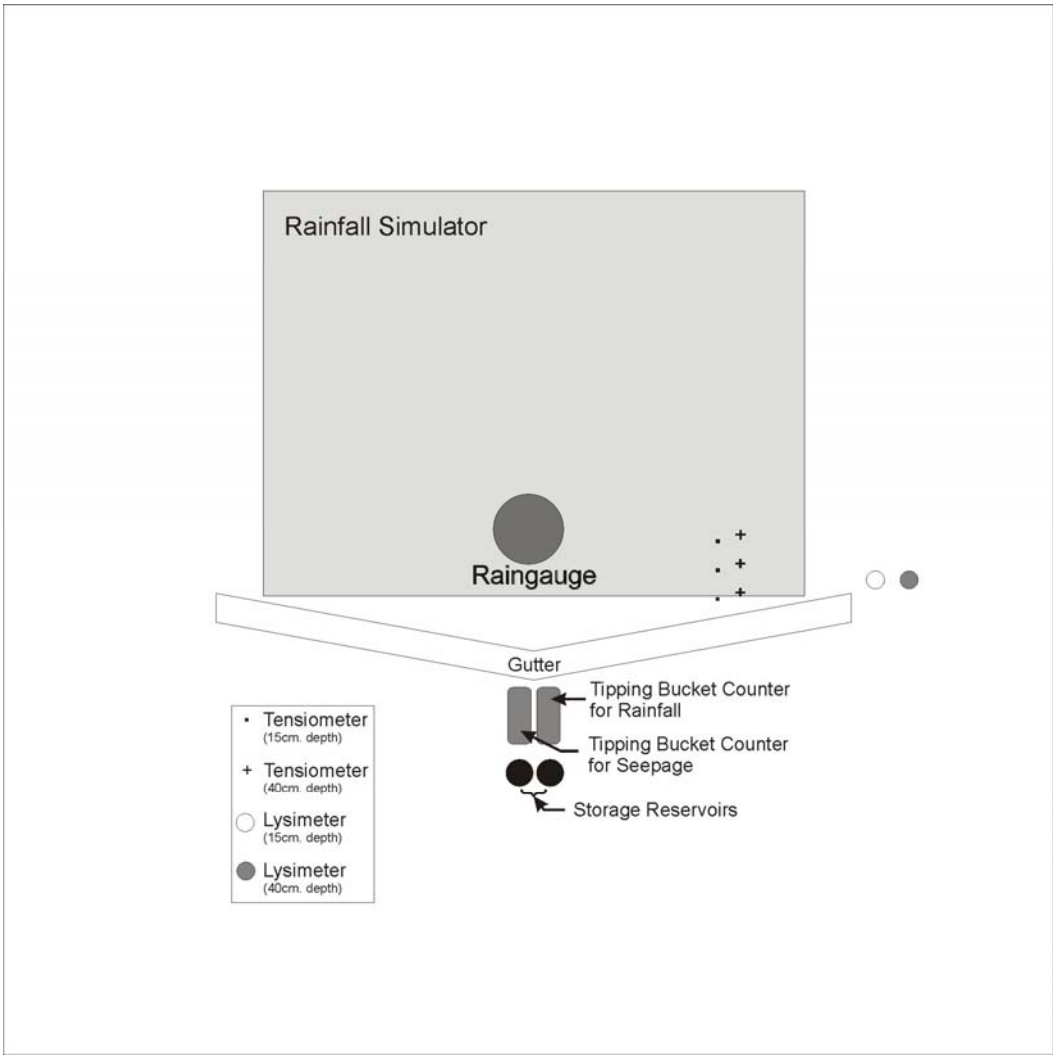

Figure 19: Rainfall simulation field site

mounted approximately 0.5 m above ground and used to record the timing, intensity, and volume of rainfall beneath the spray rig. The tensiometer field, described in Sampling Methods, was measured periodically during the second simulation. Micro-tensiometers were installed in the excavated trench soil face above the gutter and monitored during the simulations (Figure 21). A chloride tracer experiment was also conducted. The micro-tensiometer and tracer procedures are described in later sections. An infra-red/visible light web camera was used to record stormflow entering the gutters.

Figure 20: Tlaloc 3000 rainfall simulator

The first rainfall simulation took place on January 30, 2006, and was split into three "storm events." A tarp covered the ground in the field of spray so that the calibration runs of the spray nozzle would not affect the antecedent conditions. Each "storm" was set at a rate of 1.94 inches per hour to emulate a heavy, but not unlikely, storm for the study area. The spray nozzle was set at 2.5 PSI to achieve the desired 1.94 inches per hour rate, and checked regularly to ensure that the pressure reading did not vary. The first event was conducted from 11:35am-12:12pm to observe the wetting of the system. The second event was conducted from 12:30-1:00pm. Chloride tracer was added to the simulation water for the final rainfall event that day. The third rainfall event conducted from 1:30-3:21pm.

The second rainfall simulation took place on February 8, 2006, and was split into a series of nine, fifteen minute-long "storm events." The purpose of the second rainfall simulation was

to vary the rainfall intensity during the precipitation events—much like what occurs during natural rain storms. In an attempt to vary rainfall intensity, the pressure was manually changed every 15 minutes. Table 1 details the time elapsed and the pressure of each event. Event Zero is the pre-event calibration rain that was conducted from 10:26am to 11:07am. The hillslope was allowed to wet during the calibration process. The simulation began at 12:45pm and ended at 3:02pm. At Event Seven, trench one was disconnected from the tipping buckets rain gauge so that only trench two was delivering runoff.

Tensiometer Instrumentation

Micro-tensiometers (1 cm diameter x 4 cm long) were constructed and installed horizontally in the soil face at trench two. Above the gutters, the three micro-tensiometers, designated T1, T2, and T3, were placed approximately 5 cm, 7.6 cm, and 10.1 cm below the surface, respectively. T1 and T2 were placed near the forefront of the gutter while T3 was placed near the upslope end. Micro-tensiometers are utilized to provide precision and sensitivity to observe subtleties in matric potentials at high frequencies (Baldwin, 1997). Standard field tensiometers do not detect subtle shifts. T1 was damaged during the second rainfall simulation's calibration, and thus was not used on February 8, 2006. The tensiometers were calibrated to obtain a linear response function using a manometer made of glass tubing filled with water. Prior to the rainfall simulation, each tensiometer was filled with de-gassed water and attached by Tygon tubing to a pressure transducer. The transducers were wired to a Campbell Scientific CR23-X data logger. The CR23-X collected and stored soil tension readings at intervals of thirty seconds during the first rainfall simulation. Five second intervals were recorded during the second simulation.

Table 1: Rainfall Simulation Two Event Schedule

Event	Start Time	Pressure (PSI)
0	10:26am	N/A
1	12:45pm	2.2
2	1:01pm	4.5
3	1:16pm	7.0
4	1:32pm	8.0
5	1:47pm	3.5
6	2:02pm	5.5
7	2:17pm	2.2
8	2:32pm	4.0
9	2:47pm	9.0

Field tensiometers, located directly upslope of trench two, were monitored during the February 8, 2006, rainfall simulation. The tensiometer field is described in the Sampling Methods chapter. The matric potential of the soil was recorded, using a tensimeter, prior to the simulated rain (antecedent conditions) at 10:24am, and twice during the simulated rain, 12:45pm and 1:51pm.

Chloride Tracer Experiment

A tracer experiment was conducted during the January 30, 2006, rainfall simulation to determine how long it would take the chloride to infiltrate the soil and runoff into the storage reservoir. During the third simulated rainfall event that day, the chloride tracer was added to the artificial rain. A 2.6 liter mixture of 2 M $CaCl_2$ was added to the 1, 325 liters of water left in the

water tank from the two previous simulation events to achieve an approximately 278 mg/L concentration. Runoff samples were collected in sealed glass tubes at five minute intervals from the tubing that feeds the storage reservoir. The runoff samples' chloride concentration was analyzed in a laboratory using an ion chromatograph.

Figure 21: Experimental soil face and gutter

RESULTS AND DISCUSSION

Rainfall and gutter runoff was monitored from February 2005 until January 2006 at the Watkinsville, GA study plot. Appendix B contains Watkinsville, GA, precipitation data from the neighboring University of Georgia Horticulture Farm weather station, approximately one mile away from the field site. Tipping bucket response for rainfall and runoff of each individual storm event on record is presented in Appendix C. A storm event was defined as a period or periods of rainfall where 24 hours elapsed between significant amounts of rainfall. Within a given event, there were often periods where rainfall ceased for hours. Each "event within an event" was labeled *a*, *b*, *c*, etc. Results are shown in Appendix C, except for storms where equipment failed (Events 19, 20, and part of 41).

Large rainfall and runoff events are a particular focus of the study, so the events were classified by gutter flow volume, as shown in Figure 22. The size classifications include small events (< 1 L) and large events (> 1 L). Nearly one-third of the storms on record during the study are considered large events, with the largest event, Event 38, occurring on Oct. 8-10, 2005, with 3.91 in of rain. The majority of large events had over an inch of rainfall. Small storms accounted for majority of the recorded events, and presumably could be adequately described by the variable source area concept.

Storm runoff was translated to the gutters via the experimental soil face drip plates. Stable isotope evidence confirmed that gutter flow was primarily composed of soil water in the shallow subsurface as opposed to overland flow and other new water processes. The gutter flow

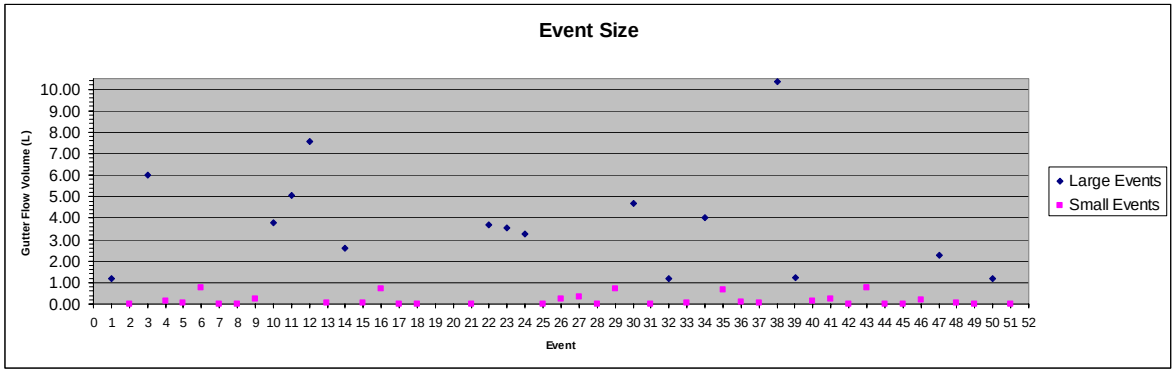

Figure 22: Event size

was also visually observed being conducted across the drip plates during several visits to the field site during storm events. However, there were instances where event water contributed to the gutter flow. The gutters were susceptible to contamination from grass-drip or saturation overland flow during long-duration events prior to June 2005, when berms were installed to deflect new water contamination, and the above-ground precipitation collectors were relocated in order to completely cover the subsurface gutter. This isolated the gutters from the surface. Repetition 2 appeared to receive more contamination than Repetition 1. The microtopography of the area was such that Repetition 2 was centered in a concave slope. This may have caused additional runoff of event water. Nonetheless, the gutter response of the two repetitions agreed closely in terms of response timing and intensity rates, as shown in figures below.

An observed rapid mobilization of flow at the study plot is consistent with a pressure wave propagation mechanism. Figure 23a shows a typical subsurface gutter and rainfall response. After an initial lag time, the gutter flow mimics rainfall. The beginning lag is due to the initial wetting of the hillslope, the amount of which is dependent on antecedent conditions. For rainfall to activate gutter flow, the hillslope subsurface has to be reasonably wet. Once the hillslope is “primed”, the gutter flow repetitively responds within minutes to the onset of rain.

Similarly, within a few minutes, the gutter flow stops with the cessation of a precipitation event. Figure 23b displays box plots that compare the “on and off” of operation times for each gutter to the rain gauge.

Gutter flow volume versus rainfall volume for repetitions is shown in Figure 24. The plots for the rain gauge are scaled to the gutter flow plots; the rain gauge collected water from a smaller area than the gutters. Generally the smaller events yielded little or no runoff, while events greater than one inch yielded measurable runoff volume. There is clearly a trend where more rainfall produces more gutter flow.

During the experimental monitoring period, fifty-one storm events were recorded. Although each event entails a unique combination of rainfall/runoff responses, δ^2H composition, and antecedent conditions, the following discussion will be illustrated with a selection of representative events.

Small storm events, such as Event 42 (0.43 in), produced little to no gutter flow (Figure 25). Storms of this size typically contribute little runoff to streams. When small storms do produce some runoff, it can be explained by the variable source area adjacent to the stream. Occasionally, such as in Figure 26, a small amount of gutter flow can occur with higher rainfall intensities several hours after the start of the rainfall.

The quick response of the subsurface runoff gutters in conjunction with rainfall was immediately noticeable during the first large storm events of the experiment. Several events had runoff gutter responses that occurred within 2-3 min after precipitation began. Event 29 (0.52 in) for example, demonstrates a nearly immediate subsurface gutter response (Figure 27). After the beginning of rainfall, three minutes pass before the subsurface gutters begin tipping. The next event, Event 30 (Figure 28), was higher in rainfall volume with 1.37 in of rain, and occurred 13.5

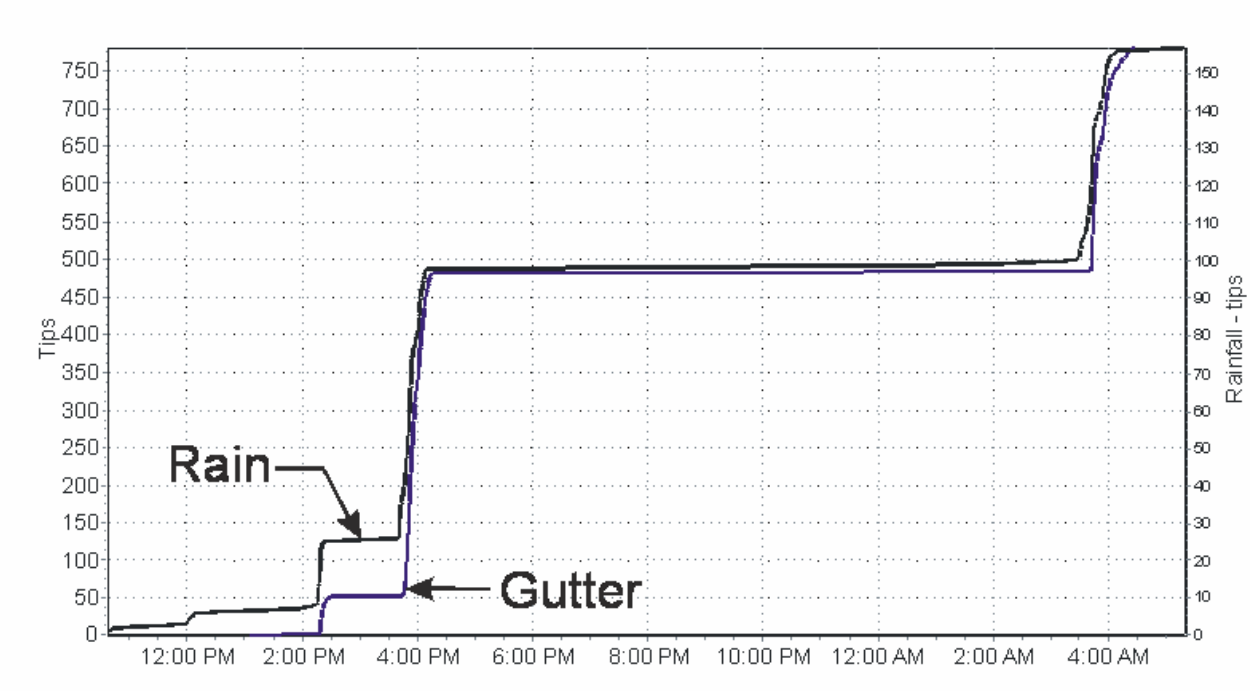

Figure 23a: Rainfall and gutter response

days later. This event took 43 minutes for the subsurface gutters to tip after the start of rainfall. More time was needed to "wet" the system and build conditions near the drip plates in order to generate flow. Antecedent conditions clearly play a role in network building. Also rainfall intensity was high at the beginning of Event 29, but was not at the beginning of Event 30. Nonetheless, once the gutters began tipping, their response closely followed that of the precipitation.

The largest storm event on record (3.91 in) took place on October 6-7, 2005, as shown in Figure 29. Event 38 exhibited a rapid initiation of gutter flow and the abrupt on and off periods mimicking the rainfall. As shown in the figure, both gutters typically showed similar patterns of response. Repetition 1 generally received more subsurface gutter flow, due to the microtopography of the hillslope

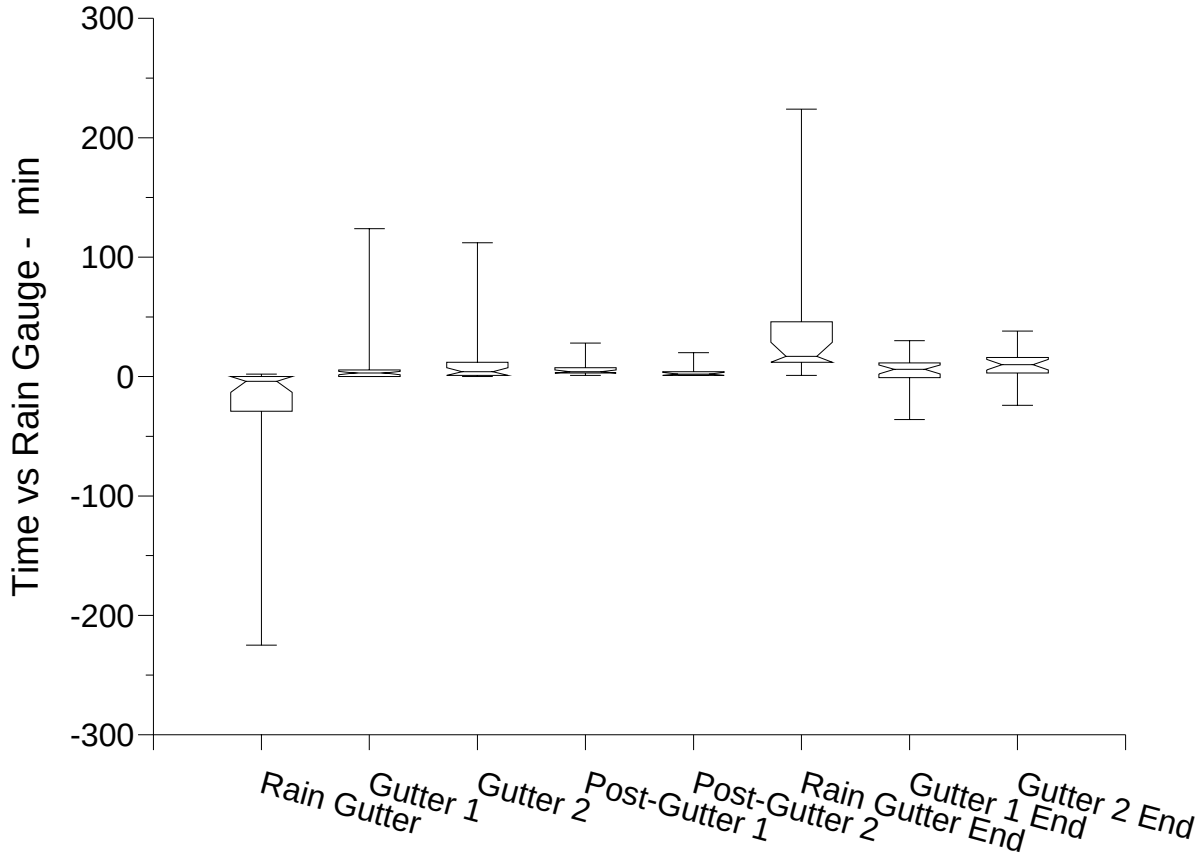

Figure 23b: Operation time per tipping bucket

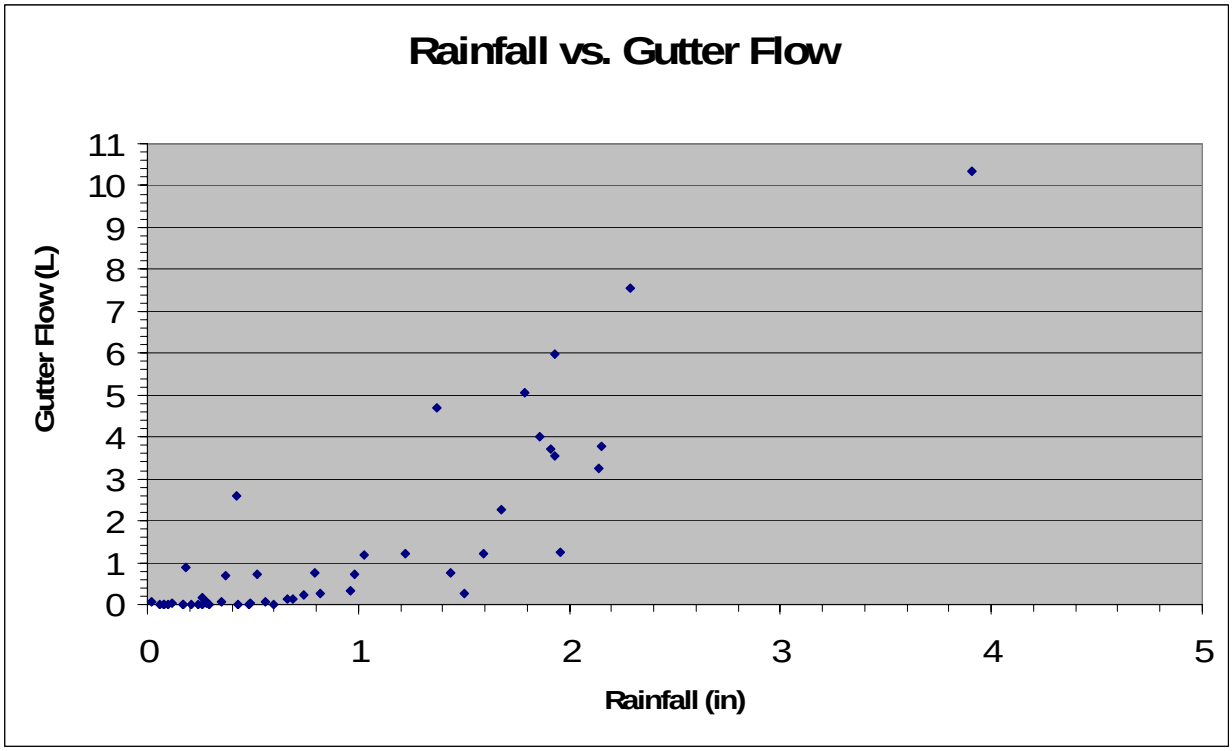

Figure 24: Gutter flow in response to rainfall event volume .

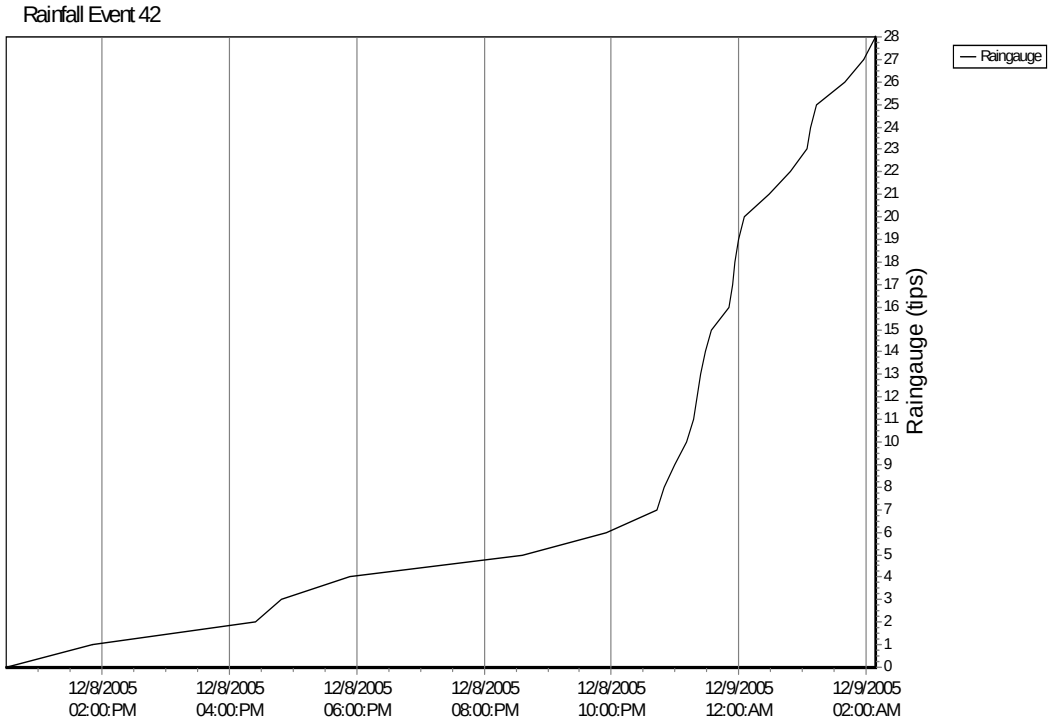

Figure 25: Rainfall Event 42 (Dec. 8-9, 2005)

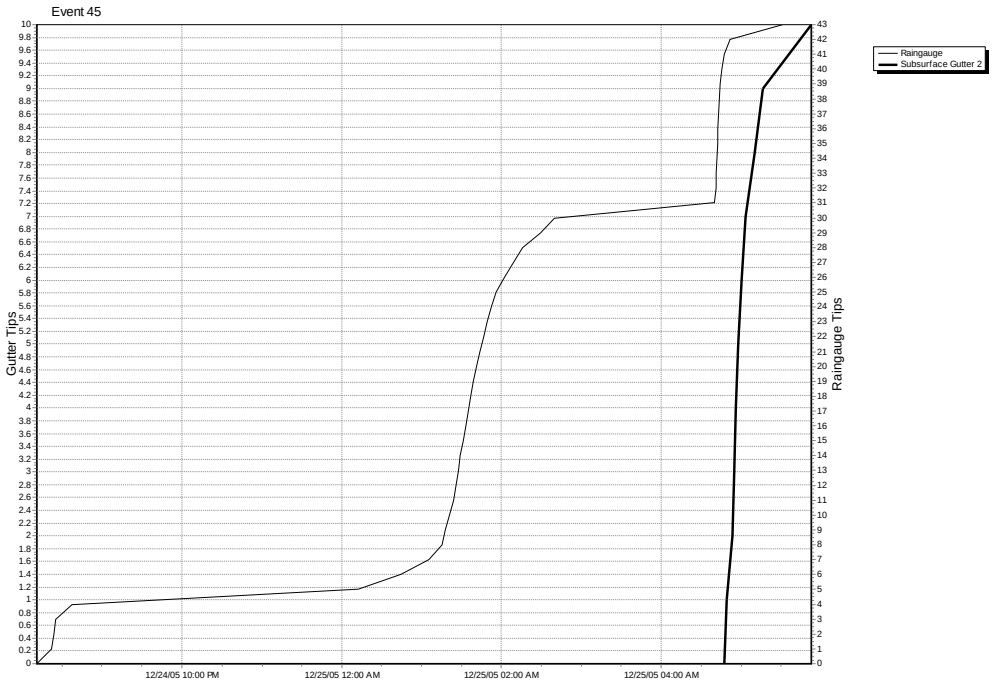

Figure 26: Rainfall Event 45 (Dec. 24-25, 2005)

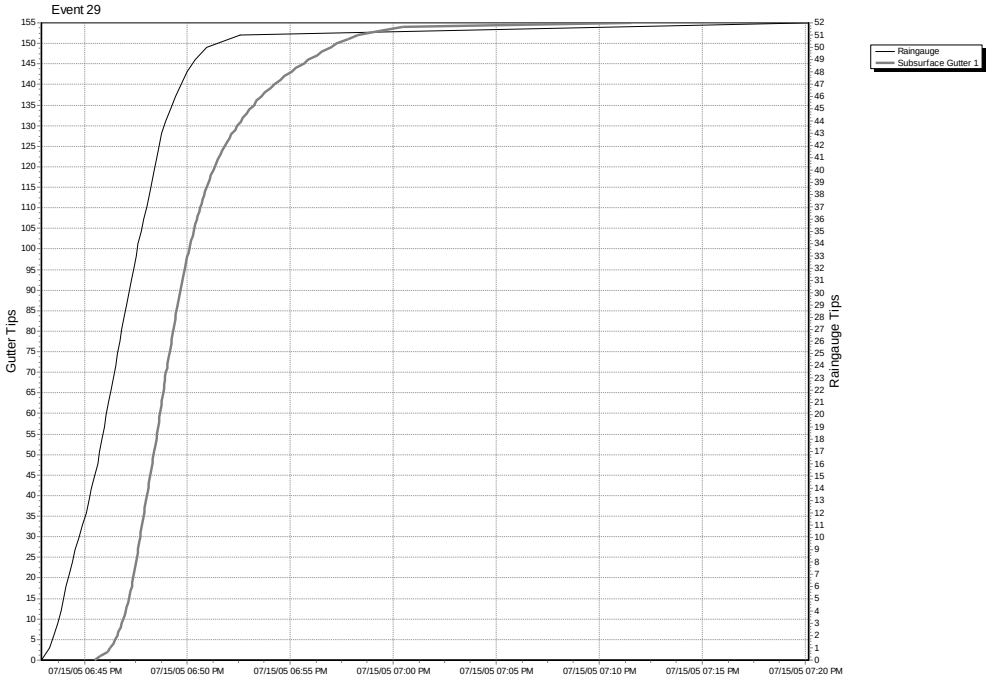

Figure 27: Rainfall Event 29 (Jul. 15, 2005)

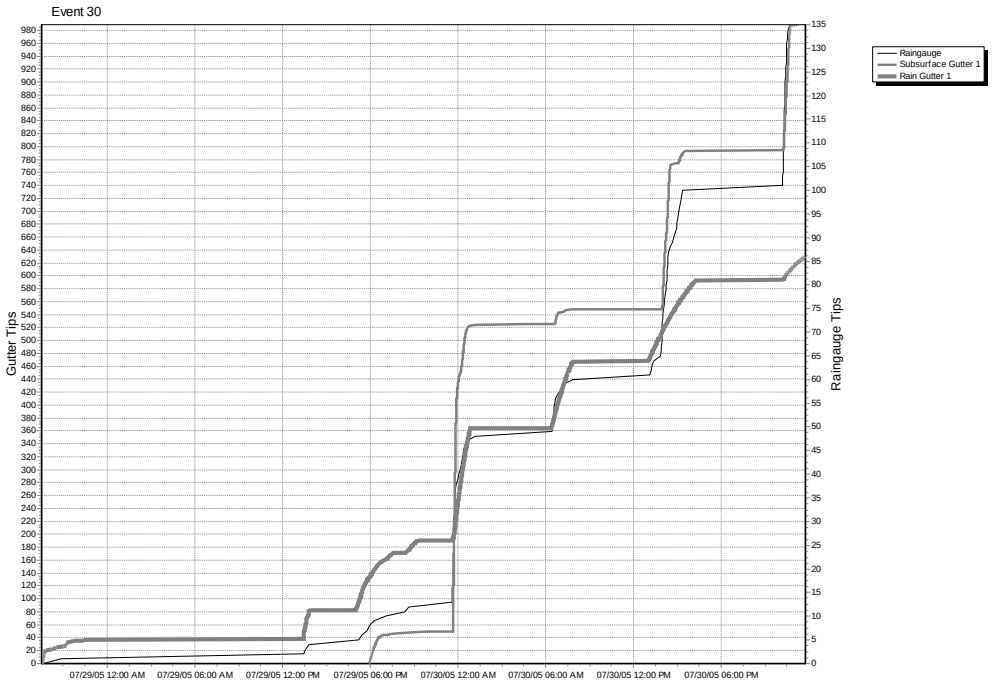

Figure 28: Rainfall Event 30 (Jul. 29-30, 2005)

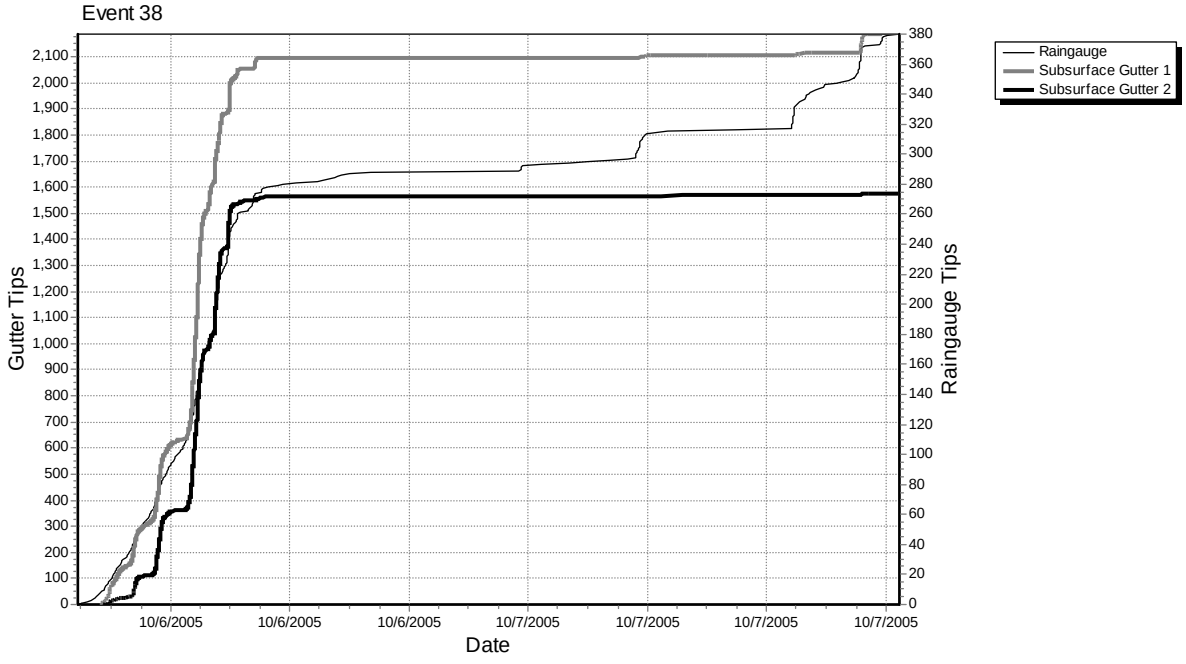

Figure 29: Event 38 (Oct. 6-7, 2005)

The storm that took place on April 22-23, 2005, designated as Event 14, is shown in Figure 30. Although it is a relatively small storm event with 0.42 in of rain, it was calculated to have the largest upslope contributing length (approx. 20 cm) to runoff, as shown in Figure 31. The incipient network that was built during this small event was roughly twice as large as that of various larger events—such as Event 11, which rained 1.79 in. The correlation between rainfall volume and contributing upslope length is highly variable, as shown in Figure 32. Eight and a half days had passed since the last storm event, so the hillslope was not significantly wet. Yet Figure 30 shows that the runoff gutters began responding almost immediately (2 min) after rainfall began. Deuterium analysis was conducted on Event 14 runoff samples and yielded the following δ^2H values: -24 $^0/_{00}$ for precipitation, -30 $^0/_{00}$ for soil water, and -29 $^0/_{00}$ for storm runoff. Hence, the storm runoff is clearly stored subsurface soil water.

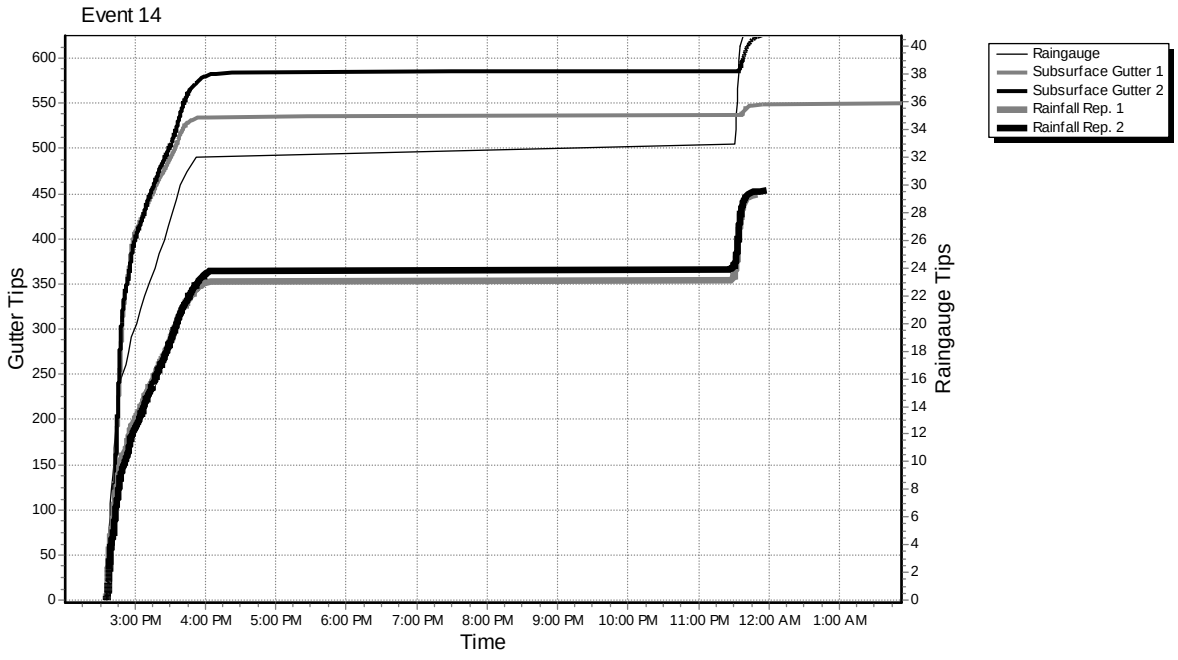

Figure 30: Rainfall Event 14 (Apr. 22, 2005)

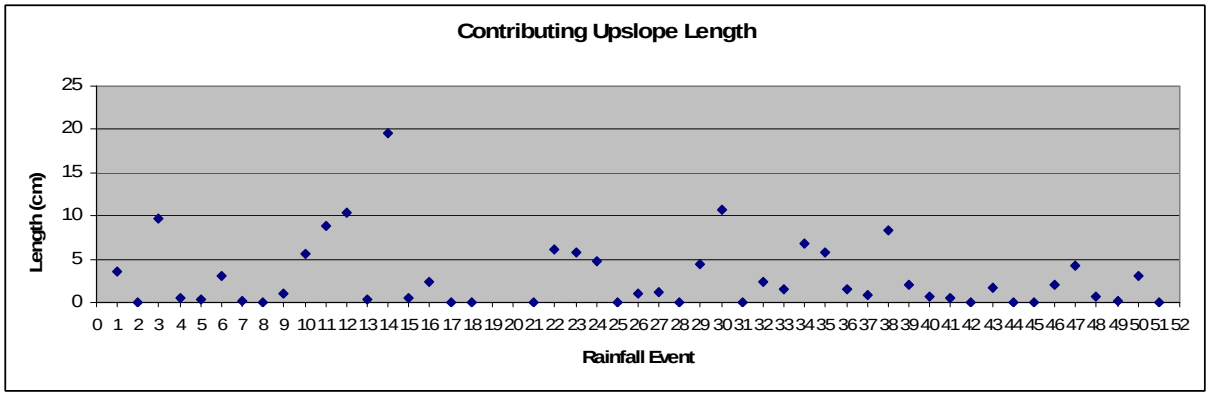

Figure 31: Contributing length for runoff from the upslope

The event that followed, Event 15 on April 26, 2005 (Figure 33), received a comparable rainfall volume of 0.35 in, yet produced 0.062 L of runoff and slope contribution was limited to the edge of the experimental soil face. Although Event 38 produced the most gutter flow and a considerable upslope contribution (8.34 cm), the contributing length was still less than half that of Event 14 (Figure 31). The larger storm events, such as Events 3, 11, 12, 22, 23, 34, 35, and 38, show a trend of approximately 6-11 cm for upslope contributing length. The June and July large events are on the lower bound of the contributing length range for large events, due to dry antecedent conditions. Small events generally demonstrated a contributing length between 0-5 cm upslope.

Although Event 14 did not consist of large rainfall volume (0.42 in), the subsurface gutters collected 2.6 L of runoff. Figure 32 shows the gutter flow during this event to be abnormally high compared to other storms of its size and duration. The factor that sets Event 14 apart from Events 15 and 38 is rainfall intensity. Event 14 exhibited the highest rainfall intensity of any storm event on record. The highest recorded rainfall intensity of the storm was 1.73 in/hr, which occurred during the first few minutes of the storm. The only other small rainfall event that exhibited a contributing length similar to large rainfall events was Event 35, which very quickly

had a rainfall intensity of up to 1.3 in/hr. Figures 34 and 35 show a trend between increasing rainfall intensity and the amount of runoff produced in a catchment.

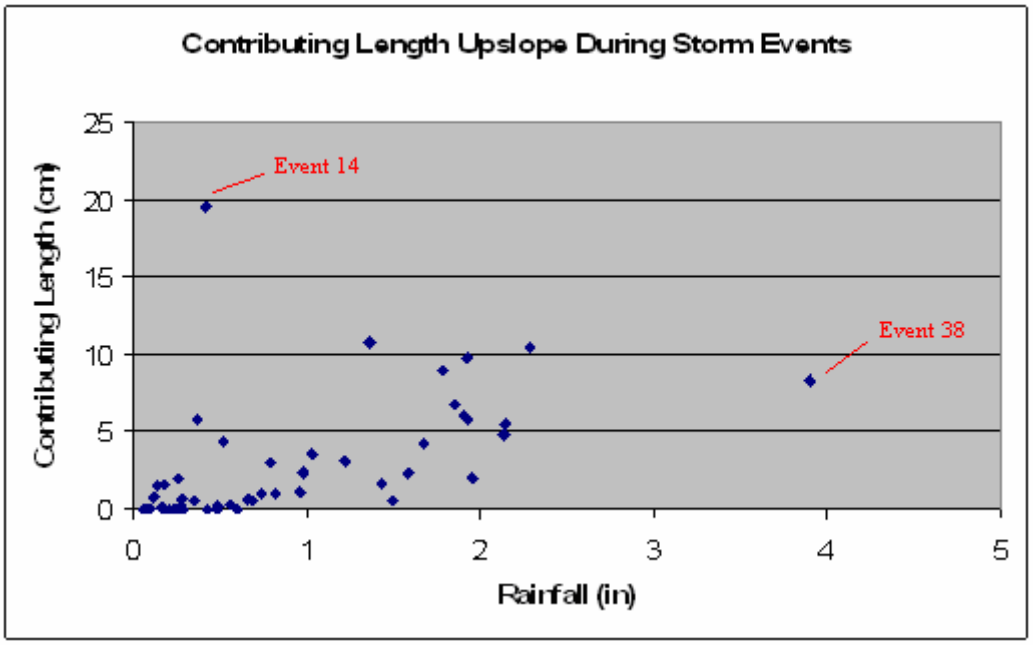

Figure 32: Upslope network contributing length during storm events

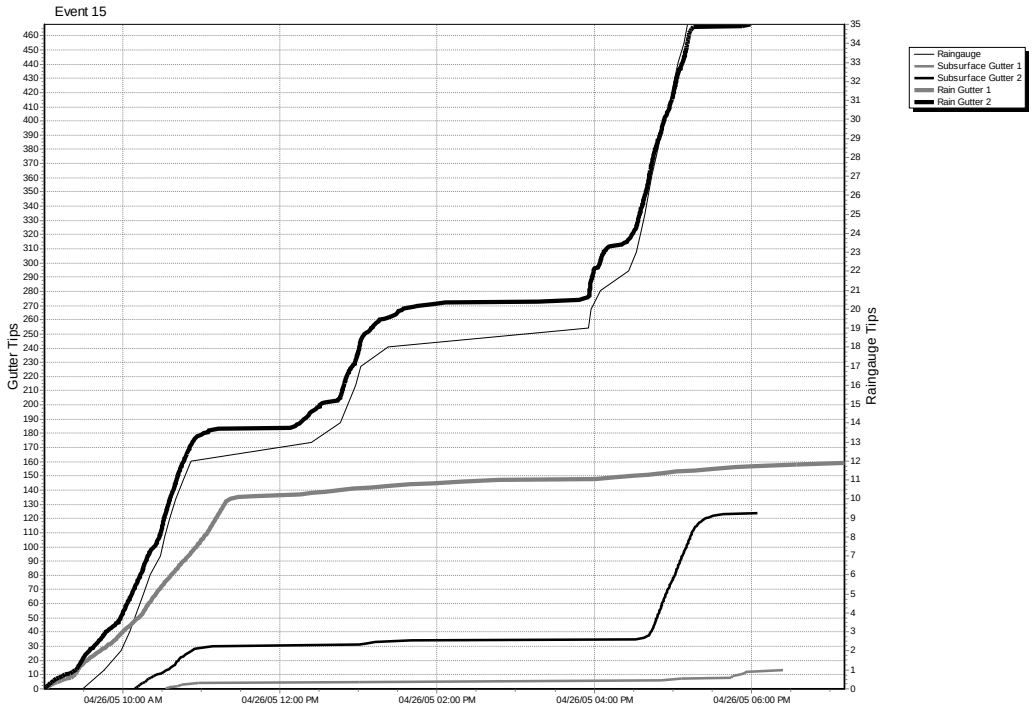

Figure 33: Rainfall Event 15 (Apr. 26, 2005)

The rainfall/runoff monitoring data of the hillslope study plot can be compared to the results of Baldwin's laboratory core experiment where pressure wave propagation was demonstrated (Rasmussen *et al*., 2000). With the application of spray, Baldwin immediately observed pressure waves within the cores that pushed water from the bottom of the core. The pressure waves and flow emission dissipated when the spray was cut off. The field experiment rainfall/runoff plots show not only a rapid translation of subsurface water to the gutters, but an abrupt cessation of gutter flow when rainfall ceases. The gutter collection systems collected subsurface water that was pushed from the experimental soil face when rain fell on the hillslope surface. The perturbation in the subsurface that is created from the rain drops causes fluctuating soil pressures that act as pressure waves. Water ceased to be ejected from the soil face when rain ceased to affect soil pressures. If standard saturated or unsaturated flow were generated in the gutters, the response would not terminate so abruptly.

Although events such as Event 14 were low in precipitation (< 0.5 in), they were able to produce high gutter flow and greater upslope contribution because of the intensity. High intensity results in more rain drops infiltrating the surface in a short period, thus causing more perturbation and a larger contributing area. For example, Event 29 had a higher initial intensity and a quicker mobilization of gutter flow than Event 30, although the events were comparable in size and soil moisture.

Stable Isotopic Analysis

Deuterium analysis was conducted on water samples collected at the field site during the rainfall/runoff monitoring period. Figure 37 displays the δ^2H values for all samples collected: precipitation samples (PRECIP), gutter flow samples (Repetition 1, Repetition 2), and soil water

samples (L1, L2, L3, L4), taken from the corresponding suction lysimeters. Appendix D gives, in detail, results and data pertaining to the stable isotope analysis.

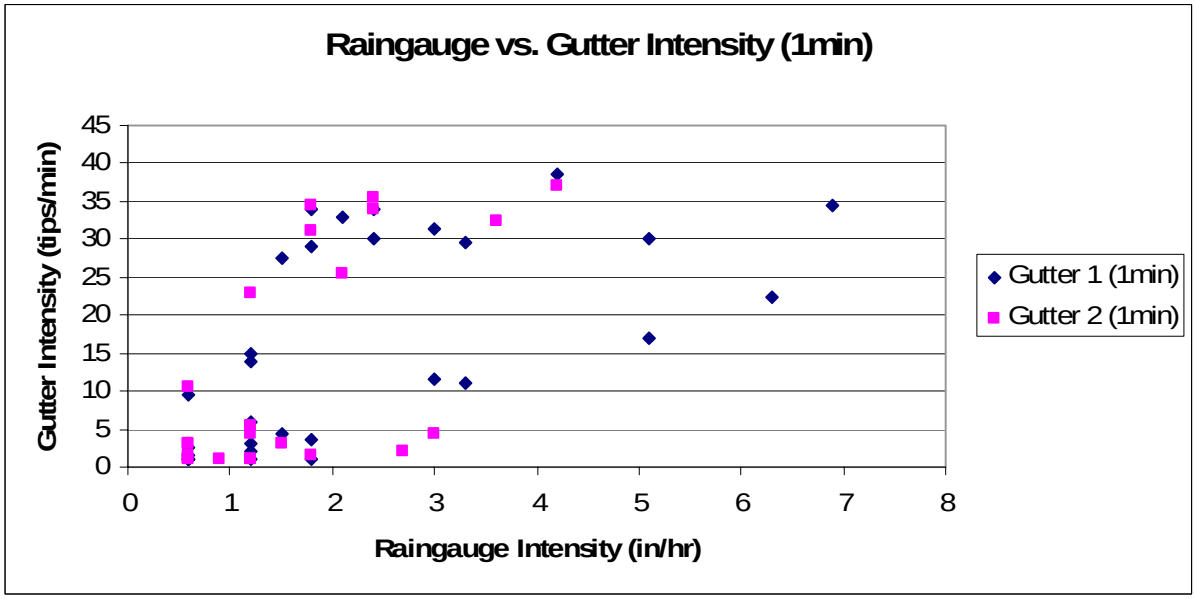

Figure 34: Gutter flow and rainfall intensity averaged over 1 min intervals

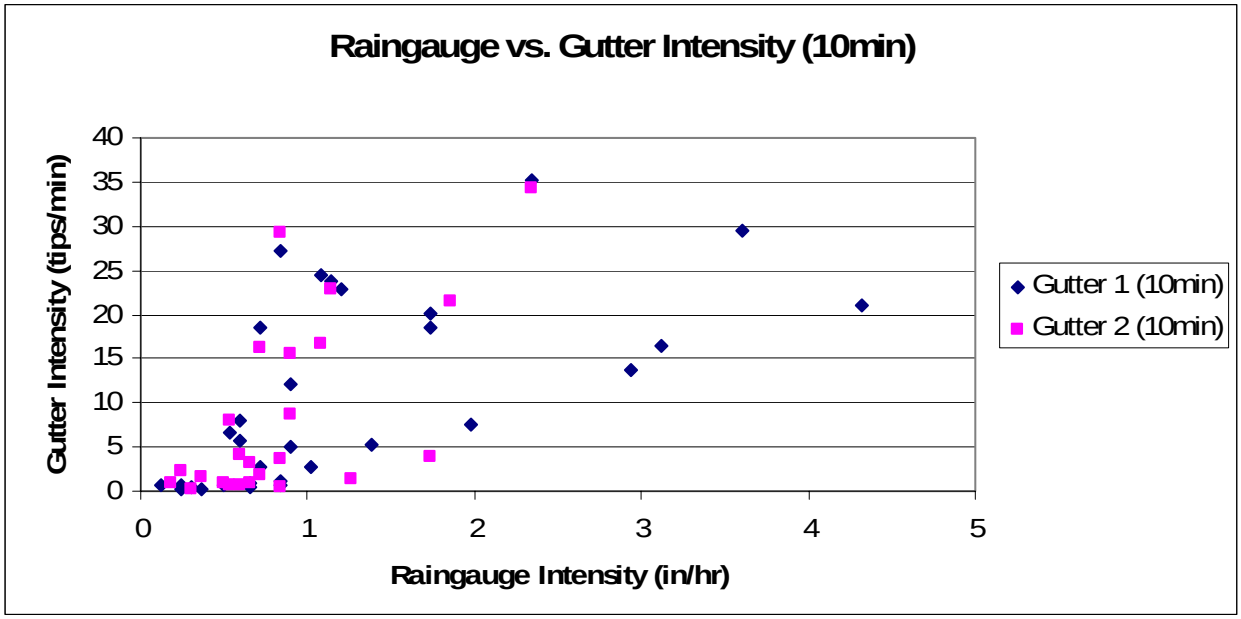

Figure 35: Gutter flow and rainfall intensity averaged over 10 min intervals

Stable isotope distribution in meteoric waters can vary spatially due to climate, latitude, altitude, and continentality (Clark and Fritz, 1997). The study was confined to a single location, so regional effects were not applicable. Local effects such as seasonal variation, temperature, and storm type contributed to the variation in δ^2H distribution. Figure 36 displays the seasonal δ^2H variation over the sampling period. Individual storm events are isotopically unique, and can vary in signature depending on properties inherent to the weather system. Therefore, there is bound to be variation in deuterium for precipitation, as shown in Figure 37. The underlying trend in seasonal variation, however, is enrichment of heavier δ^2H during warmer months (Figure 36). Higher temperatures result in increased evaporation, causing fractionation. The Watkinsville results agree with the seasonal variations reported in Rozanski *et al*., (1993).

In terms of annual average rainfall, a relatively small portion of precipitation reaches the water table or surface water bodies via overland flow, direct precipitation, etc. A large percentage of rainfall is returned to the atmosphere by evapotranspiration. The remaining volume is relegated to storage in the vadose zone or runoff. This vadose zone soil water was sampled for deuterium analysis by two repetitions of suction lysimeters, at depths of 15 cm (L1 and L3) and 40 cm (L2 & L4). Soil water is reasonably isotopically homogenous. After infiltration below the influence of the root zone, water in storage is shielded from fractionation due to evapotranspiration. Unsaturated zone soil water can be seen as a long term average of the different storms that are represented as stored infiltration (Kendall and McDonnell, 1998). The thirty-eight soil water samples, taken over the course of a year, yielded an average δ^2H of -32 $^0/_{00}$. The δ^2H values ranged from -24 to -43 $^0/_{00}$; although the outlying values can be attributed to rainwater contamination of the lysimeters. Each time there was an anomalous soil water δ^2H value, it was similar to that of the rainfall. Also, the anomalous values occurred in the shallow

lysimeters. It was suspected that the suction lysimeters were occasionally sampling flow that ran down the sides of the lysimeters. Soil water samples yielded an approximate range of -27 to -30 $^{0}/_{00}$. As shown in Figure 37, there was close agreement between the four lysimeters.

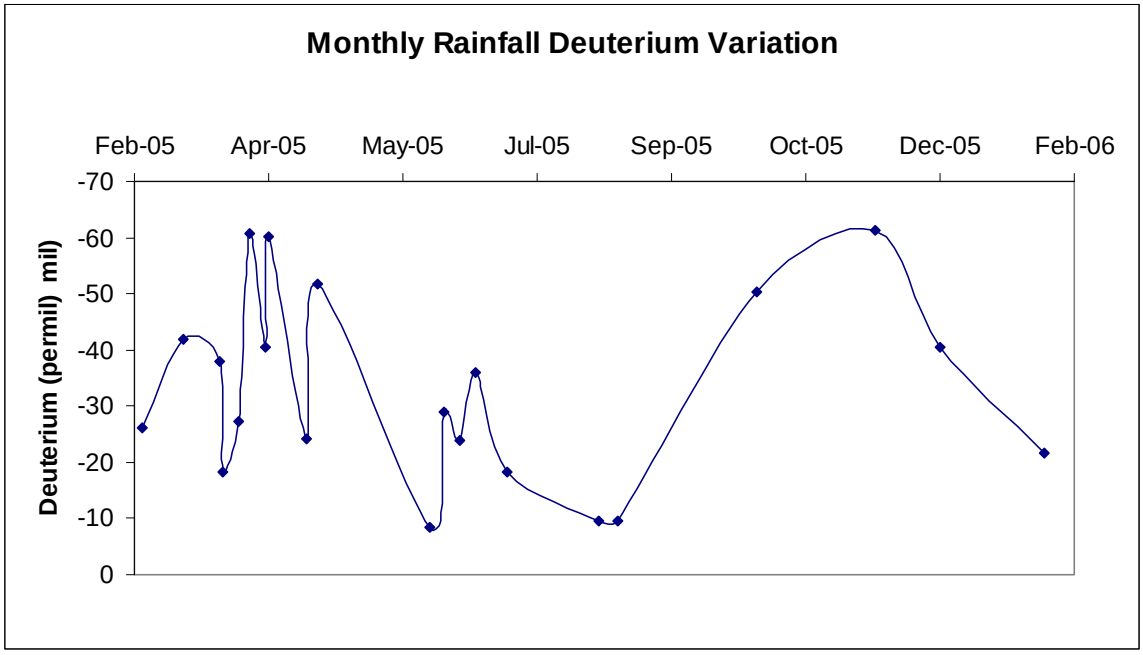

Figure 36: Monthly Rainfall δ^2H Variation—Watkinsville, GA

The primary purpose of deuterium analysis was to determine if subsurface stormflow is "old" water. There can be considerable inter-storm variation of isotopic composition, so deuterium analysis is often useful to differentiate between storm water and the relatively static soil water (Pionke and DeWalle, 1992; Kendall and McDonnell, 1998). The gutter flow is called "old" water if the isotopic value is similar to the soil water samples, and dissimilar to the rainfall values. Appendix E gives all δ^2H values for runoff found during the study, while Figure 37 compares rainfall, soil water, and runoff for each storm event that was analyzed.

The deuterium results presented in Figure 37 show that the stormflow is dominated by old water. One of the clearest examples is the storm of April 22, 2005. The event water had an average δ^2H composition of -24 $^{0}/_{00}$. Pre-event lysimeter samples had an average δ^2H

composition of -31 $^{0}/_{00}$. The gutter flow sampled from the gutter collection system yielded a δ^2H composition of -29 $^{0}/_{00}$. The percentage of old water comprising gutter flow was calculated for a selection of events where lysimeter samples were present and there was no clear indication of contamination of the gutter samples. The range of old water contribution was 97%-25%, with an average of 70% old water contribution and 30% new water contribution to gutter flow.

Several storms, especially in the first months of the sampling period, had runoff values that were similar in composition to rainfall. The early design of the gutter collection system, however, was not completely closed to the atmosphere or impervious to drip from grass. The subsurface gutters were observed to receive contamination from direct precipitation into the gutters. The collection system was redesigned in June, 2005 to limit this contamination. When antecedent conditions are near saturation and the storm has a long duration, such as during the winter months where more contamination was noticed, the system is more likely to translate event water through rapid pathways. Kendall and McDonnell (1998) note that it can be difficult to meet the requirements set forth by Sklash and Farvolden (1979) for isotopic hydrograph separation. Occasionally precipitation and soil water are similar isotopically, as was the case on such as April 7, 2005.

Some storms demonstrated a runoff composition that was dissimilar to both rainfall and lysimeter samples. For example, June 13, 2005 (Event 22), yielded the following results: -28 to -30 $^{0}/_{00}$ for precipitation, -31 to -33 $^{0}/_{00}$ for lysimeter water, and -38 to -40 $^{0}/_{00}$ for runoff. There are several possible explanations for these results. The isotopic value of the storm event could have changed significantly during the duration of the storm and the observed runoff is a mixture of that range--although this assumes that the precipitation made its way to the gutters via overland flow which rarely happened, especially in the summer months. A more likely

explanation is that the shallow subsurface can store various values from previous storms. The storm preceding Event 22 was a very small storm that didn't result in any runoff for sampling. However, Event 20 (June 2, 2005) was the second largest storm that took place during the study. Thus, water from events such as Event 20 could still be present in the soil and later pushed onto the gutter during Event 22.

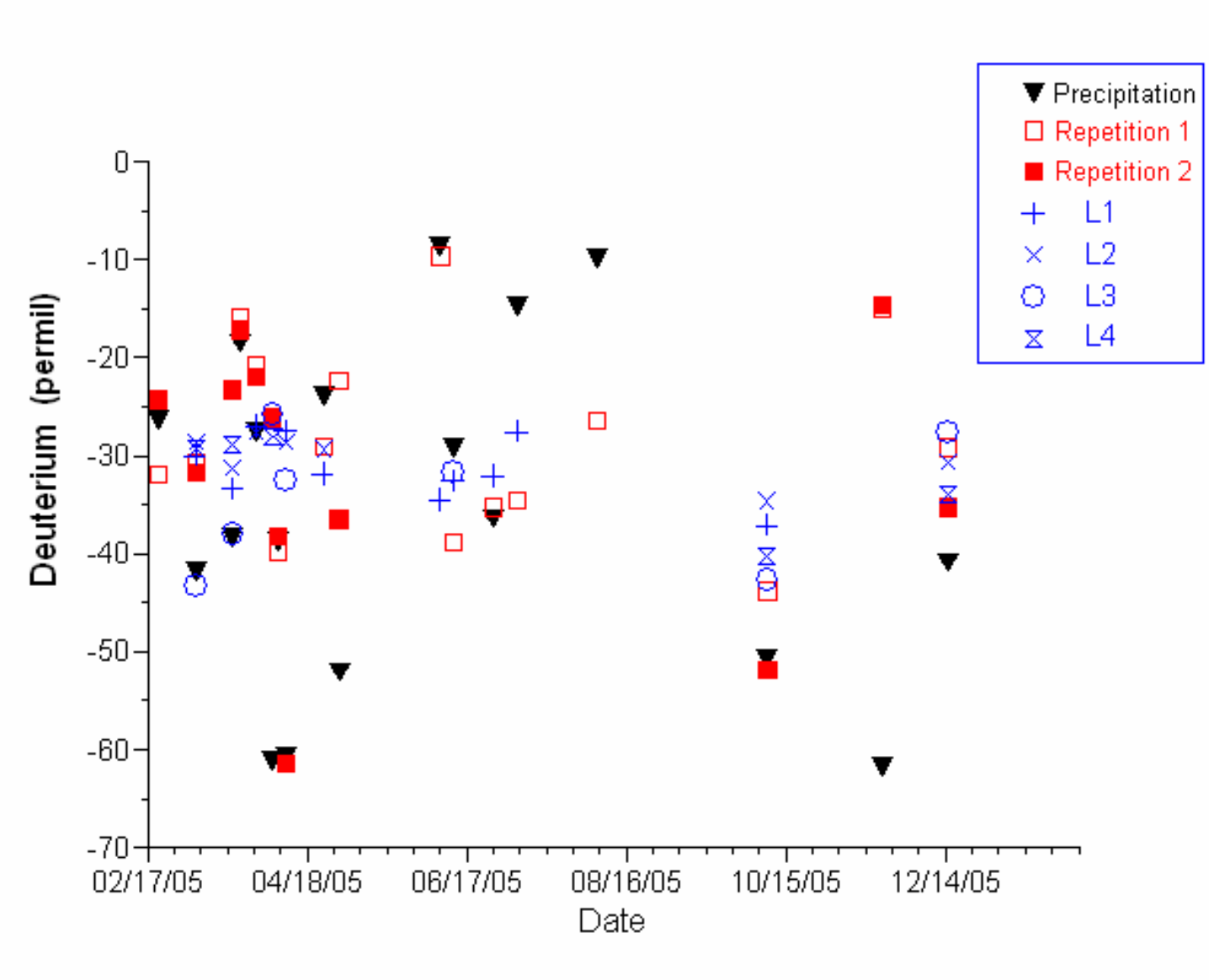

Figure 37: Field Experiment Deuterium Analysis Result

Artificial Rainfall Simulations

A Tlaloc 3000 rainfall simulator sprayed artificial rain on an approximately 2.5 m X 2.5 m area immediately upslope of the Repetition 1 gutter collection system (Figure 19). The rainfall and gutter flow response for the first rainfall simulation, conducted on January 30, 2006, is shown in Figure 38. Soil moisture conditions were typical for the region in the winter months. There was 0.16 in of rain the day before the simulation, and an inch of rain on Jan. 23, 2006. The soil properties of the study area were examined and discussed in Appendix E.

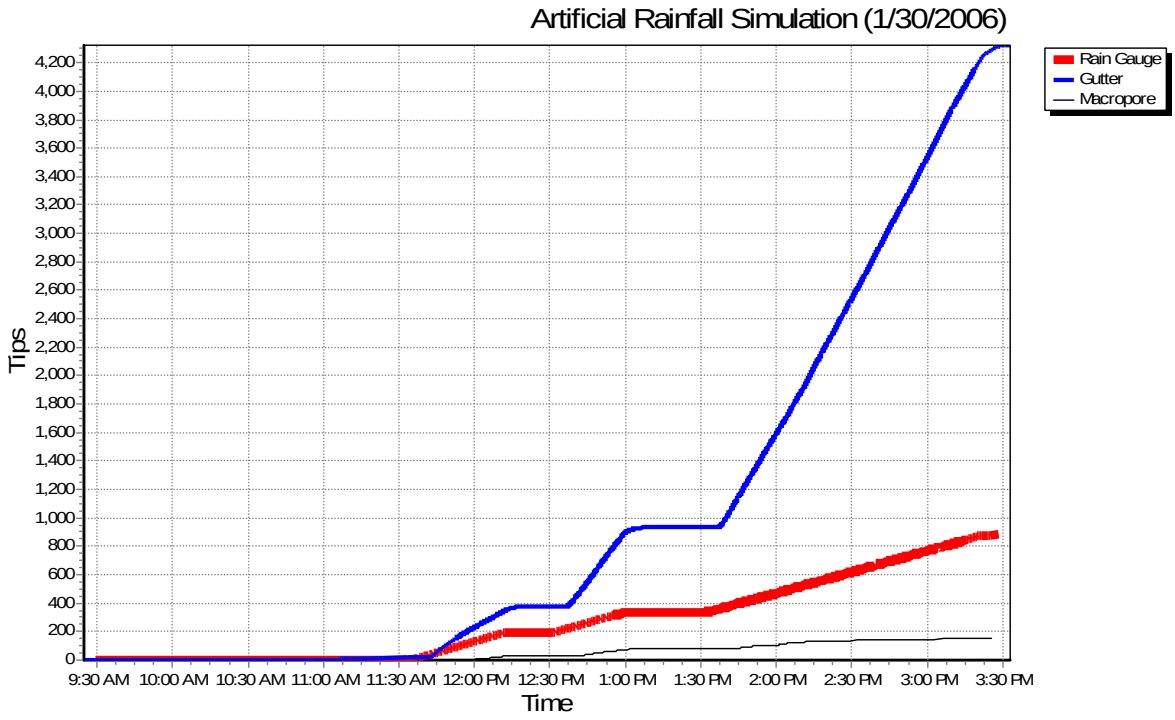

Figure 38: Rainfall Simulation One—January 30, 2006

The Tlaloc 3000 simulator was set to simulate large storms with high rainfall intensities averaging slightly over three inches per hour. Table 2 gives the maximum rate of flow for each tipping bucket at one and ten minute intervals for each "event". The Tlaloc 3000 sprayed a total of 8.8 in of artificial rain on the study plot during the first rainfall simulation and the subsurface gutter collected 20.439 L of water. The artificial macropore produced 0.7144 L of water.

Table 2: Simulation 1 maximum tipping bucket rates

Event	Precip. Rate 1min (in/hr)	Precip. Rate 10min (in/hr)	Gutter Rate 1min (tips/min)	Gutter Rate 10min (tips/min)	Macropore Rate 1min (tips/min)	Macropore Rate 10min (tips/min)
1	3.3	3.24	15.5	11.9	2.5	1.4
2	3.3	3.06	24.5	23.9	3	2.5
3	3.6	3.12	35.5	34.3	4	2

Compared to data from natural rainfall/runoff event monitoring, the tipping bucket response operated similarly during the artificial rain simulation. After the initiation of rainfall, the subsurface stormflow gutters collected flow following a lag time on the order of 5-10 minutes. The artificial macropore received flow approximately twenty minutes after the onset of heavy rainfall. Once the gutters began tipping, the gutter flow plots, including the artificial macropore, mirrored that of the un-scaled rain gauge plot (Figure 38). When each event was concluded, the gutter flow abruptly stopped, and the gutter flow abruptly switches back on with the start of each new event.

A web camera was mounted in the gutter trench and filmed the drip plates as they conducted water from the soil. Approximately eight minutes into the first application of spray, water began to drip off of the most down-gradient drip plate into the gutter. Within another minute, water was being conducted rapidly across all of the drip plates.

The micro-tensiometers emplaced in the trench soil face operated throughout the duration of the rainfall simulation. The subsurface pressure fluctuations behind the soil face, in conjunction with the spray and gutter flow plots, are shown in Figure 39. Tensiometer 1 had an average matric potential of 10.29 cm during the experiment, while Tensiometer 2 had an average of 11.14 cm. The matric potential readings prior to rainfall can be attributed to noise in the system, produced during installation and the set-up of the simulator. With the onset of falling

artificial rain, both micro-tensiometers recorded sharp, immediate increase in soil pressure at the same time as the runoff response began in the subsurface gutters. The system pressure fluctuate much like the soil pressures in Baldwin's (1997) soil core experiment. Baldwin's tensiometer response appears more "jagged". However, the data loggers used at the simulation took a reading every thirty seconds, while Baldwin's recorded every second. When the spray ceases, the pressure drops rapidly.

During each rainfall event, the matric potential gradually decreases after a certain point. The threshold for maximum pressure in the system during the three events is approx. -10.5 cm, -9.5 cm, and -7.5 cm, respectively. The relation between these pressures and the pressure wave is not known.

Rainfall and runoff response for the second artificial rainfall simulation, that took place on Feb. 8, 2006, is shown in Figure 40. The soil was relatively moist, as it had rained 1.67 in two days prior to the simulation. A total volume of 5.8 in of artificial rain was sprayed on the surface cover of the study plot during the second rainfall simulation. The subsurface gutter collected 23.310 L of runoff. The macropore response was not recorded due to data logger malfunction. Simulation 2 differed from the first. Rather than simulating three distinct events at three different intensities, one event with varying intensity was attempted. Figure 40 shows two events. The first is the calibration of the simulator before the main event that began at 12:45pm. The intensity steps are denoted in Table 1. However, it was found that the Tlaloc 3000 rainfall simulator did not effectively produce varying rates of spray. The tipping bucket rain gauge did not record extensive changes in intensity during the event, despite adjustments to the pressure gauge at regular intervals during the experiment.

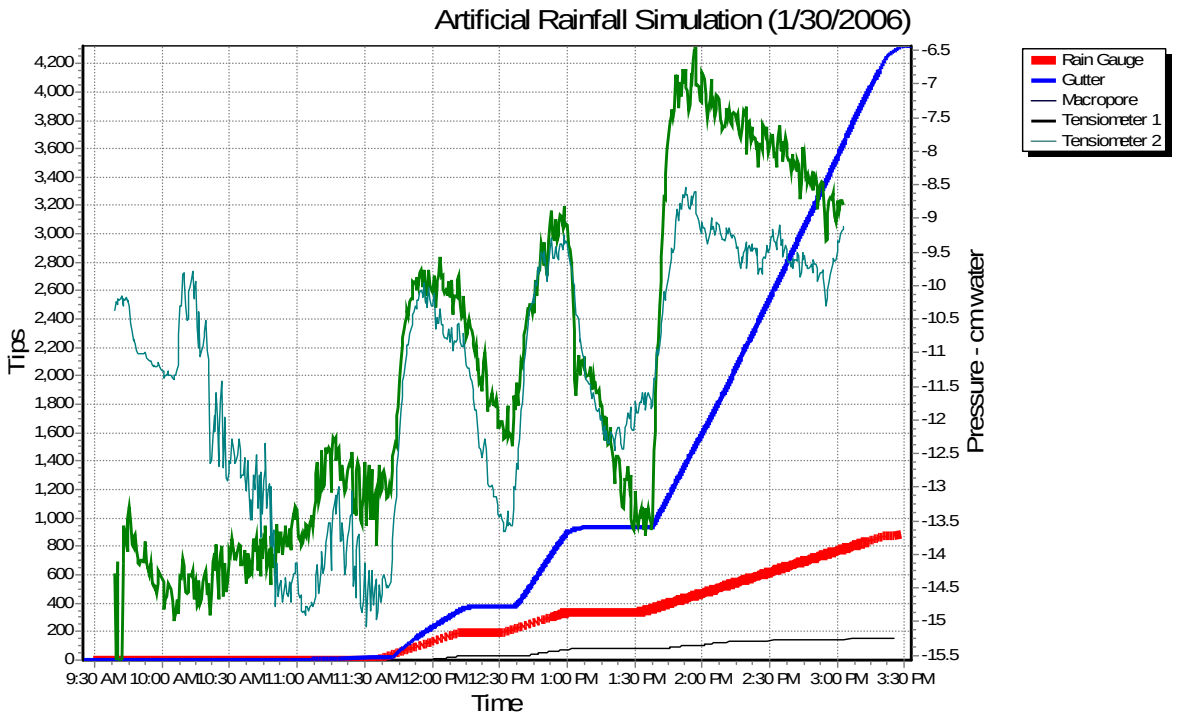

Figure 39: Rainfall Simulation One tensiometer response

Lag times between the onset of heavy rainfall and gutter responses were in agreement with the previous simulation and natural rainfall. Overall, the rainfall intensity for the simulation averaged between 2.1-2.6 in/hr. The maximum rate of rainfall was calculated to be 3 in/hr at a one minute interval and 2.64 in/hr at a ten minute interval. The maximum rate for subsurface runoff was calculated to be 40 tips/min at the one minute time interval and 39.7 tips/min at the ten minute time interval.

The average matric potential during the second rainfall simulation was 22.47 cm for Tensiometer 2. The seal on Tensiometer 1 was accidentally broken during the set-up of the simulator, and could not be used. The matric potential response of Tensiometer 2 was similar to the response of the Jan. 30, 2006, simulation. The pressure near the soil

face exhibited a sharp increase in sync with the "switching on" of the hillslope as the runoff gutters begin to exhibit flow after the onset of rainfall. The threshold of maximum pressure and

pressure wave fluctuations were similar to the first experiment. After the conclusion of the experiment, the tensiometer was left to record the matric potential for 24 hours. Figure 41 shows the natural fluctuations of pressure. The gradual decline in pressure at the latter portion of the recording period was caused by drying of the soil.

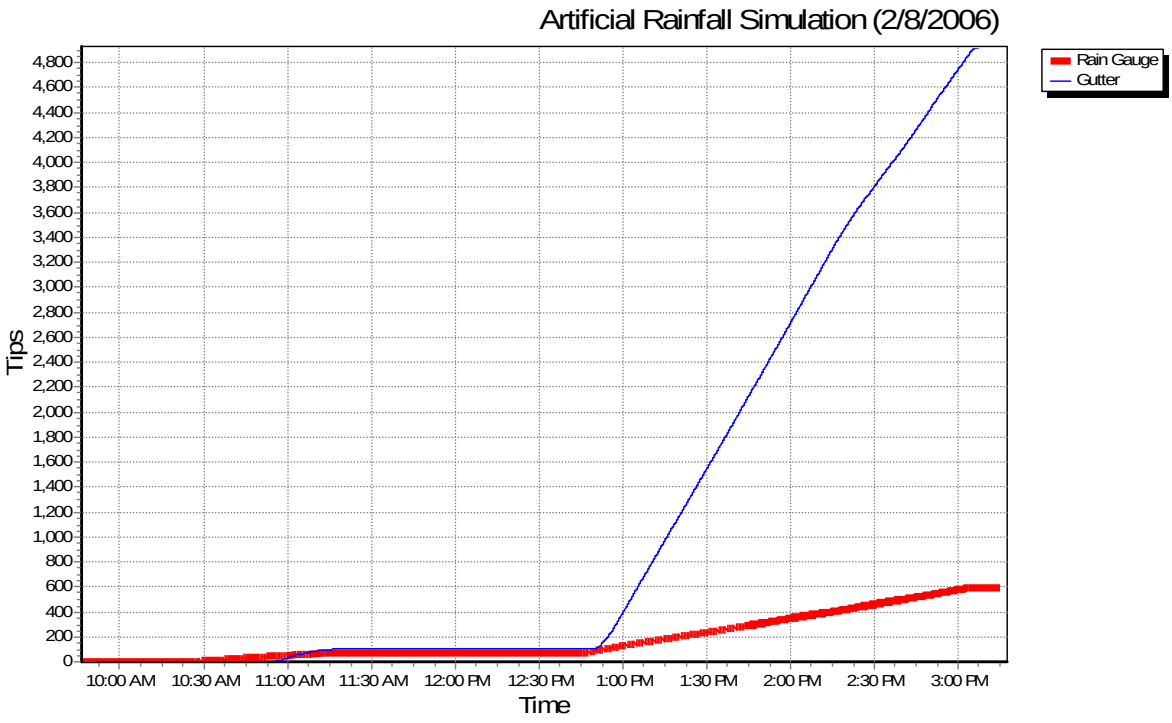

Figure 40: Rainfall Simulation Two—February 8, 2006

Chloride Tracer Experiment

A chloride tracer was added to the artificial rain during the third event of the Jan. 30 simulation to determine how quickly water moves through the system. Results are shown in Table 3. Samples P1-P5 were collected directly from simulator spray at the hillslope surface to compare to chloride concentrations in the runoff. The runoff samples, R0-R20, were collected at 5 minute intervals after the runoff tipping buckets began tipping. The first sample, R0, yielded a relatively small chloride value of 33 mg/L, although approx. 7 mg/L is an average background value. The second sample taken, R1, yielded a chloride concentration of 243 mg/L. Samples

R2-R20 generally exhibited a chloride concentration comparable to those in the precipitation samples (e.g. P1-P5), with the exception of a couple of outliers that exhibited very high concentrations. The rapidity of the rapid flow network (macropores and rills) was

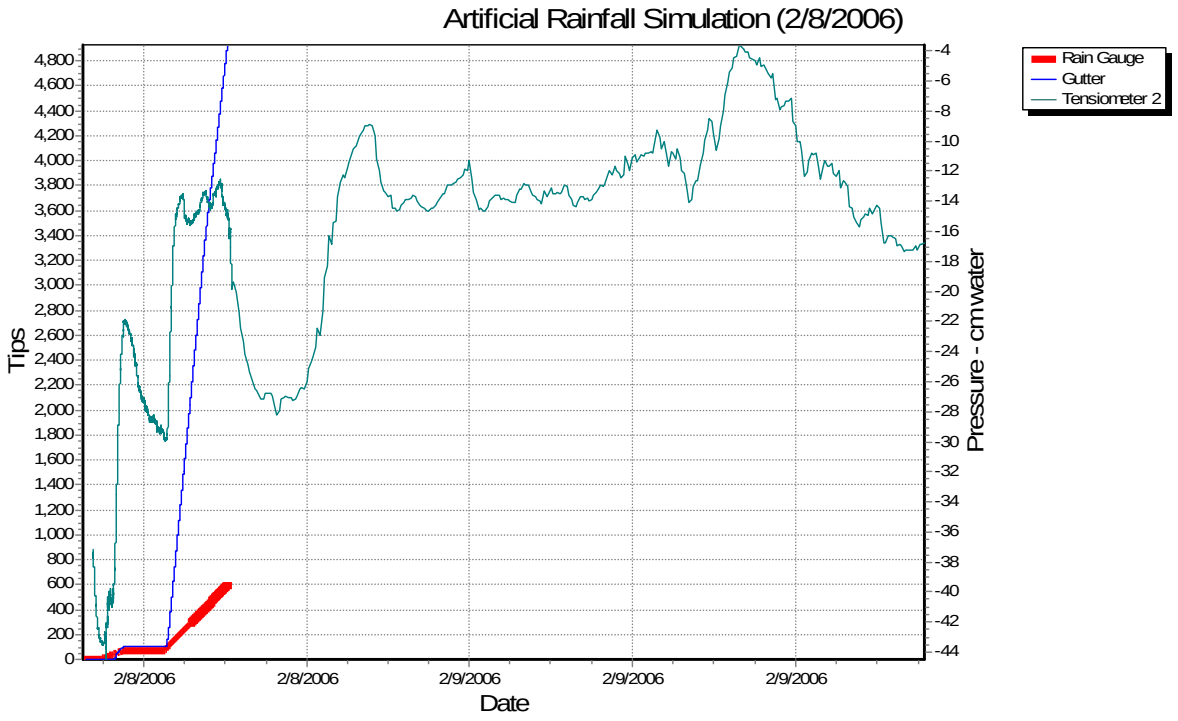

Figure 41: Rainfall Simulation Two tensiometer response

demonstrated as the chloride tracer traveled through the system or across the surface in minutes. Conducting the tracer test during the third event was a mistake. The hillslope had already been wetted beyond natural conditions during the calibration of the simulator and the first two events of the simulation and therefore the tracer spray simply ran over the surface. The experiment did show that saturation overland flow conditions can be achieved when the hillslope displays near-saturation conditions. However, the amount of rainfall needed to reach near-saturation was far beyond any precipitation event recorded over the year.

Samples R21-R26 were collected during the Feb. 8 simulation to determine whether natural rainfall events had pushed out all of the chloride tracer during the interim period between

the two simulations. The runoff averaged a concentration of 50 mg/L, which is slightly higher than background levels, but considerably less than the concentration that was applied to the hillslope. Future tracer experiments would benefit from applying the tracer before the hillslope receives any spray. Calibration could be carried out without wetting the hillslope by covering the study plot with a water-proof tarp.

Table 3: Chloride Tracer Test Results

Date	Sample	Chloride Concentration (mg/L)
1/30/2006	P1	296
1/30/2006	P2	324
1/30/2006	P3	321
1/30/2006	P4	331
1/30/2006	P5	298
1/30/2006	R0	33
1/30/2006	R1	243
1/30/2006	R2	324
1/30/2006	R3	282
1/30/2006	R4	290
1/30/2006	R5	806
1/30/2006	R6	322
1/30/2006	R7	322
1/30/2006	R8	436
1/30/2006	R9	337
1/30/2006	R10	298
1/30/2006	R11	304
1/30/2006	R12	288
1/30/2006	R13	352
1/30/2006	R14	304
1/30/2006	R15	336
1/30/2006	R16	326
1/30/2006	R17	380
1/30/2006	R18	356
1/30/2006	R19	441
1/30/2006	R20	274
2/8/2006	R21	70
2/8/2006	R22	72
2/8/2006	R23	38
2/8/2006	R24	26
2/8/2006	R25	56
2/8/2006	R26	39

CONCLUSIONS

Traditional explanations of storm runoff hold that runoff commonly occurs over the entire watershed as rainfall rate exceeds the infiltration rate and quickly flows over land. Small storm events, where rainfall does not exceed the infiltration capacity of soils, can be described by the variable source area concept. However, stable isotopic analysis of larger storm events has shown that stream discharge is primarly pre-event, or old water (Pearce *et al*., 1986a, 1986b; Kirchner, 2003). The seemingly counter-intuitive relationship between the rapid movement of runoff and the old water dominance of stream discharge has long raised questions regarding the mechanism that rapidly mobilizes catchment water.

The rainfall and gutter runoff experiments, conducted on a hillslope at the J. Phil Campbell, Jr., Natural Resource Conservation Center in Watkinsville, GA, demonstrate a kinematic process that delivers stormflow into rapid flowpaths. Deuterium analysis of rainfall, soil water, and gutter flow confirmed old water dominance of stormflow from the catchment. Tipping bucket rain gauge data, of rainfall and gutter flow, demonstrated a rapid mobilization of the old water in the subsurface. Once the soil water conditions were moist, the gutter flow began within minutes of the onset of rainfall. If the process had been traditional overland flow, there would have been a longer time gap between rainfall and gutter response in order to exceed the infiltration capacity of the hillslope. Once flow was initiated in the gutters, both gutters responded similarly to each other and to the rainfall.

The subsurface gutters simulate the ephemeral, rapid flow network that exists on hillslopes, via macropores and rills. The network is a dynamic one that becomes more connected as the hillslope is "primed." After the network becomes well-connected rainfall at the surface causes water to be ejected into the rapid flow paths. The "turning off" of gutter flow demonstrates the kinematic mechanism that pushes water from the soil matrix into the rapid pathways that the gutters represent. With the cessation of rainfall, the gutters abruptly stop, typically within minutes. Had the mechanism been Darcian in nature, the gutter flow would have tailed off like a storm hydrograph recession curve. Instead, gutter flow began and ended abruptly with the initiation and cessation of rainfall, signifying a kinematic delivery. The pressure waves are propagated through the subsurface from the soil pressures changes that are created by the perturbation of falling rain infiltrating the system once the system is wet enough to conduct the waves.

Rainfall intensity was shown to push more flow through the system by increasing the number of rain drops that infiltrated the surface. It is likely that with increased intensity, there are more pressure waves operating that increase gutter flow rate and volume.

The rainfall simulation experiments produced similar gutter responses under artificial conditions. The micro-tensiometers measured rapid fluctuations in matric potential upslope of the gutter trenches that occurred and ceased with the artificial rainfall intervals and the periods of induced gutter flow. The micro-tensiometer data is similar to that of Baldwin's laboratory results.

The pressure wave mechanism has been demonstrated in the field in this study. Future work should be directed towards understanding the ephemeral network that is fed by this mechanism.

REFERENCES

Ammozegar, A., 1989. A compact constant head permeameter for measuring saturated hydraulic conductivity of the vadose zone. *Soil Science Society of America Journal*, 5:1356-1351.

Baldwin, R.H., 1997. *Water and tracer behavior in undisturbed saprolite soil cores*. Unpublished MS Thesis, University of Georgia; 106pp.

Beldring, S., S. Gottschalk, A. Rodhe, and L.M. Tallaksen, 2000. Kinematic wave approximations to hillslope hydrological processes. *Hydrological Processes*, 14:727-745.

Beven, K.F. and P. Germann, 1982. Macropores and water flow in soils. *Water Resources Research*, 17(5): 1311-1325.

Bruce, R.R., J.H. Dane, V.L. Quisenberry, N.L. Powell, and A.W. Thomas, 1983. Physical characterization of soils in the southern region: Cecil. Southern Coop. Series Bull. No. 267. University of Georgia, Athens, GA.

Buttle, J.M., 1998. Fundamentals of small catchment hydrology: in *Isotope Tracers In Catchment Hydrology*, C. Kendall and J.J. McDonnell editors, Amsterdam: Elsevier Science B.V., p. 1-49.

Buttle, J.M., 1994. Isotope hydrograph separations and rapid delivery of pre-event water from drainage basins. *Progress In Physical Geography*, 18: 16-41.

Clark, I. and P. Fritz, 1997. *Environmental Isotopes In Hydrogeology*. New York: Lewis Publishers.

Dowd, J.F. and A.G. Williams, 1989. Calibration and use of pressure transducer in soil hydrology. *Hydrological Processes*, 3(1): 43-49.

Dowd, J., A. Williams, and R. McKinnon, 2005. Holne Moor Watershed, Dartmoor, U. K. Conference proceedings. Portland, Oregon.

Dowd, J.F., A.G. Williams, E.W. Meyles, D. Scholefield, L. Deeks, and M. Leng, 2006. Kinematic stormflow generation and network development: Case studies from contrasting areas. Unpublished manuscript.

Dunne, T. and R.D. Black, 1970a. An experimental investigation of runoff production in permeable soils. *Water Resources Research*, 6(2): 478-490.

Dunne, T. and R.D. Black, 1970b. Partial area contributions to storm runoff in a small New England watershed. *Water Resources Research*, 6(5): 1296-1311.

Dunne and Leopold, 1978. *Water In Environmental Planning*. W.H. Freeman and Company, San Francisco, Calif. 818p.

Endale, D., M. Cabrera, J. Steiner, D. Radcliffe, W. Vencill, H. Schomberg, L. Lohr, 2002. Impact of conservation tillage and nutrient management on soil water and yield of cotton fertilized with poultry litter and or ammonium nitrate in the Georgia Piedmont. *Soil and Tillage Research*, 66: 55-68.

Fetter, C.W., 2001. *Applied Hydrogeology*. New Jersey: Prentice Hall.

Gaskin, J.W., J.F. Dowd, and W.L. Nutter, 1989. Vertical and lateral components of soil nutrient flux in a hillslope. *Journal of Environmental Quality* 18(4): 403-410.

Genereux D.P. and R.P. Hooper, 1998. Oxygen and hydrogen isotopes in rainfall-runoff studies. In *Isotope Tracers in Catchment Hydrology*, Kendall C. and J.J. McDonnell (eds). Amsterdam: Elsevier, pp. 319-343.

Hewlett, J.D. and A.R. Hibbert, 1967. Factors affecting the response of small watersheds to precipitation in humid areas. In Sopper, W.E. and H.W. Lull (eds.), *Forest Hydrology*. New York: Pergamon Press. pp. 275-290.

Horton, R.E., 1933. The role of infiltration in the hydrologic cycle. *Transactions of the American Geophysical Union*, 14: 446-460.

Hursh, C.R., 1944. Report of subcommittee on subsurface flow. *Transactions of the American Geophysical Union*, Part V, pp. 745-746.

Ingraham, N.L., 1998. Isotopic variations in precipitation. In *Isotope Tracers in Catchment Hydrology*, Kendall C. and J.J. McDonnell (eds). Amsterdam: Elsevier, pp. 87-115.

Jones, J.A.A., 1971. Soil piping and stream channel initiation. *Water Resources Research*, 7:602-610.

Kirchner, J.W., 2003. A double paradox in catchment hydrology. *Hydrologic Processes*, 17: 871-874.

Kubota, T., and Y. Tsuboyama, 2002. Intra- and inter-storm oxygen-18 and deuterium variations of rain, throughfall, and stemflow, and two-component hydrograph separation in a small forested catchment in Japan. *Journal of Forest Resources,* 8: 179-190.

Meyles, E., A. Williams, L. Ternan, and J. Dowd, 2003. Runoff generation in relation to soil moisture patterns in a small Dartmoor catchment, Southwest England. *Hydrological Processes*, 17: 251-264.

McDonnell, J.J., 1990. A rationale for old water discharge through macropores in a steep, humid catchment. *Water Resources Research*, 26(11): 2821-2832.

Nutter, W.L., 1973. The role of soil water in the hydrologic behavior of upland basins. In *Field Soil Moisture Regime*. Soil Science Society of America. Madison, WI. (Monograph Series). pp. 181-193.

Pearce, A.J., M.K. Stewart, and M.G. Sklash, 1986a. Storm runoff generation in humid headwater catchments: 1. Where does the water come from? *Water Resources Research*, 22(8): 1263-1272.

Pearce, A.J., M.K. Stewart, and M.G. Sklash, 1986b. Storm runoff generation in humid headwater catchments: 2. A case study of hillslope and low-order stream response. *Water Resources Research*, 22(8): 1273-1282.

Perkins, H.F., 1987. Characterization data for selected Georgia soils. Georgia Agric. Exp. Stn. University of Georgia, Athens, GA.

Pionke, H.B. and DeWalle, D.R., 1992. Intra- and inter-storm 18-O trends for selected rainstorms in Pennsylvania. *Journal of Hydrology*, 138: 131-143.

Polluted! EPA-841-F-94-005. United States Environmental Protection Agency brochure, 1994.

Radcliffe, D. *Soil Physics*. Class lecture notes packet. University of Georgia, 2005.

Railsback L.B., P.A. Bouker, T.P. Feeney, E.A. Goddard, A.S. Hall, B.P. Jackson, A.A. McClain, M.C. Orsega, M.A. Rafter, and J.W. Webster, 1996. A survey of the major-element geochemistry of Georgia groundwater. *Southeastern Geology*, 36(3): 99-122.

Rasmussen, T., R.H. Baldwin, J. Dowd, and A. Williams, 2000. Tracer vs. pressure wave velocities *through* unsaturated saprolite. *Soil Science Society of America Journal*, 64(1): 75-85.

Shanley, J., C. Kendell, T. Smith, D. Wolock, and J. McDonnell, 2002. Controls on old and new water contributions to stream flow at some nested catchments in Vermont, USA. *Hydrologic Processes*, 16: 589-609.

Sklash, M.G. and R.N. Farvolden, 1979. The role of groundwater in storm runoff. *Journal of Hydrology*, 43: 45-65.

Torres, R., 2002. A threshold condition for soil-water transport. *Hydrological Processes*, 16: 2703-2706.

Torres, R., and L. Alexander, 2002. Intensity-duration effects on drainage: Column experiments at near-zero pressure head. *Water Resources Research*, 38(11): 221-225.

Torres, R., W.E. Dietrich, D.R. Montgomery, S. P. Anderson, K. Loague, 1998. Unsaturated zone processes and the hydrologic response of a steep, unchanneled catchment. *Water Resources Research*, 34(8): 1865-1879.

Williams, A., J. Dowd, and E. Meyles, 2002. A new interpretation of kinematic stormflow generation. *Hydrological Processes*, 16: 2791-2803.

APPENDIX A: HOLNE MOOR, DARTMOOR, UK

The Holne Moor research watershed, as described by Dowd *et al*. (2005), is a valley with steep slopes located 8 km east of Princetown, southwest England (Figure). The watershed (Figure 42) is approximately 0.7 km^2 in area. Altitude ranges 290 to 450 m above mean sea level. The study area climate is typical of southwestern England; temperatures are moderate and there is high annual rainfall (2104 mm yr^{-1}). "Well drained humose podzolic soil are found on the slopes and poorly drained peat soils are situated on the plateau. The soils in the valley floor area tend to be gleyed and are typified by lateral seepage from the slopes" (Dowd *et al*., 2005). The bedrock underlying the catchment is Dartmoor granite. Vegetation in the catchment is comprised of heath species and bracken, found on the steep slopes, and grasses, found on the poorly-drained soils on the valley floor and plateau.

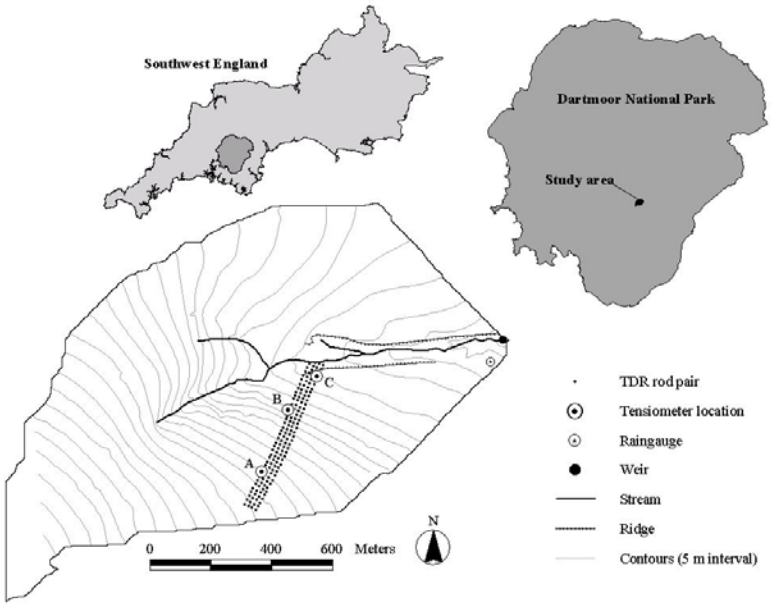

Figure 42: Holne Moor, Dartmoor National Park, UK

APPENDIX B: PRECIPITATION AT UGA HORTICULTURE FARM, WATKINSVILLE, GA

Date	Max. Temp. (°F)	Min. Temp. (°F)	Rain (in)
Jan 1, 2005	69.4	39.7	0.00
Jan 2, 2005	68.4	39.7	0.00
Jan 3, 2005	68.4	42.8	0.00
Jan 4, 2005	72.3	45.5	0.00
Jan 5, 2005	69.3	47.1	0.00
Jan 6, 2005	65.7	49.8	0.18
Jan 7, 2005	65.5	45.9	0.00
Jan 8, 2005	71.2	47.8	0.00
Jan 9, 2005	66.0	35.2	0.00
Jan 10, 2005	67.1	37.9	0.00
Jan 11, 2005	68.0	46.0	0.00
Jan 12, 2005	65.5	49.1	0.02
Jan 13, 2005	67.5	53.1	2.11
Jan 14, 2005	60.6	38.7	0.08
Jan 15, 2005	51.1	32.9	0.00
Jan 16, 2005	56.8	28.9	0.00
Jan 17, 2005	41.7	21.7	0.00
Jan 18, 2005	40.1	16.2	0.00
Jan 19, 2005	42.1	16.9	0.00
Jan 20, 2005	59.0	30.0	0.00
Jan 21, 2005	68.2	39.6	0.00
Jan 22, 2005	41.9	27.3	0.02
Jan 23, 2005	35.1	19.6	0.00
Jan 24, 2005	49.6	12.9	0.00
Jan 25, 2005	59.9	31.6	0.00
Jan 26, 2005	68.9	45.3	0.00
Jan 27, 2005	54.0	36.0	0.00
Jan 28, 2005	39.9	30.4	0.00
Jan 29, 2005	31.5	25.7	0.00
Jan 30, 2005	44.6	29.1	1.13
Jan 31, 2005	48.6	31.1	0.00
Feb 1, 2005	47.1	37.8	0.02
Feb 2, 2005	42.1	33.4	0.57
Feb 3, 2005	44.1	29.5	0.78
Feb 4, 2005	61.0	26.4	0.01

Feb 5, 2005	62.4	27.9	0.00
Feb 6, 2005	61.9	30.0	0.00
Feb 7, 2005	63.5	37.9	0.00
Feb 8, 2005	64.0	42.1	0.08
Feb 9, 2005	59.7	52.3	0.95
Feb 10, 2005	53.1	29.3	0.00
Feb 11, 2005	53.4	25.5	0.00
Feb 12, 2005	61.9	31.8	0.00
Feb 13, 2005	56.3	39.7	0.00
Feb 14, 2005	50.2	44.6	0.48
Feb 15, 2005	57.0	47.8	0.00
Feb 16, 2005	70.9	49.6	0.00
Feb 17, 2005	55.2	36.1	0.00
Feb 18, 2005	55.6	29.8	0.00
Feb 19, 2005	60.3	33.3	0.00
Feb 20, 2005	52.5	39.9	0.27
Feb 21, 2005	63.0	45.0	1.65
Feb 22, 2005	75.2	49.3	0.01
Feb 23, 2005	72.1	41.4	0.37
Feb 24, 2005	53.6	47.5	0.32
Feb 25, 2005	58.8	39.2	0.00
Feb 26, 2005	58.8	29.8	0.00
Feb 27, 2005	48.4	39.7	0.39
Feb 28, 2005	48.9	37.2	0.19
Mar 1, 2005	43.0	28.4	0.00
Mar 2, 2005	49.6	25.5	0.00
Mar 3, 2005	56.3	30.4	0.00
Mar 4, 2005	62.1	29.7	0.00
Mar 5, 2005	67.5	40.3	0.00
Mar 6, 2005	63.5	31.5	0.00
Mar 7, 2005	70.5	35.6	0.78
Mar 8, 2005	55.2	34.2	0.15
Mar 9, 2005	49.5	28.0	0.00
Mar 10, 2005	55.0	32.9	0.00
Mar 11, 2005	60.8	38.1	0.00
Mar 12, 2005	75.2	37.0	0.00
Mar 13, 2005	77.4	52.0	0.04
Mar 14, 2005	64.4	43.2	0.13
Mar 15, 2005	59.5	40.1	0.00
Mar 16, 2005	50.5	38.7	0.74
Mar 17, 2005	39.6	36.3	0.04

Mar 18, 2005	58.1	30.4	0.00
Mar 19, 2005	60.6	29.5	0.00
Mar 20, 2005	68.0	37.9	0.00
Mar 21, 2005	63.3	46.4	0.07
Mar 22, 2005	55.6	46.8	0.74
Mar 23, 2005	70.7	46.9	0.25
Mar 24, 2005	71.1	44.2	0.00
Mar 25, 2005	80.1	42.8	0.00
Mar 26, 2005	79.0	48.6	0.00
Mar 27, 2005	62.2	55.4	2.45
Mar 28, 2005	63.3	45.9	0.09
Mar 29, 2005	78.1	46.0	0.00
Mar 30, 2005	80.2	42.4	0.00
Mar 31, 2005	65.1	56.3	2.05
Apr 1, 2005	63.3	54.0	0.27
Apr 2, 2005	60.4	41.4	0.15
Apr 3, 2005	68.5	42.6	0.00
Apr 4, 2005	77.4	45.0	0.00
Apr 5, 2005	80.2	47.1	0.00
Apr 6, 2005	75.6	48.7	0.00
Apr 7, 2005	70.0	56.3	2.19
Apr 8, 2005	69.8	55.8	0.51
Apr 9, 2005	73.6	55.2	0.00
Apr 10, 2005	79.3	47.7	0.00
Apr 11, 2005	77.9	51.3	0.00
Apr 12, 2005	76.5	58.1	0.44
Apr 13, 2005	68.9	46.8	0.56
Apr 14, 2005	67.1	44.4	0.00
Apr 15, 2005	72.1	38.8	0.00
Apr 16, 2005	69.3	42.8	0.00
Apr 17, 2005	75.4	35.2	0.00
Apr 18, 2005	82.4	45.0	0.00
Apr 19, 2005	81.9	46.2	0.00
Apr 20, 2005	80.2	49.1	0.00
Apr 21, 2005	82.0	49.8	0.00
Apr 22, 2005	79.5	56.3	0.56
Apr 23, 2005	61.9	46.0	0.01
Apr 24, 2005	57.0	34.7	0.00
Apr 25, 2005	67.8	36.3	0.00
Apr 26, 2005	56.7	47.1	0.42
Apr 27, 2005	68.2	44.6	0.00

Apr 28, 2005	73.2	38.8	0.01
Apr 29, 2005	78.4	57.0	0.00
Apr 30, 2005	65.8	57.4	1.15
May 1, 2005	72.0	46.8	0.03
May 2, 2005	71.1	41.4	0.00
May 3, 2005	68.9	43.7	0.00
May 4, 2005	73.8	40.6	0.00
May 5, 2005	63.1	50.7	0.00
May 6, 2005	76.3	45.3	0.00
May 7, 2005	78.6	46.4	0.00
May 8, 2005	84.6	50.4	0.00
May 9, 2005	85.3	56.3	0.00
May 10, 2005	81.7	59.7	0.00
May 11, 2005	83.5	52.7	0.00
May 12, 2005	87.4	54.7	0.00
May 13, 2005	86.4	57.0	0.00
May 14, 2005	82.2	57.0	0.47
May 15, 2005	72.0	60.4	0.12
May 16, 2005	78.4	50.4	0.00
May 17, 2005	82.9	51.1	0.00
May 18, 2005	81.3	60.6	0.00
May 19, 2005	84.4	60.4	0.00
May 20, 2005	80.8	61.0	0.31
May 21, 2005	75.2	58.1	0.00
May 22, 2005	79.5	57.2	0.00
May 23, 2005	86.4	64.6	0.00
May 24, 2005	81.7	56.7	0.00
May 25, 2005	75.2	45.9	0.00
May 26, 2005	81.7	48.4	0.00
May 27, 2005	85.6	54.5	0.00
May 28, 2005	82.6	56.8	0.00
May 29, 2005	75.6	50.9	0.42
May 30, 2005	64.9	57.6	0.65
May 31, 2005	72.3	59.7	0.28
Jun 1, 2005	64.6	58.8	1.87
Jun 2, 2005	66.4	59.2	0.67
Jun 3, 2005	70.3	61.0	0.02
Jun 4, 2005	83.7	64.6	0.00
Jun 5, 2005	89.2	65.8	0.00
Jun 6, 2005	91.4	65.8	0.00
Jun 7, 2005	89.2	62.6	0.12

Jun 8, 2005	88.0	68.7	0.02
Jun 9, 2005	87.8	66.7	0.01
Jun 10, 2005	85.3	69.8	0.00
Jun 11, 2005	80.2	70.0	0.08
Jun 12, 2005	83.3	71.2	1.40
Jun 13, 2005	89.2	72.1	0.51
Jun 14, 2005	92.3	69.3	0.00
Jun 15, 2005	91.6	71.1	0.00
Jun 16, 2005	88.2	64.9	0.00
Jun 17, 2005	84.6	63.9	0.00
Jun 18, 2005	85.5	61.0	1.44
Jun 19, 2005	81.9	61.0	0.01
Jun 20, 2005	81.3	60.1	0.51
Jun 21, 2005	84.2	59.0	1.88
Jun 22, 2005	87.4	61.5	0.00
Jun 23, 2005	88.9	63.7	0.00
Jun 24, 2005	88.2	64.9	0.00
Jun 25, 2005	84.6	64.8	0.07
Jun 26, 2005	78.6	64.9	0.43
Jun 27, 2005	88.7	71.2	0.49
Jun 28, 2005	82.2	70.3	0.03
Jun 29, 2005	85.8	70.7	0.00
Jun 30, 2005	91.0	69.1	0.02
Jul 1, 2005	92.8	69.8	0.28
Jul 2, 2005	92.1	68.2	0.00
Jul 3, 2005	85.3	70.5	0.14
Jul 4, 2005	83.8	69.4	0.26
Jul 5, 2005	89.6	67.6	0.00
Jul 6, 2005	85.1	68.4	0.11
Jul 7, 2005	77.2	66.7	3.60
Jul 8, 2005	87.4	63.3	0.00
Jul 9, 2005	89.2	65.5	0.07
Jul 10, 2005	80.6	68.9	0.73
Jul 11, 2005	86.7	73.9	0.30
Jul 12, 2005	88.0	70.2	0.00
Jul 13, 2005	86.5	68.0	0.05
Jul 14, 2005	86.7	70.2	0.00
Jul 15, 2005	86.2	70.2	0.51
Jul 16, 2005	86.4	70.2	0.01
Jul 17, 2005	89.2	71.8	0.00
Jul 18, 2005	93.0	71.6	0.00

Jul 19, 2005	90.7	70.7	0.00
Jul 20, 2005	92.8	71.2	0.00
Jul 21, 2005	94.5	72.0	0.00
Jul 22, 2005	94.5	72.9	0.00
Jul 23, 2005	93.0	70.9	0.00
Jul 24, 2005	91.8	71.6	0.00
Jul 25, 2005	94.3	72.3	0.00
Jul 26, 2005	98.2	73.8	0.00
Jul 27, 2005	95.9	75.6	0.00
Jul 28, 2005	94.6	72.0	0.05
Jul 29, 2005	78.1	70.3	0.59
Jul 30, 2005	79.9	69.8	1.05
Jul 31, 2005	84.6	70.5	0.03
Aug 1, 2005	83.5	70.0	0.18
Aug 2, 2005	88.0	67.5	0.00
Aug 3, 2005	91.0	66.9	0.00
Aug 4, 2005	93.0	69.3	0.17
Aug 5, 2005	91.0	68.7	0.00
Aug 6, 2005	90.5	67.1	0.26
Aug 7, 2005	79.5	70.2	0.98
Aug 8, 2005	83.5	70.0	0.35
Aug 9, 2005	85.5	70.7	0.00
Aug 10, 2005	86.5	71.2	0.14
Aug 11, 2005	90.0	68.4	0.01
Aug 12, 2005	91.4	69.8	0.00
Aug 13, 2005	90.1	69.8	0.00
Aug 14, 2005	92.3	68.2	0.00
Aug 15, 2005	93.9	69.1	0.00
Aug 16, 2005	93.0	73.2	0.26
Aug 17, 2005	94.1	71.2	1.87
Aug 18, 2005	89.4	70.3	0.00
Aug 19, 2005	93.6	69.8	0.00
Aug 20, 2005	96.3	70.9	0.00
Aug 21, 2005	97.7	74.5	0.00
Aug 22, 2005	95.5	69.8	0.19
Aug 23, 2005	88.2	68.9	0.17
Aug 24, 2005	86.7	70.0	0.00
Aug 25, 2005	85.1	69.3	0.00
Aug 26, 2005	84.9	65.5	0.00
Aug 27, 2005	88.0	63.9	0.00
Aug 28, 2005	90.1	69.1	0.00

Aug 29, 2005	89.2	71.8	0.25
Aug 30, 2005	89.2	74.5	0.01
Aug 31, 2005	89.2	66.0	0.00
Sep 1, 2005	89.2	62.2	0.00
Sep 2, 2005	89.6	62.2	0.00
Sep 3, 2005	89.2	65.5	0.00
Sep 4, 2005	88.9	63.0	0.00
Sep 5, 2005	83.8	61.9	0.00
Sep 6, 2005	83.5	60.6	0.00
Sep 7, 2005	85.5	62.6	0.00
Sep 8, 2005	87.4	60.1	0.00
Sep 9, 2005	88.5	58.6	0.00
Sep 10, 2005	88.0	57.0	0.00
Sep 11, 2005	86.7	60.4	0.00
Sep 12, 2005	87.6	57.4	0.00
Sep 13, 2005	91.8	60.4	0.00
Sep 14, 2005	91.6	62.4	0.00
Sep 15, 2005	95.0	64.4	0.00
Sep 16, 2005	93.2	69.6	0.00
Sep 17, 2005	91.8	67.6	0.00
Sep 18, 2005	92.3	62.4	0.00
Sep 19, 2005	94.1	58.3	0.00
Sep 20, 2005	93.7	62.6	0.00
Sep 21, 2005	92.8	66.2	0.00
Sep 22, 2005	90.0	65.5	0.00
Sep 23, 2005	90.3	64.0	0.00
Sep 24, 2005	90.9	64.0	0.00
Sep 25, 2005	88.0	65.5	0.00
Sep 26, 2005	79.7	70.2	0.00
Sep 27, 2005	89.6	65.7	0.00
Sep 28, 2005	81.9	66.6	0.03
Sep 29, 2005	90.0	64.2	0.00
Sep 30, 2005	81.0	62.6	0.00
Oct 1, 2005	86.4	61.7	0.00
Oct 2, 2005	83.8	65.5	0.00
Oct 3, 2005	86.7	65.8	0.00
Oct 4, 2005	86.7	63.3	0.00
Oct 5, 2005	79.2	66.2	0.00
Oct 6, 2005	70.9	67.1	3.08
Oct 7, 2005	72.5	69.1	1.04
Oct 8, 2005	82.9	63.5	0.15

Oct 9, 2005	71.6	63.5	0.03
Oct 10, 2005	72.0	66.9	0.00
Oct 11, 2005	76.3	65.5	0.00
Oct 12, 2005	77.9	60.8	0.00
Oct 13, 2005	77.9	60.4	0.00
Oct 14, 2005	82.8	56.3	0.00
Oct 15, 2005	81.7	52.3	0.00
Oct 16, 2005	77.5	49.1	0.00
Oct 17, 2005	75.2	42.4	0.00
Oct 18, 2005	84.4	44.8	0.00
Oct 19, 2005	85.3	53.8	0.00
Oct 20, 2005	84.0	57.2	0.00
Oct 21, 2005	82.0	55.0	0.00
Oct 22, 2005	71.8	45.3	0.00
Oct 23, 2005	71.4	39.4	0.00
Oct 24, 2005	59.4	42.8	0.00
Oct 25, 2005	56.3	41.4	0.00
Oct 26, 2005	63.7	34.7	0.00
Oct 27, 2005	63.5	32.2	0.00
Oct 28, 2005	65.5	35.1	0.00
Oct 29, 2005	64.4	36.5	0.00
Oct 30, 2005	72.3	33.3	0.00
Oct 31, 2005	71.8	34.9	0.00
Nov 1, 2005	75.4	46.4	0.00
Nov 2, 2005	74.1	42.4	0.00
Nov 3, 2005	73.6	36.0	0.00
Nov 4, 2005	75.9	41.4	0.00
Nov 5, 2005	73.9	47.8	0.00
Nov 6, 2005	77.7	49.5	0.01
Nov 7, 2005	81.5	49.3	0.01
Nov 8, 2005	83.3	43.2	0.00
Nov 9, 2005	81.3	55.8	0.00
Nov 10, 2005	70.9	41.4	0.00
Nov 11, 2005	65.8	30.9	0.00
Nov 12, 2005	69.4	31.1	0.00
Nov 13, 2005	72.0	42.4	0.00
Nov 14, 2005	77.9	54.9	0.00
Nov 15, 2005	77.9	57.9	0.00
Nov 16, 2005	68.7	41.4	0.03
Nov 17, 2005	56.8	30.9	0.00
Nov 18, 2005	54.1	22.3	0.00

Nov 19, 2005	59.4	23.4	0.00
Nov 20, 2005	60.8	46.0	0.46
Nov 21, 2005	55.0	40.6	1.75
Nov 22, 2005	50.4	36.3	0.01
Nov 23, 2005	53.1	31.6	0.00
Nov 24, 2005	68.0	45.0	0.00
Nov 25, 2005	57.0	35.6	0.00
Nov 26, 2005	58.5	34.0	0.00
Nov 27, 2005	51.3	43.3	0.00
Nov 28, 2005	66.0	46.8	0.20
Nov 29, 2005	66.2	44.1	0.60
Nov 30, 2005	59.7	35.2	0.00
Dec 1, 2005	57.6	28.8	0.00
Dec 2, 2005	52.5	31.1	0.00
Dec 3, 2005	41.5	25.5	0.04
Dec 4, 2005	71.2	39.9	0.79
Dec 5, 2005	59.0	36.1	0.96
Dec 6, 2005	51.4	28.8	0.00
Dec 7, 2005	54.0	25.2	0.00
Dec 8, 2005	43.5	34.3	0.24
Dec 9, 2005	50.0	27.1	0.11
Dec 10, 2005	54.7	21.7	0.00
Dec 11, 2005	52.2	32.9	0.00
Dec 12, 2005	57.6	32.9	0.00
Dec 13, 2005	53.6	29.5	0.00
Dec 14, 2005	37.8	30.2	0.11
Dec 15, 2005	37.6	29.5	1.58
Dec 16, 2005	47.8	30.4	0.01
Dec 17, 2005	45.0	37.6	0.03
Dec 18, 2005	55.0	32.5	0.04
Dec 19, 2005	57.0	27.5	0.00
Dec 20, 2005	50.5	27.3	0.00
Dec 21, 2005	49.6	23.7	0.00
Dec 22, 2005	53.4	20.7	0.00
Dec 23, 2005	57.4	23.7	0.00
Dec 24, 2005	56.7	22.5	0.06
Dec 25, 2005	55.2	44.1	0.45
Dec 26, 2005	50.7	34.7	0.00
Dec 27, 2005	64.9	31.1	0.00
Dec 28, 2005	57.4	41.0	0.19
Dec 29, 2005	52.3	37.6	0.00

Dec 30, 2005	60.8	31.1	0.00
Dec 31, 2005	62.1	38.1	0.01
Jan 1, 2006	67.1	30.0	0.25
Jan 2, 2006	61.2	50.4	1.68
Jan 3, 2006	58.6	41.0	0.00
Jan 4, 2006	64.2	33.3	0.00
Jan 5, 2006	63.1	39.0	0.00
Jan 6, 2006	47.7	30.9	0.00
Jan 7, 2006	50.2	25.5	0.00
Jan 8, 2006	64.8	31.1	0.00
Jan 9, 2006	72.0	47.3	0.00
Jan 10, 2006	68.5	40.8	0.00
Jan 11, 2006	64.4	47.5	0.40
Jan 12, 2006	68.9	43.9	0.00
Jan 13, 2006	64.0	40.6	0.36
Jan 14, 2006	43.3	30.9	0.00
Jan 15, 2006	57.4	30.0	0.00

APPENDIX C: EVENT TIPPING BUCKET DATA

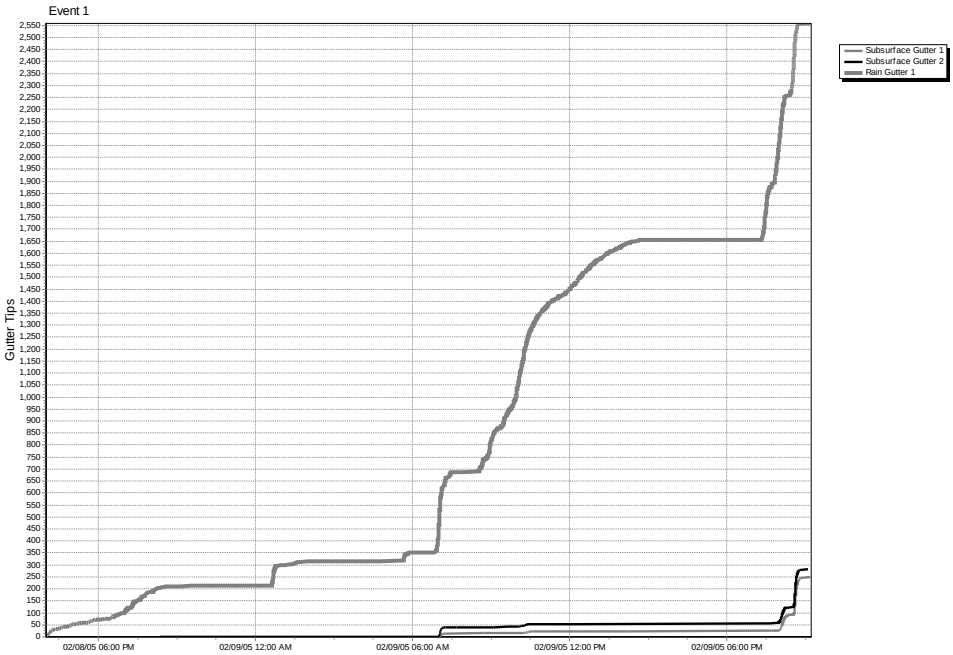

Figure 43: Rain Event 1 (Feb 2-9, 2005)

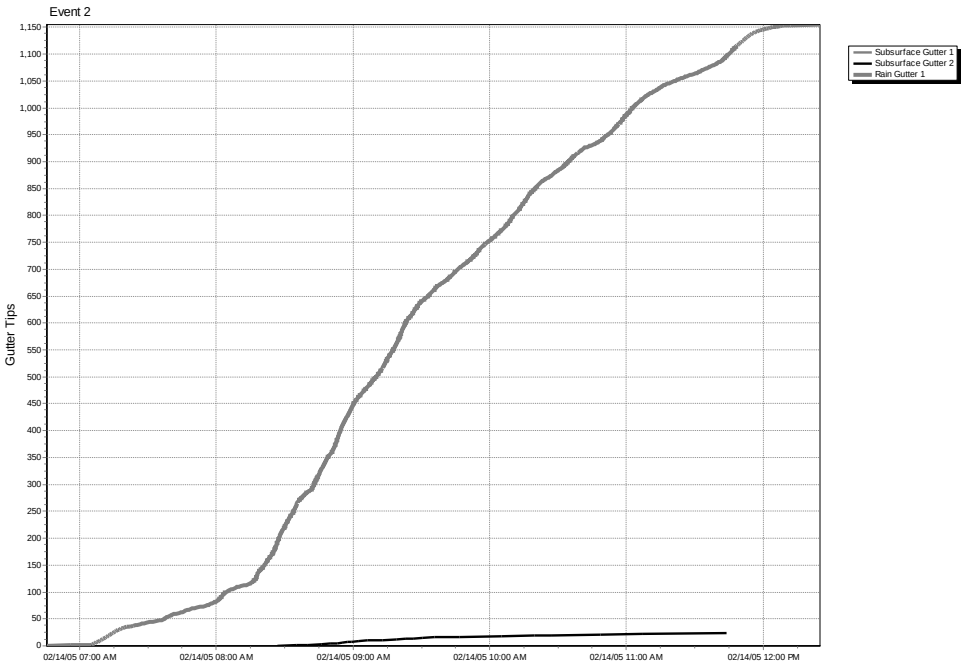

Figure 44: Rainfall Event 2 (Feb. 14, 2005)

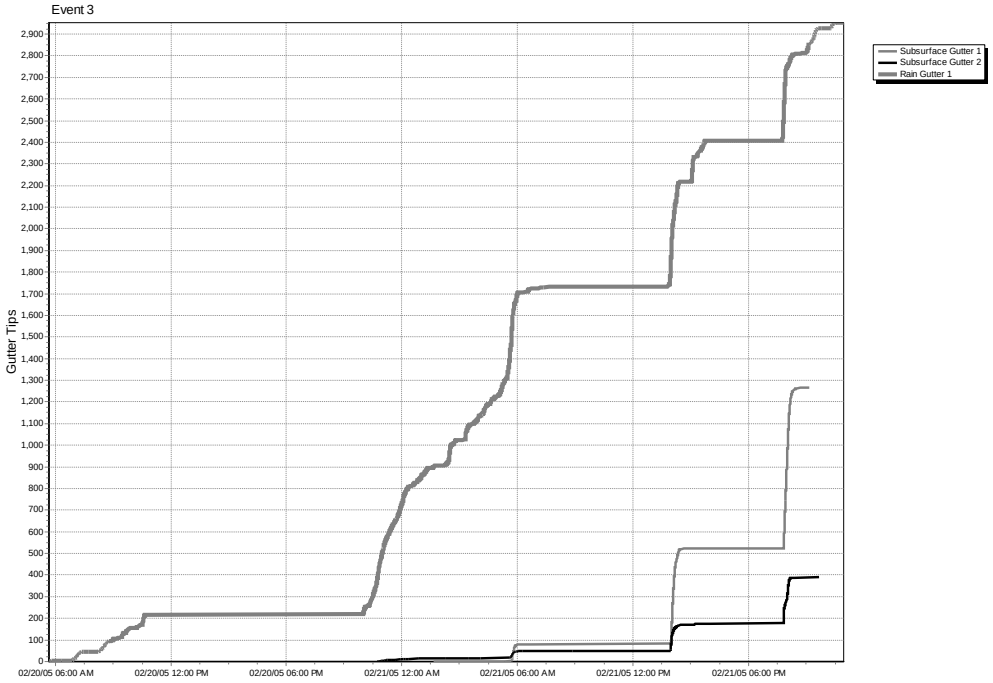

Figure 45: Rainfall Event 3 (Feb. 20-21, 2005)

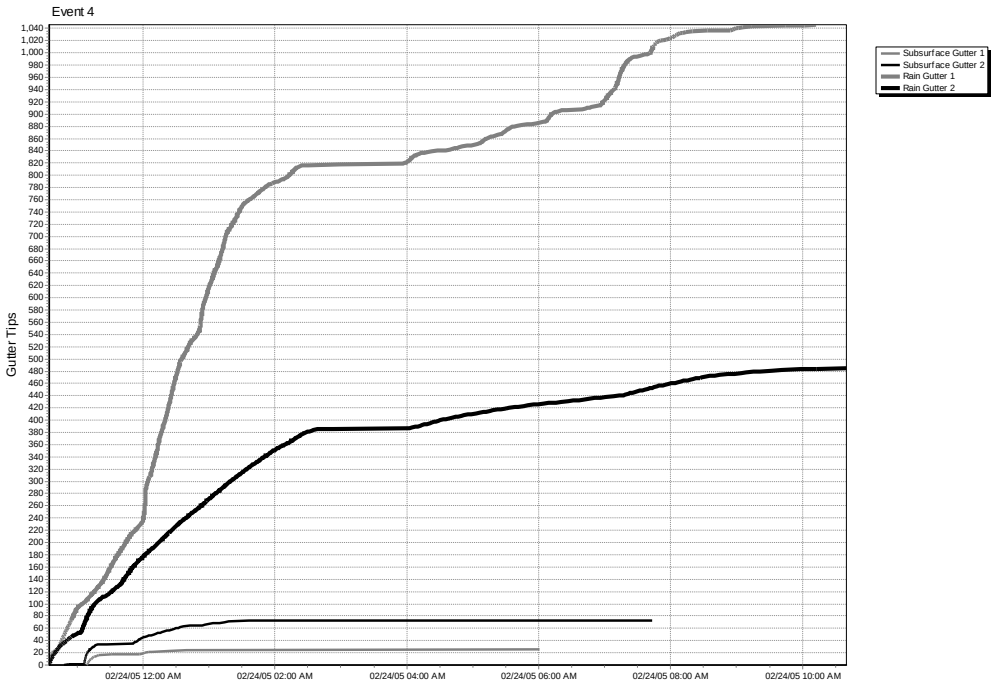

Figure 46: Rainfall Event 4 (Feb. 23-24, 2005)

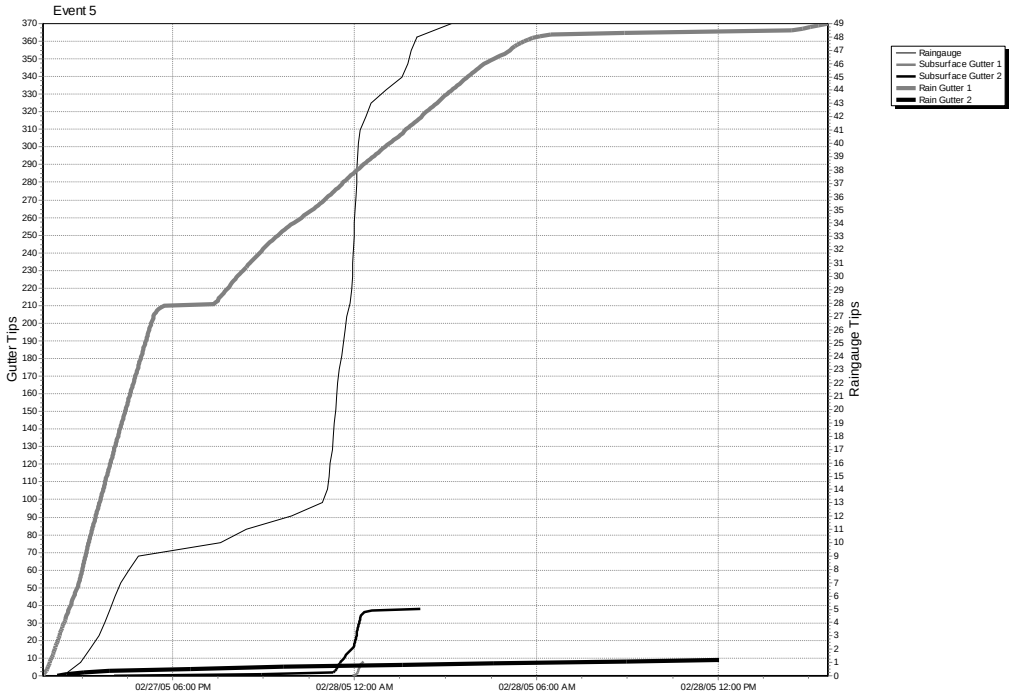

Figure 47: Rainfall Event 5 (Feb. 27-28, 2005)

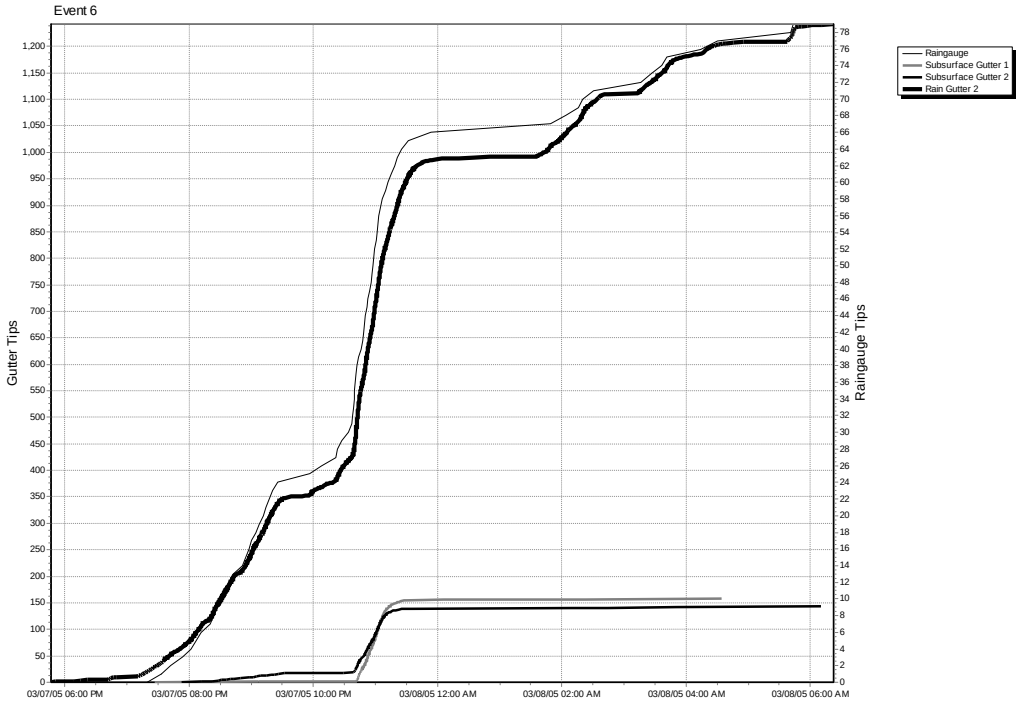

Figure 48: Rainfall Event 6 (Mar. 7-8, 2005)

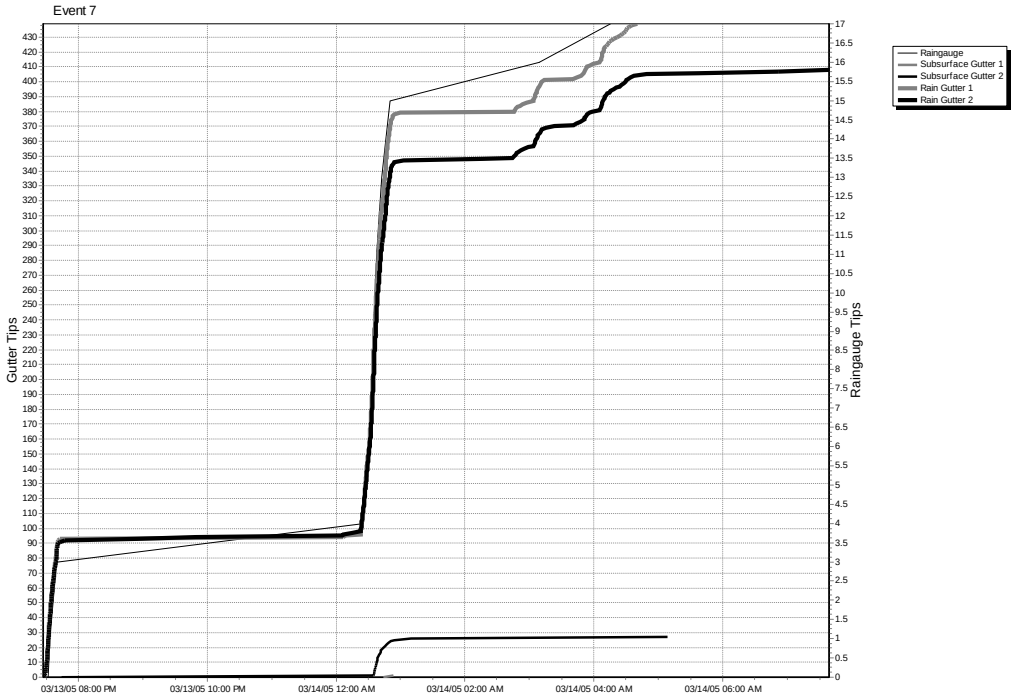

Figure 49: Rainfall Event 7 (Mar. 14, 2005)

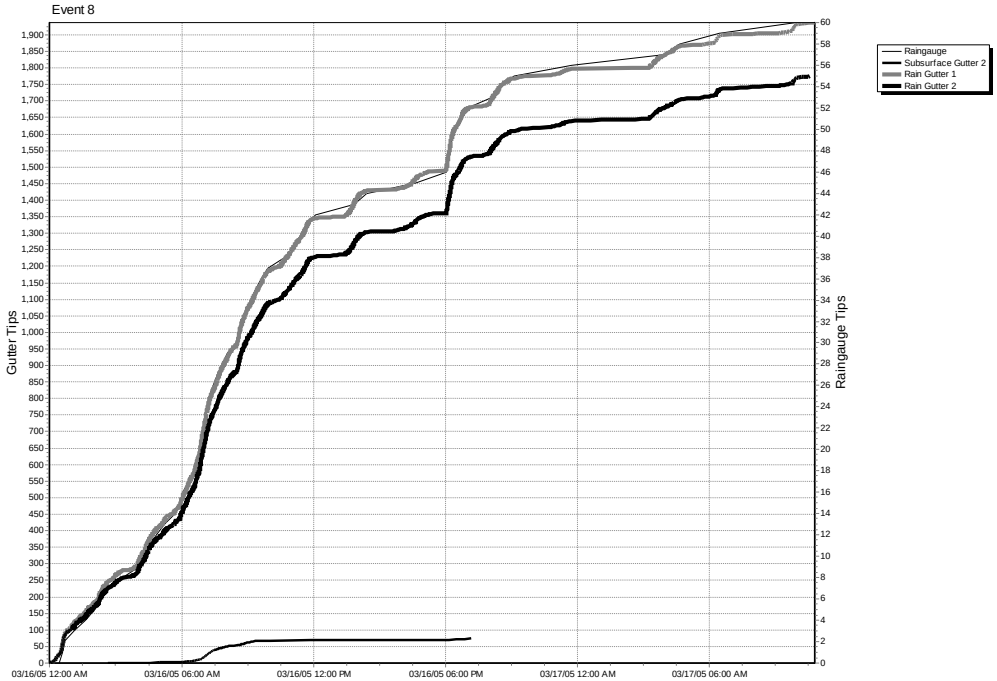

Figure 50: Rainfall Event 8 (Mar. 16-17, 2005)

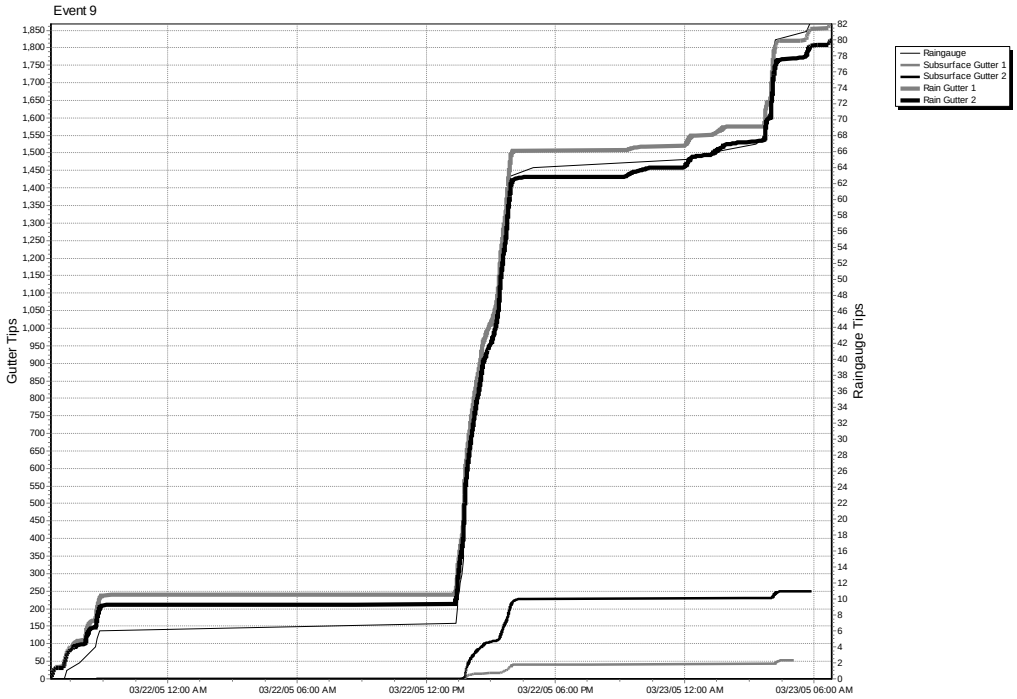

Figure 51: Rainfall Event 9 (Mar. 22-23, 2005)

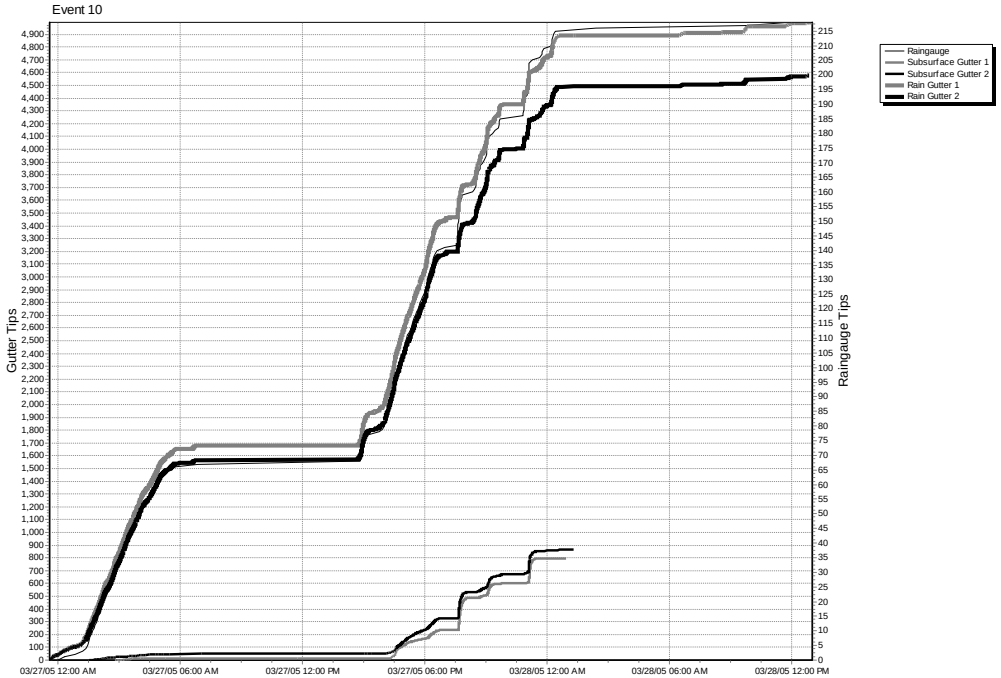

Figure 52: Rainfall 10 (Mar. 27-28, 2005)

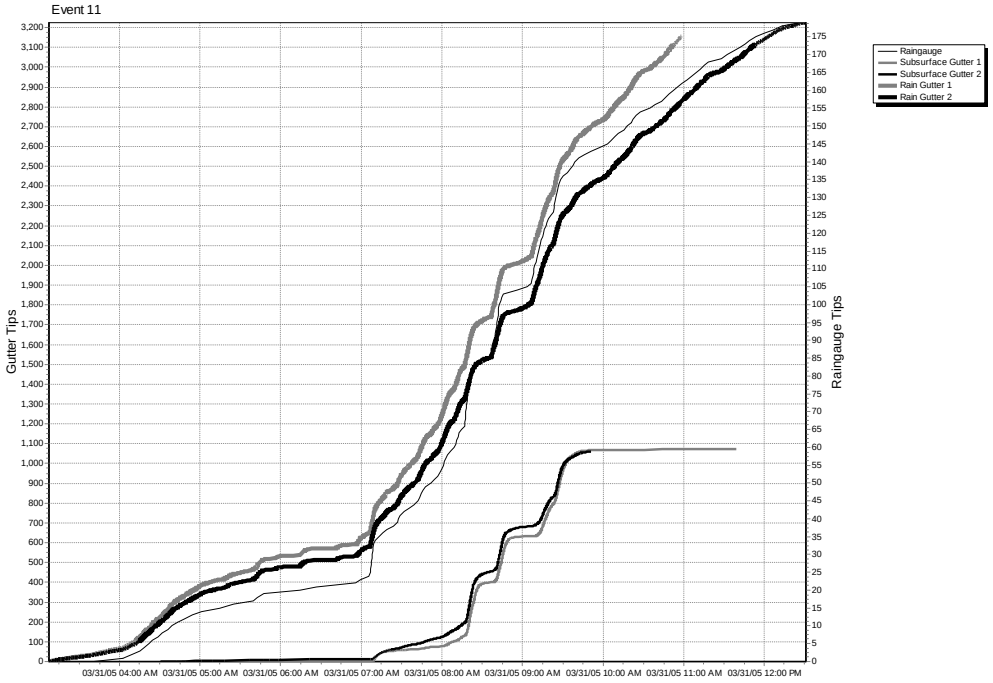

Figure 53: Rainfall Event 11 (Mar. 31, 2005)

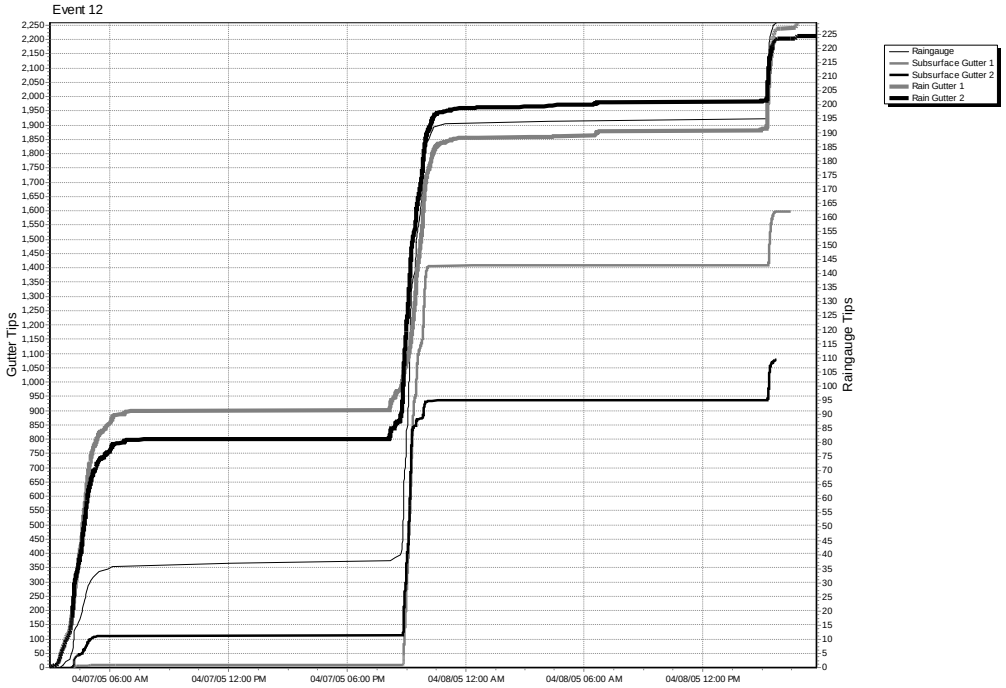

Figure 54: Rainfall Event 12 (April 7-8, 2005)

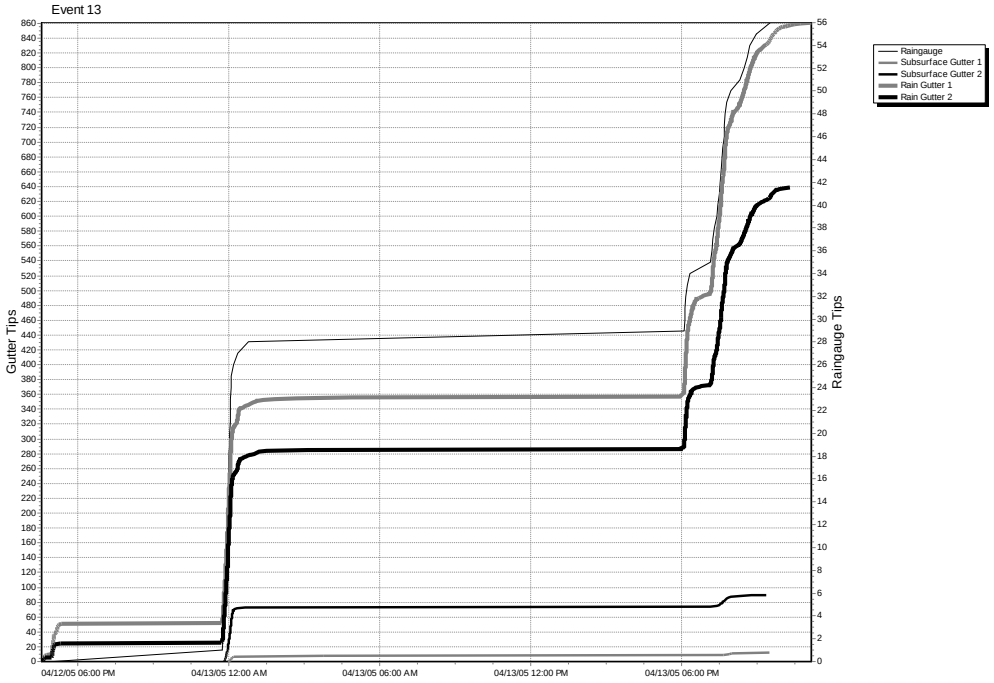

Figure 55: Rainfall Event 13 (Apr. 12-13, 2005)

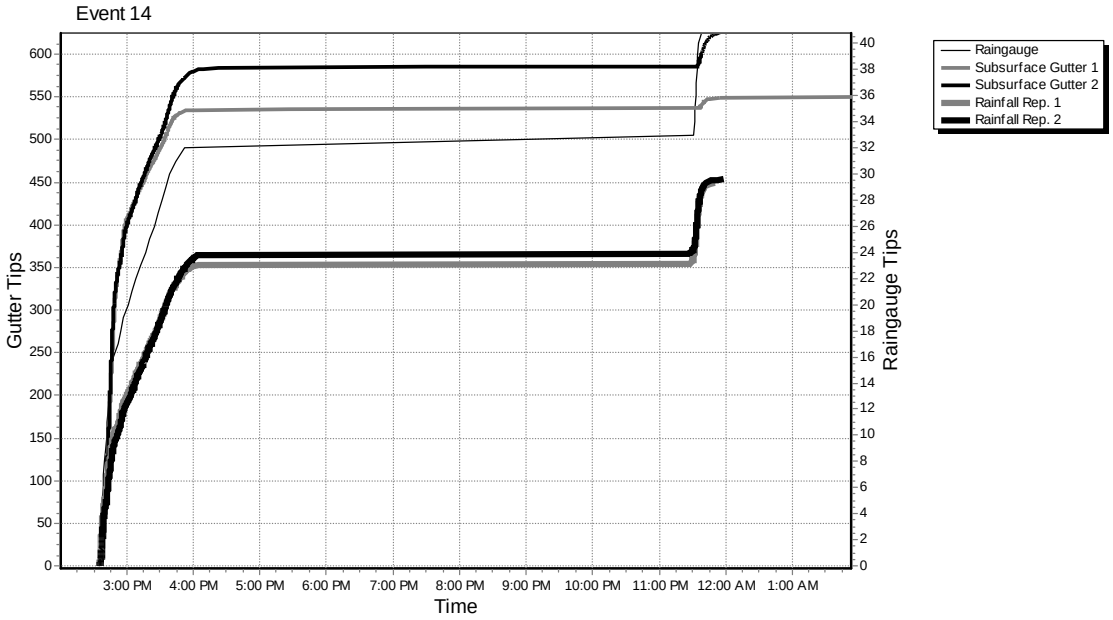

Figure 56: Rainfall Event 14 (Apr. 22-23, 2005)

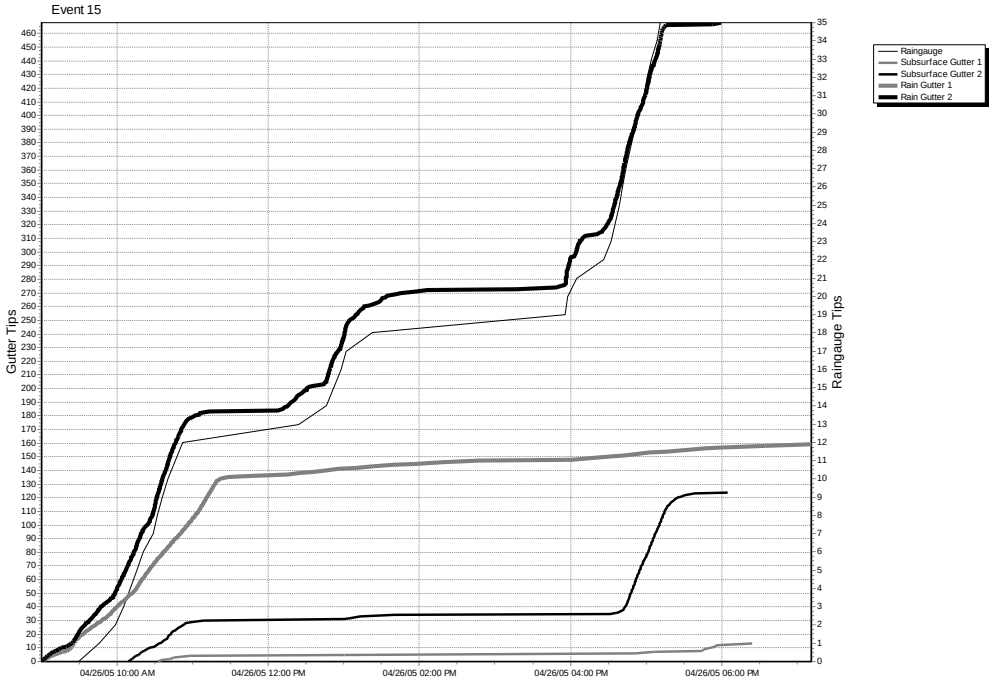

Figure 57: Rainfall Event 15 (Apr. 26, 2005)

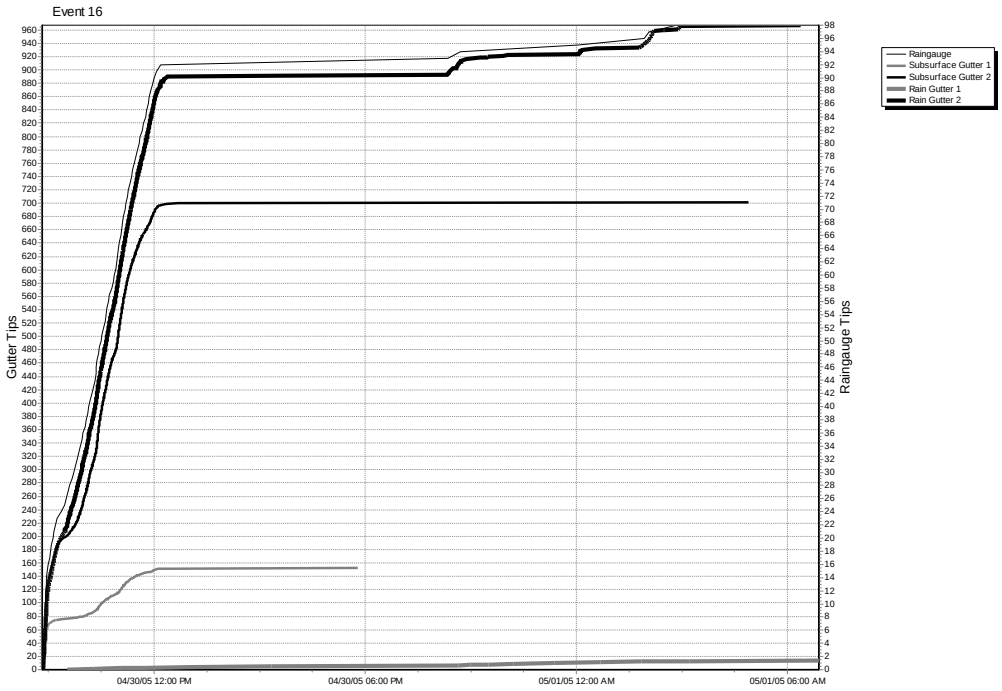

Figure 58: Rainfall Event 16 (April 30-May 1, 2005)

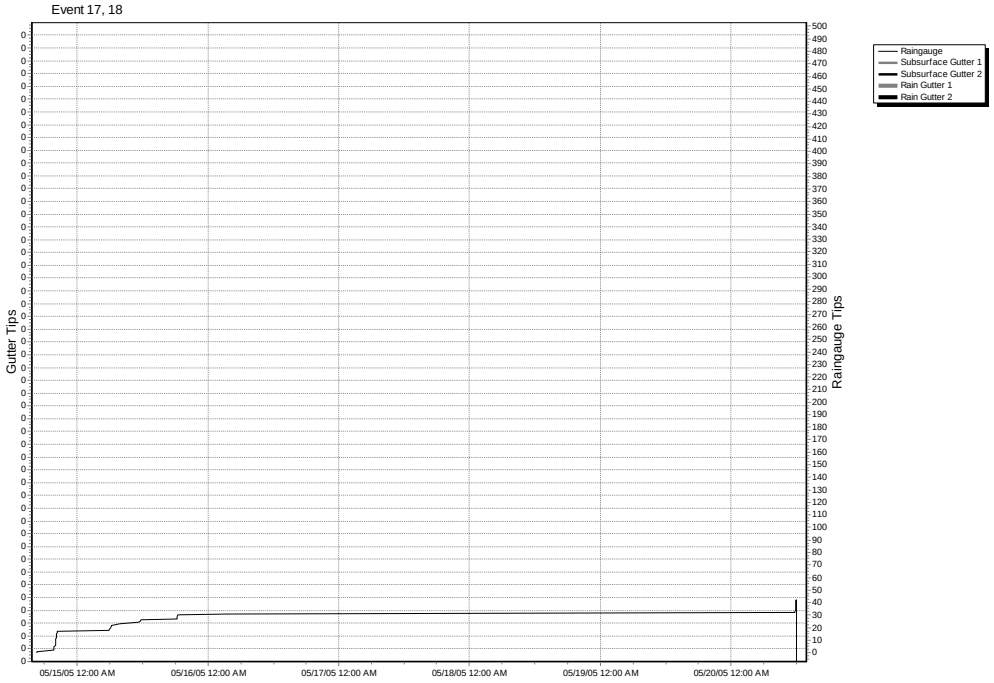

Figure 59: Rainfall Event 17, 18 (May 15-20, 2005)

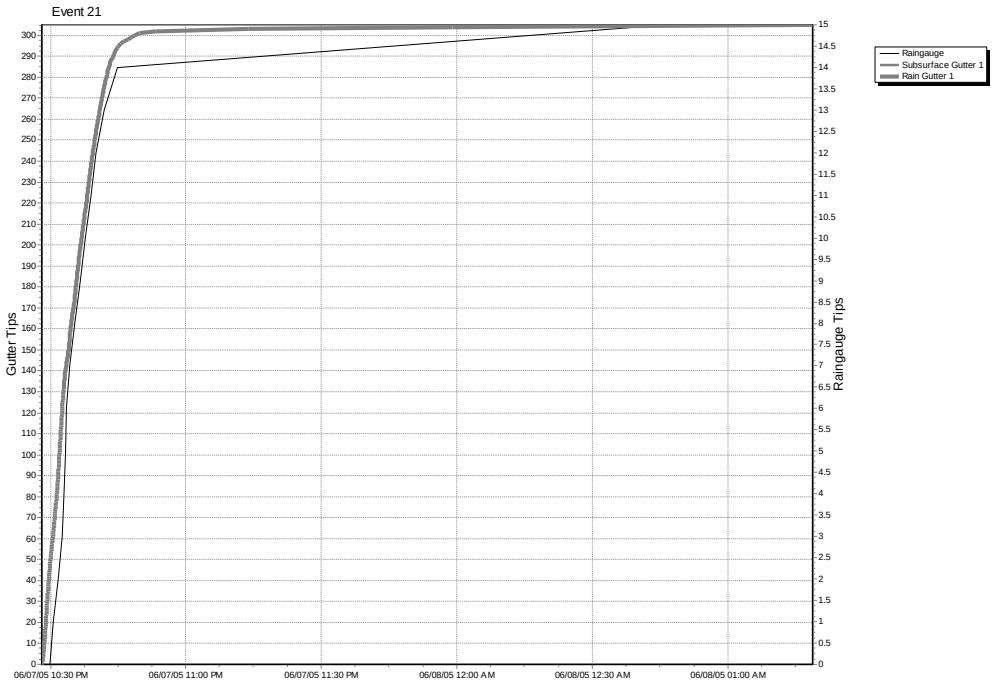

Figure 60: Rainfall Event 21 (Jun. 7-8, 2005)

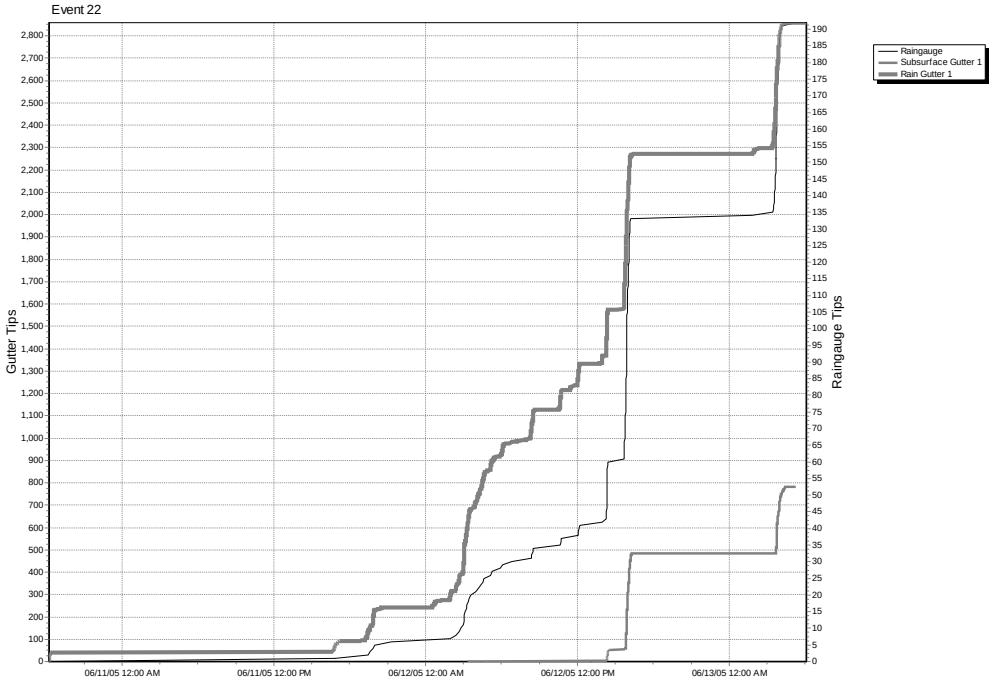

Figure 61: Rainfall Event 22 (Jun. 11-13, 2005)

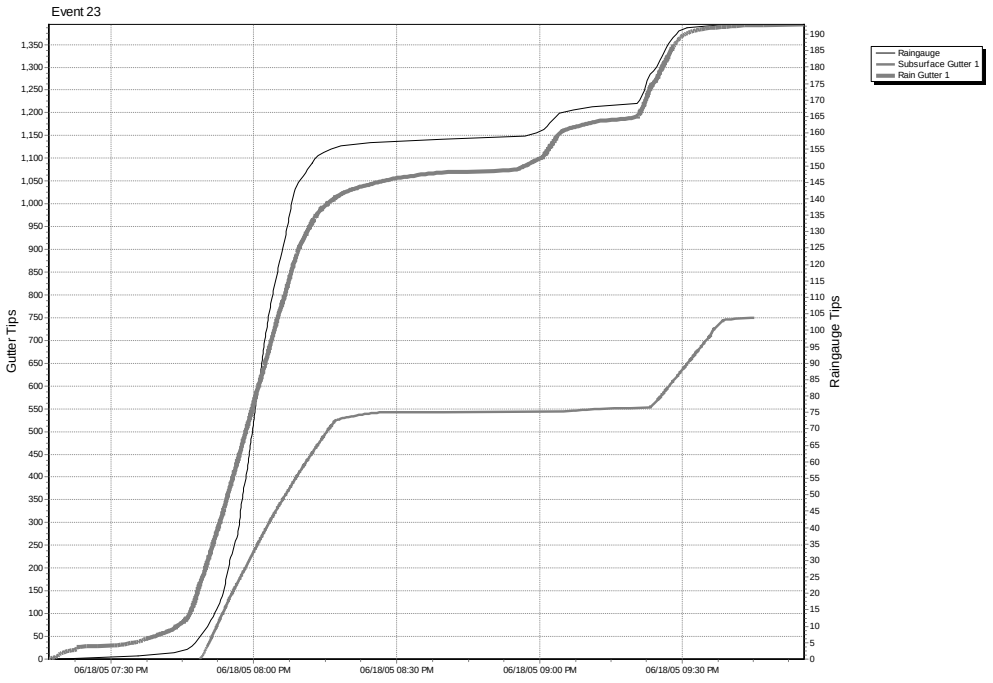

Figure 62: Rainfall Event 23 (Jun. 18, 2005)

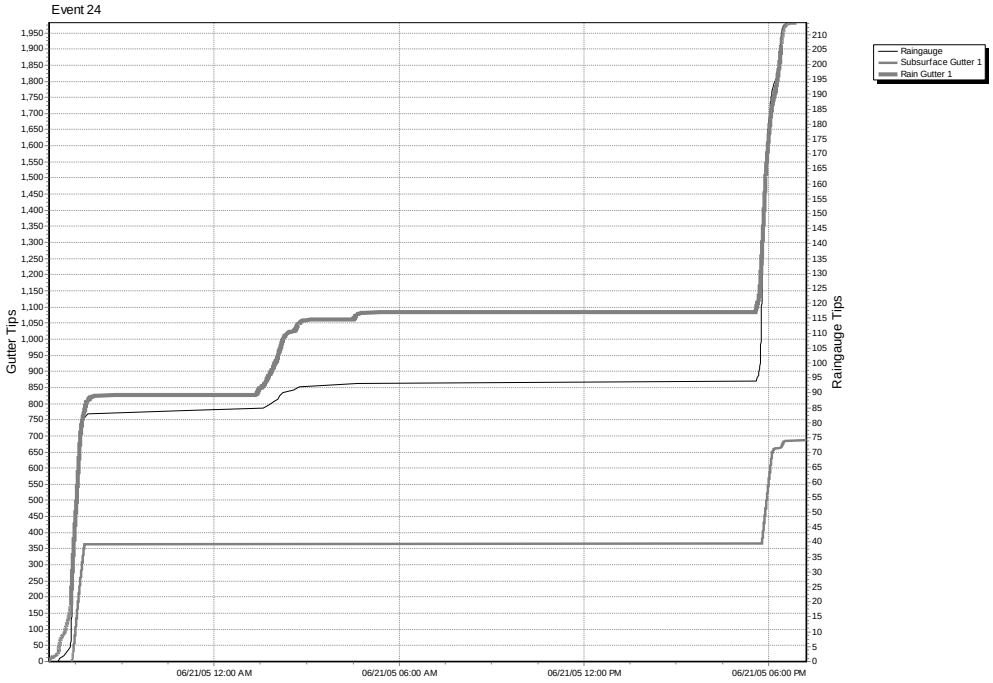

Figure 63: Rainfall Event 24 (June 20, 2005)

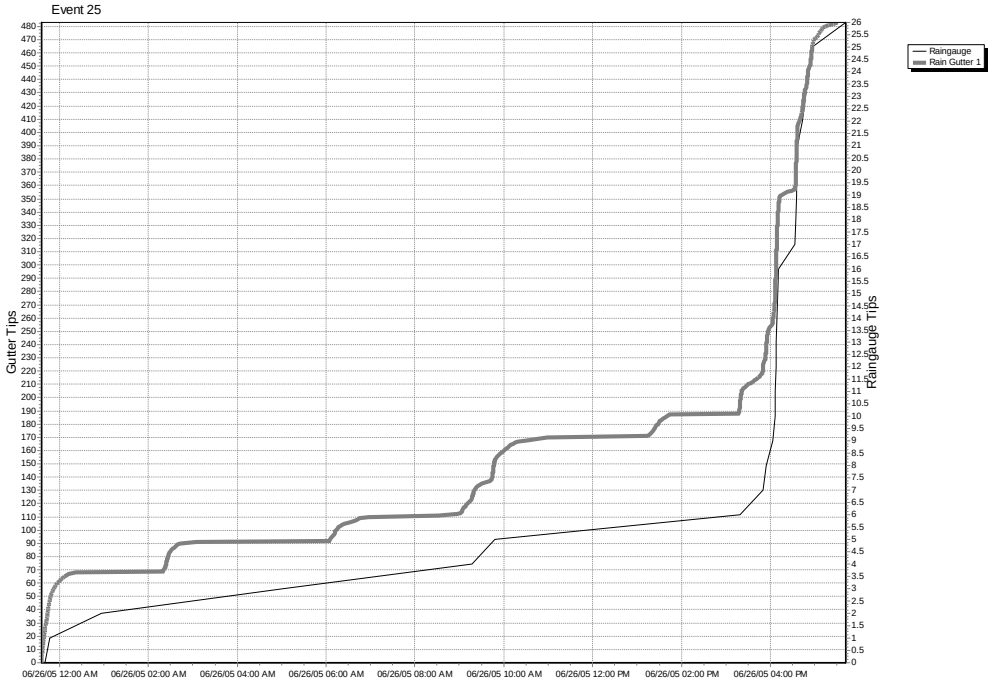

Figure 64: Rainfall Event 25 (June 26, 2005)

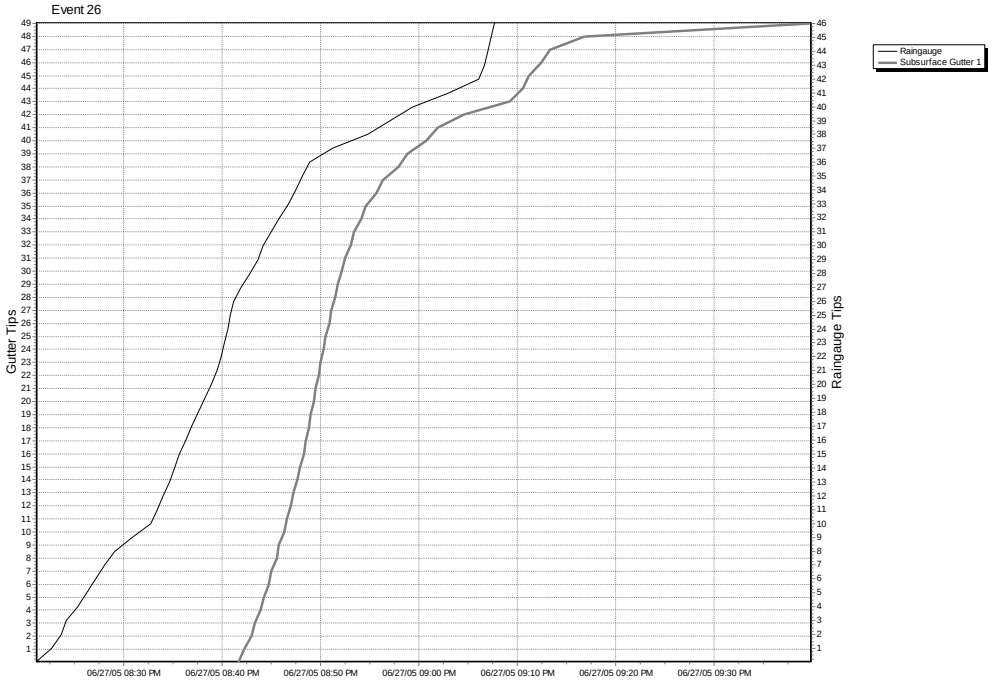

Figure 65: Rainfall Event 26 (Jun. 27, 2005)

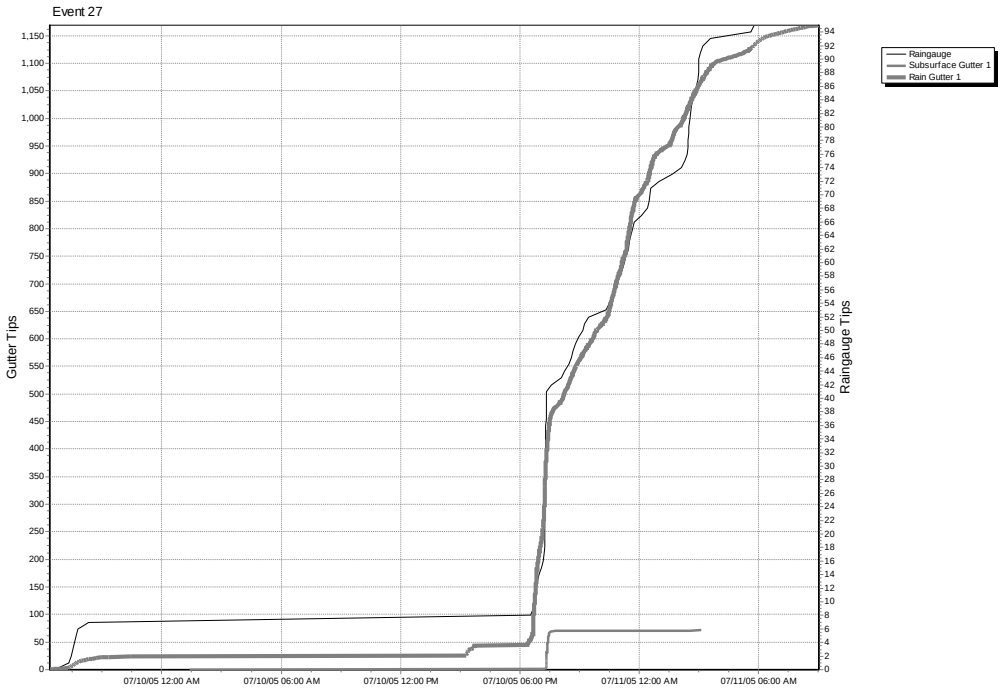

Figure 66: Rainfall Event 27 (Jul. 10-11, 2005)

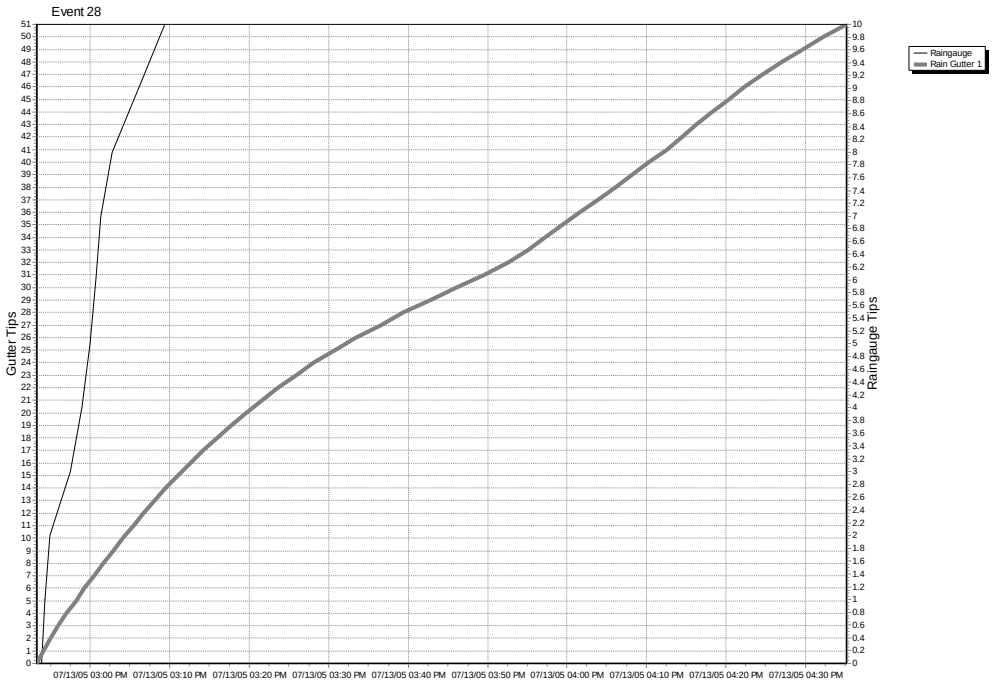

Figure 67: Rainfall Event 28 (Jul. 13, 2005)

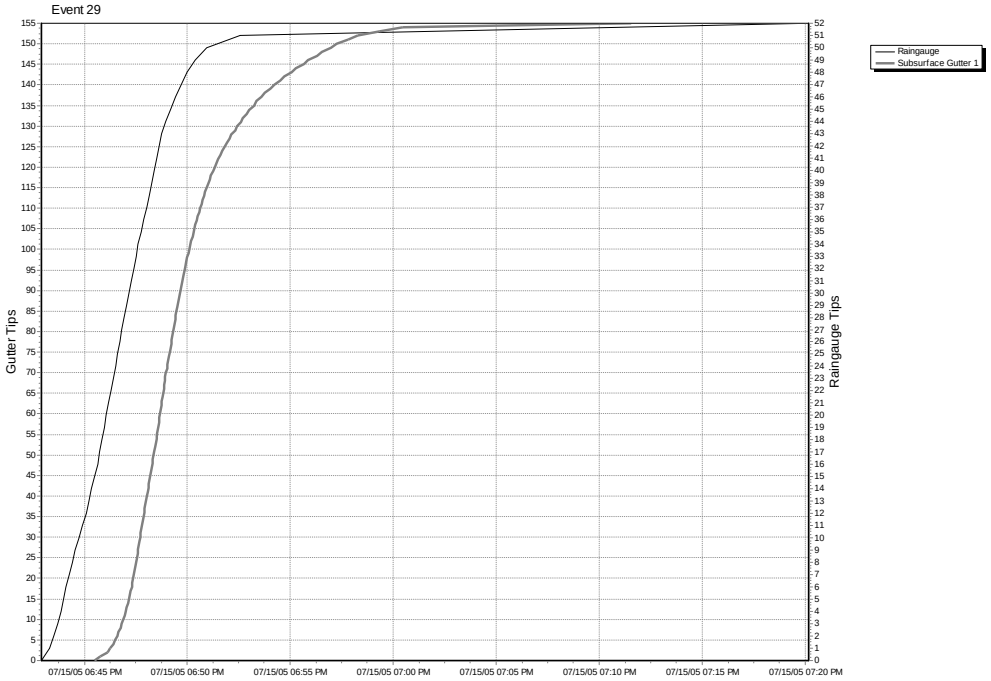

Figure 68: Rainfall Event 29 (Jul. 15, 2005)

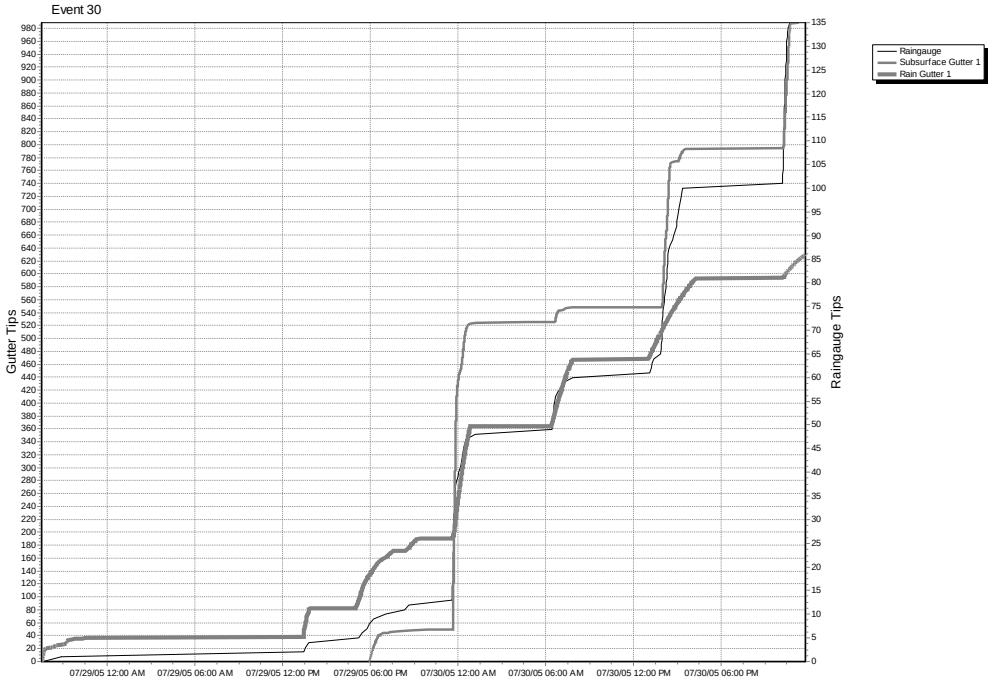

Figure 69: Rainfall Event 30 (Jul. 29-30, 2005)

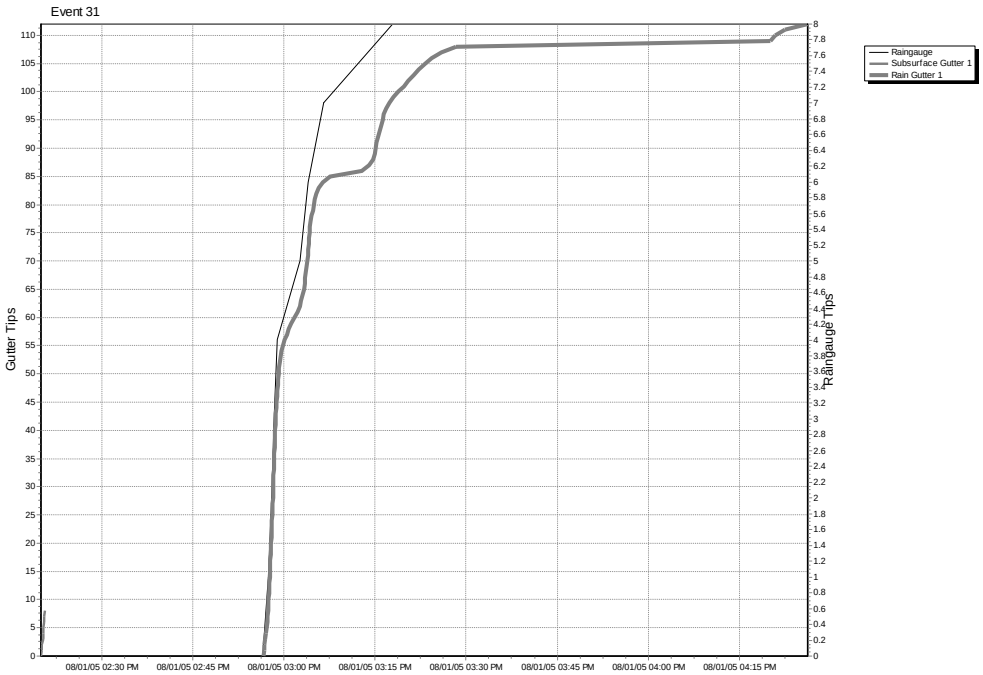

Figure 70: Rainfall Event 31 (Aug. 1, 2005)

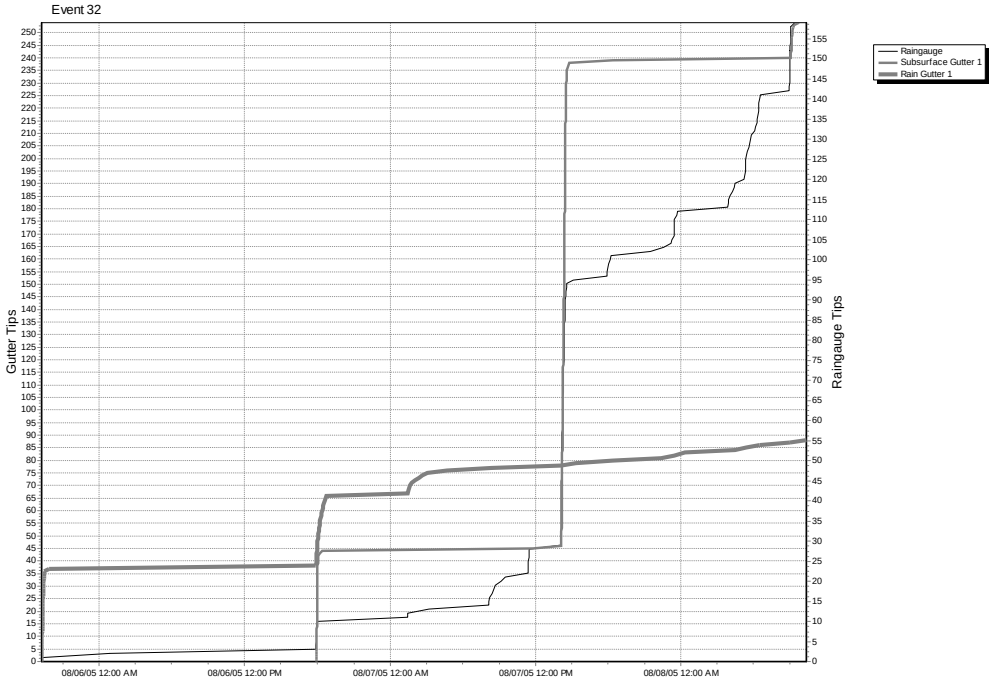

Figure 71: Rainfall Event 32 (Aug. 6-8, 2005)

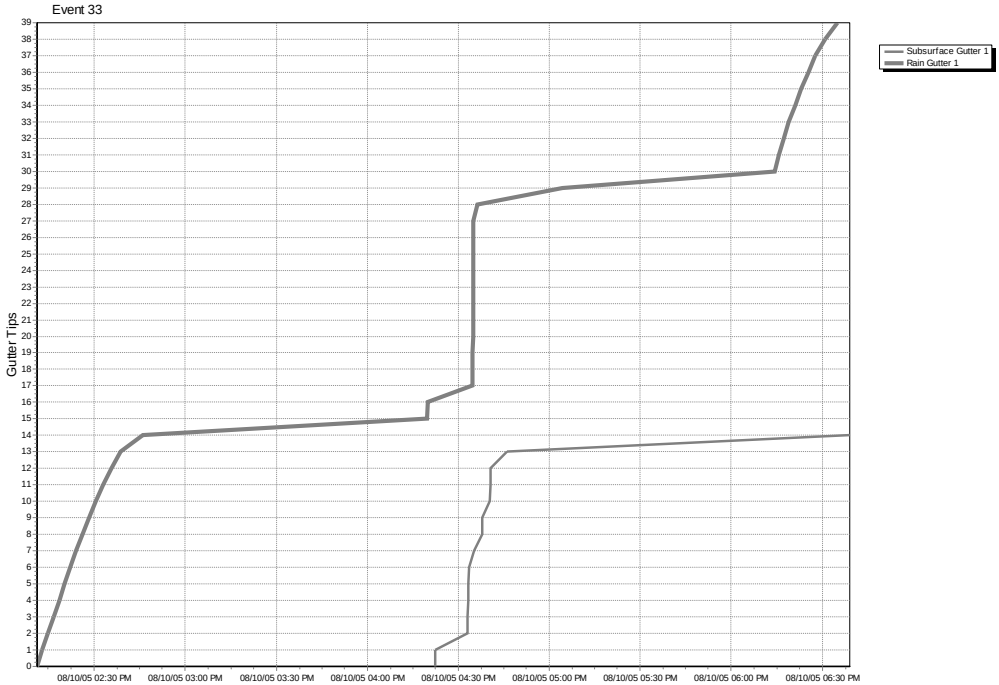

Figure 72: Rainfall Event 33 (Aug. 10, 2005)

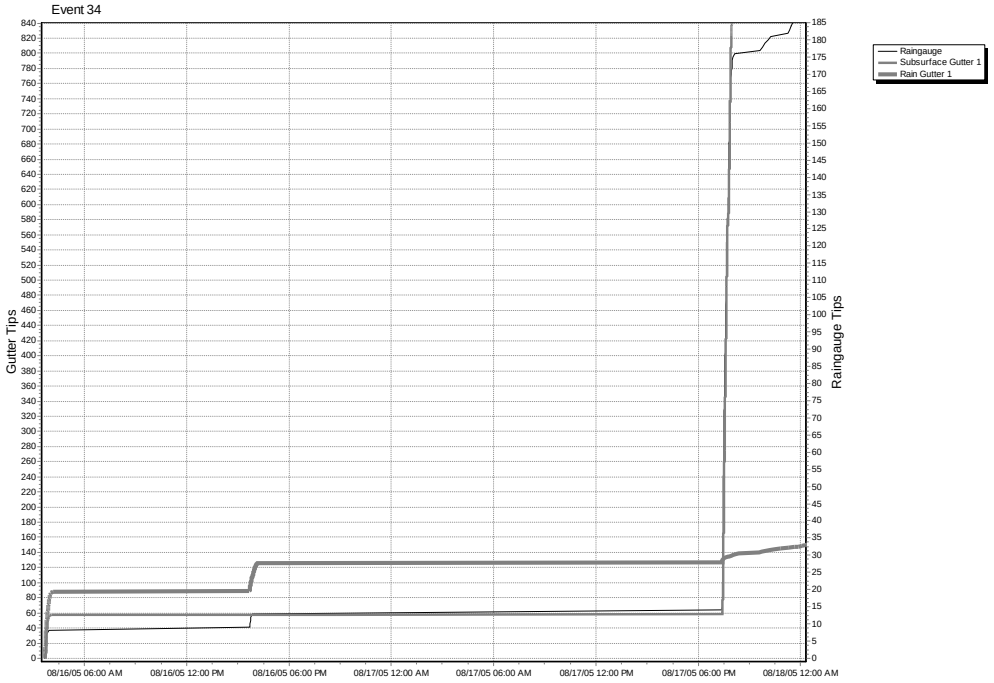

Figure 73: Rainfall Event 34 (Aug. 16-17, 2005)

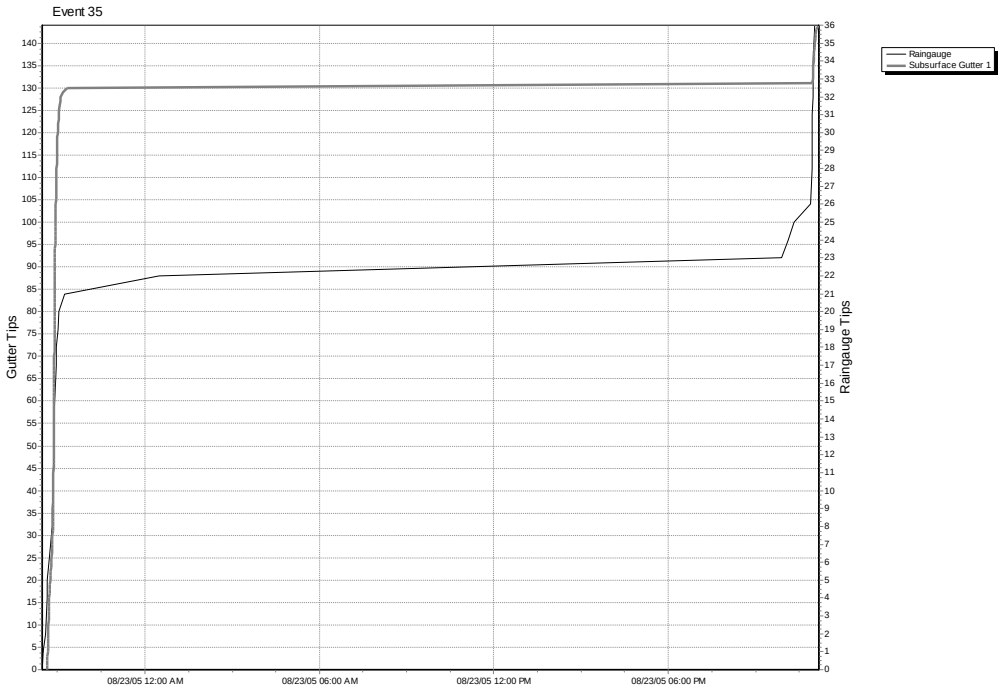

Figure 74: Rainfall Event 35 (Aug. 23, 2005)

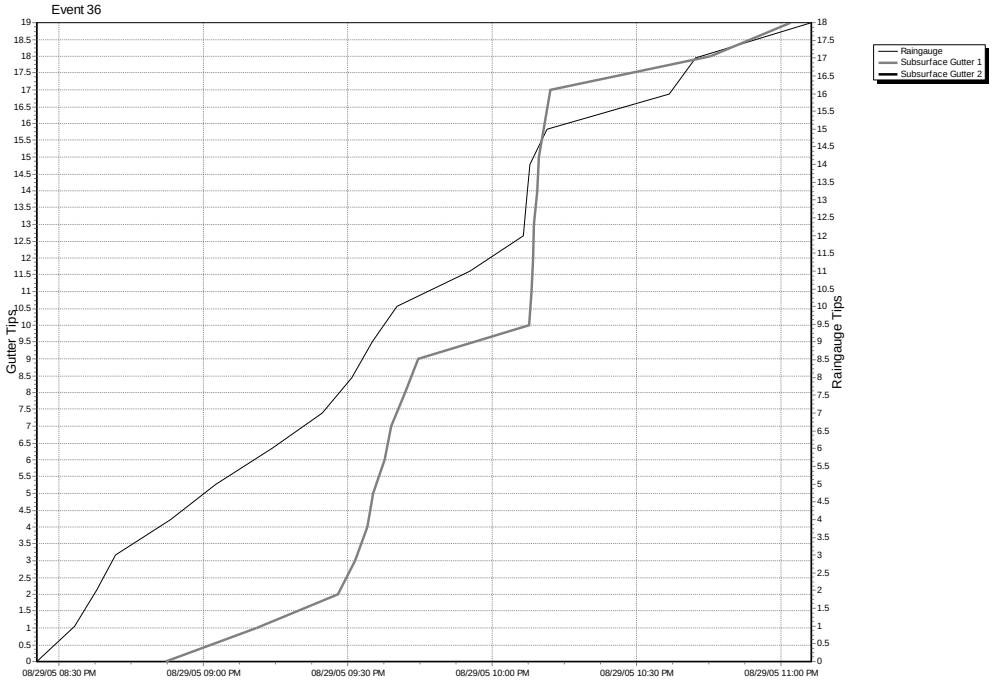

Figure 75: Rainfall Event 36 (Aug. 29, 2005)

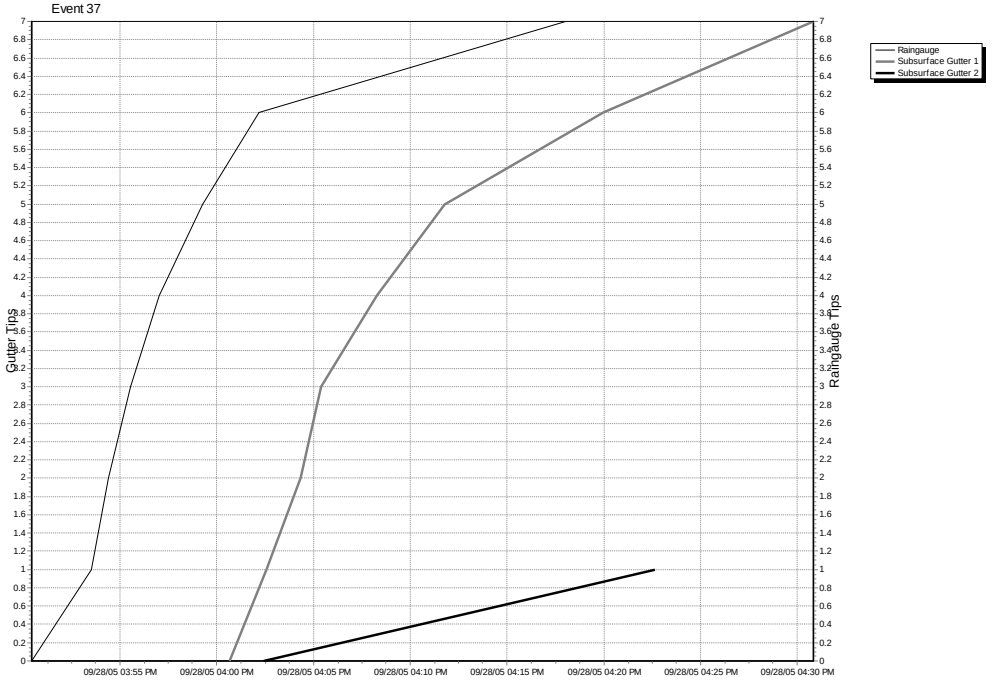

Figure 76: Rainfall Event 37 (Sep. 28, 2005)

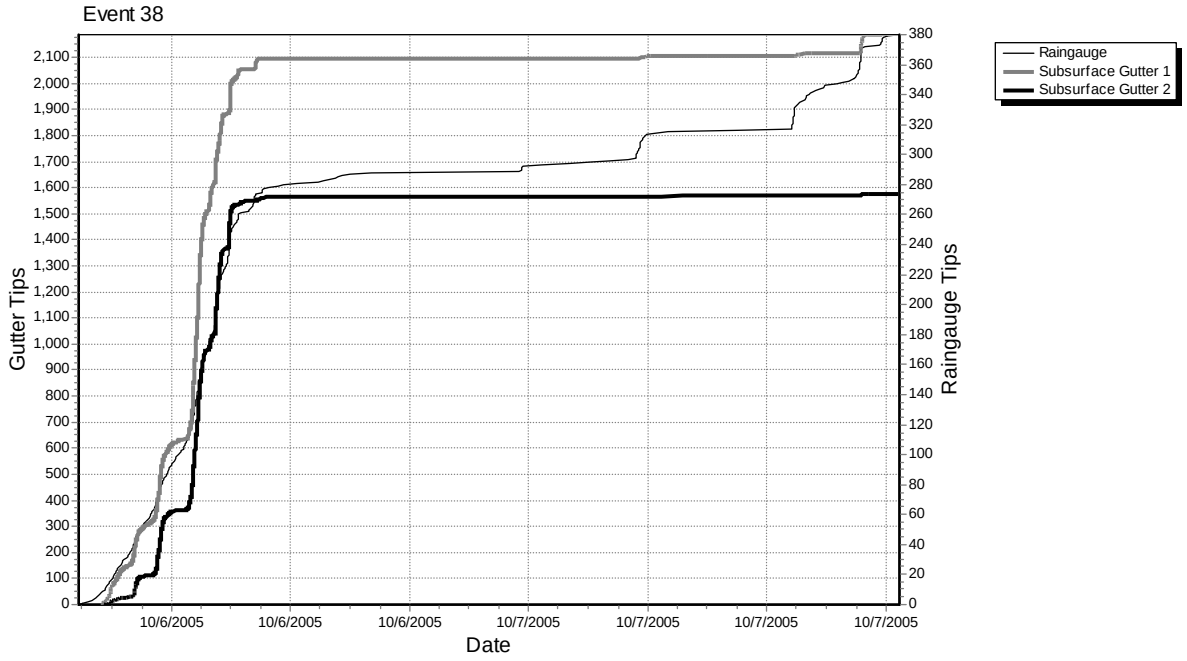

Figure 77: Rainfall Event 38 (Oct. 6-8, 2005)

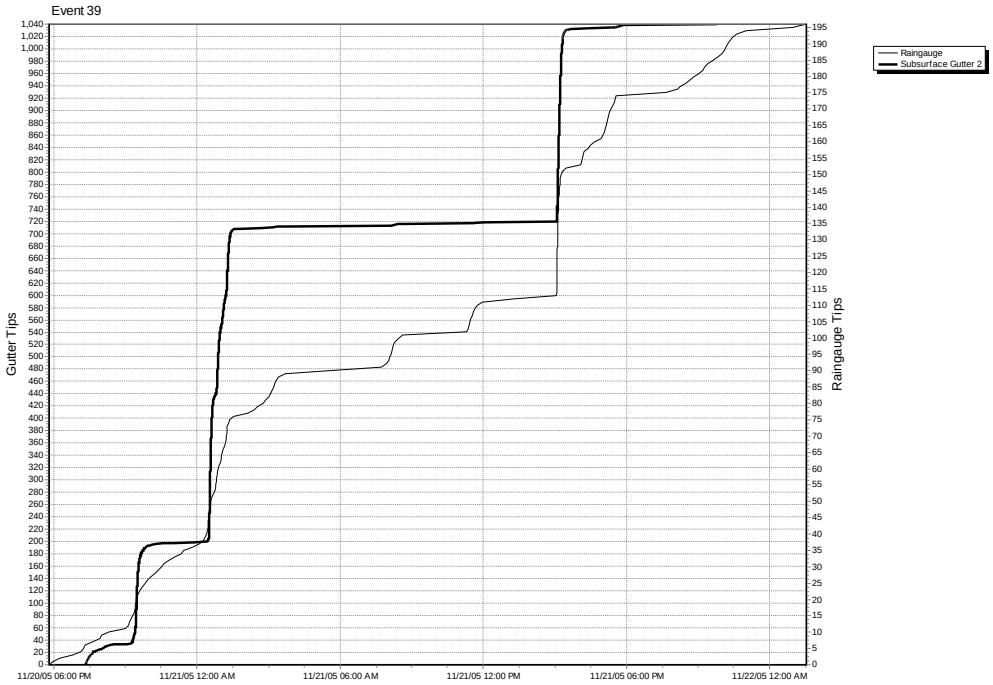

Figure 78: Rainfall Event 39 (Nov. 20-22, 2005)

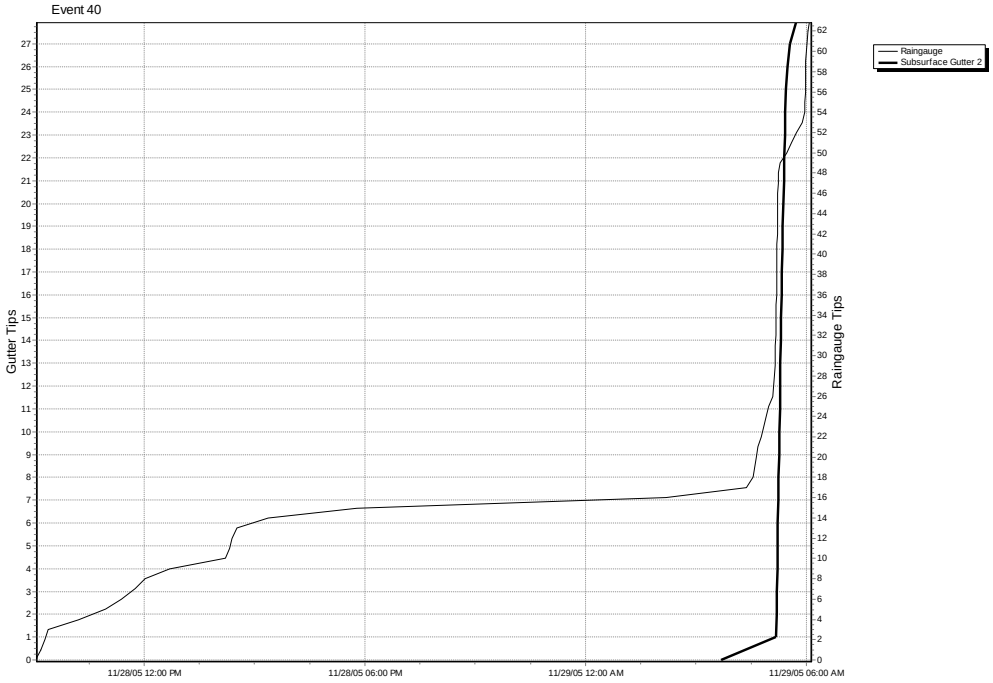

Figure 79: Rainfall Event 40 (Nov. 28-29, 2005)

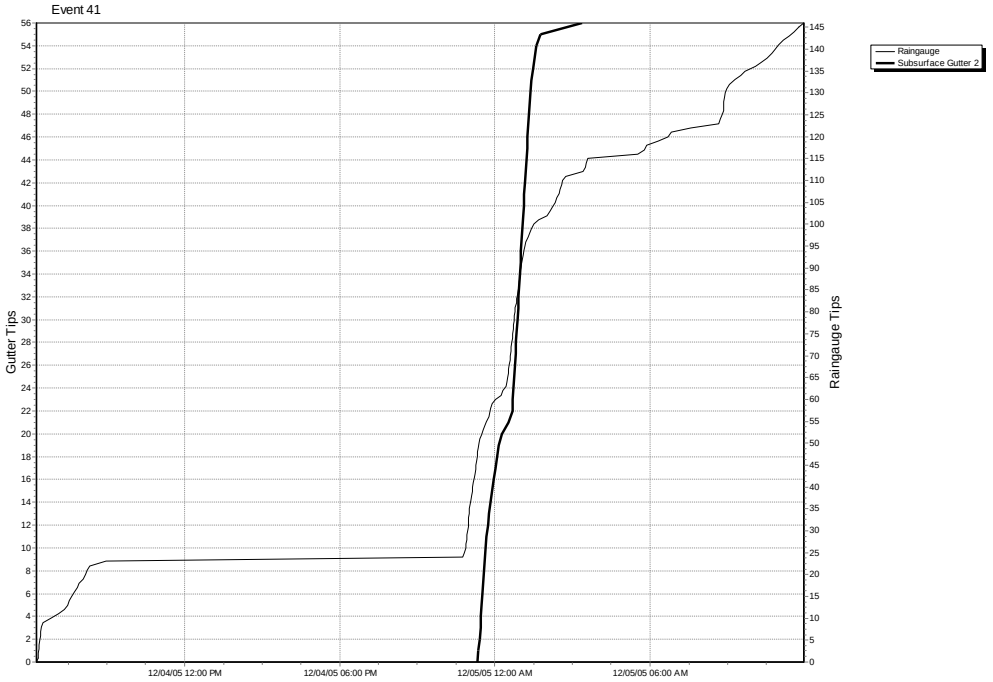

Figure 80: Rainfall Event 41 (Dec. 4-5, 2005)

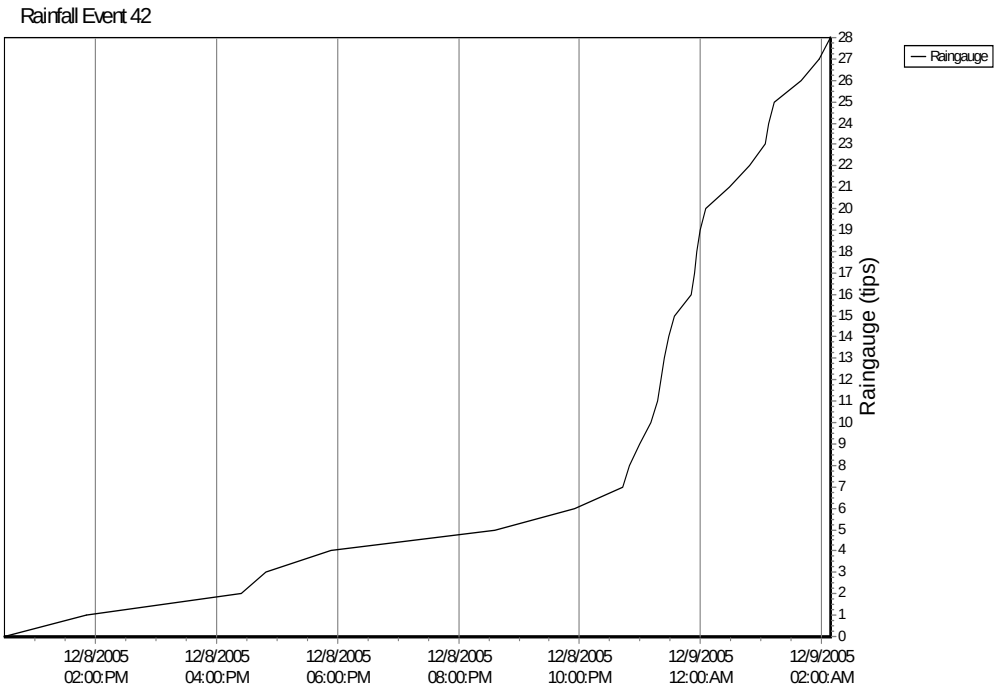

Figure 81: Rainfall Event 42 (Dec. 8-9, 2005)

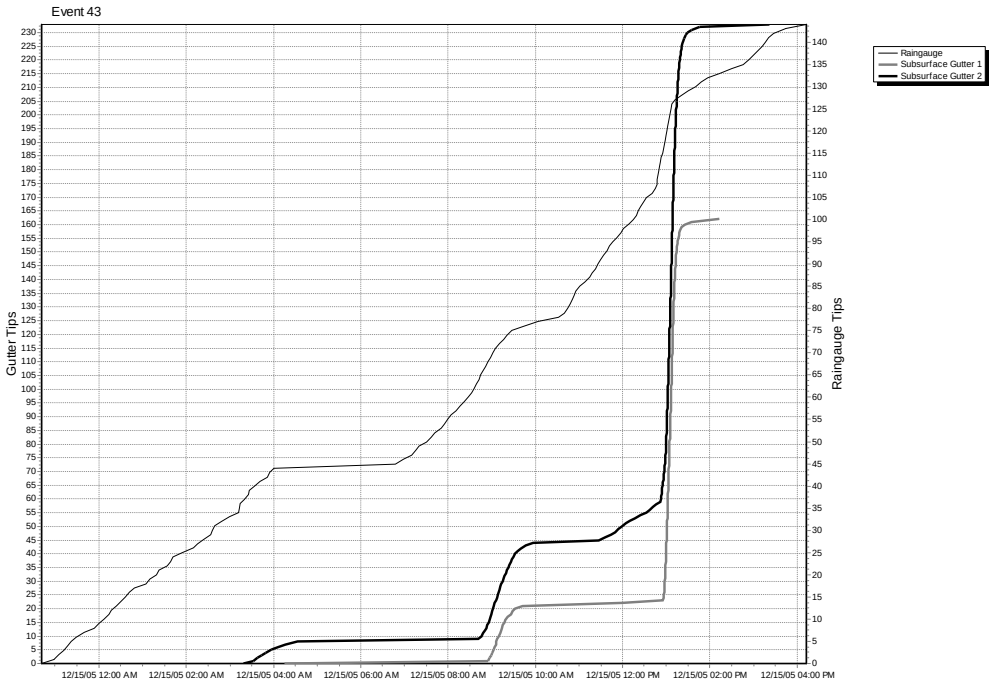

Figure 82: Rainfall Event 43 (Dec. 15, 2005)

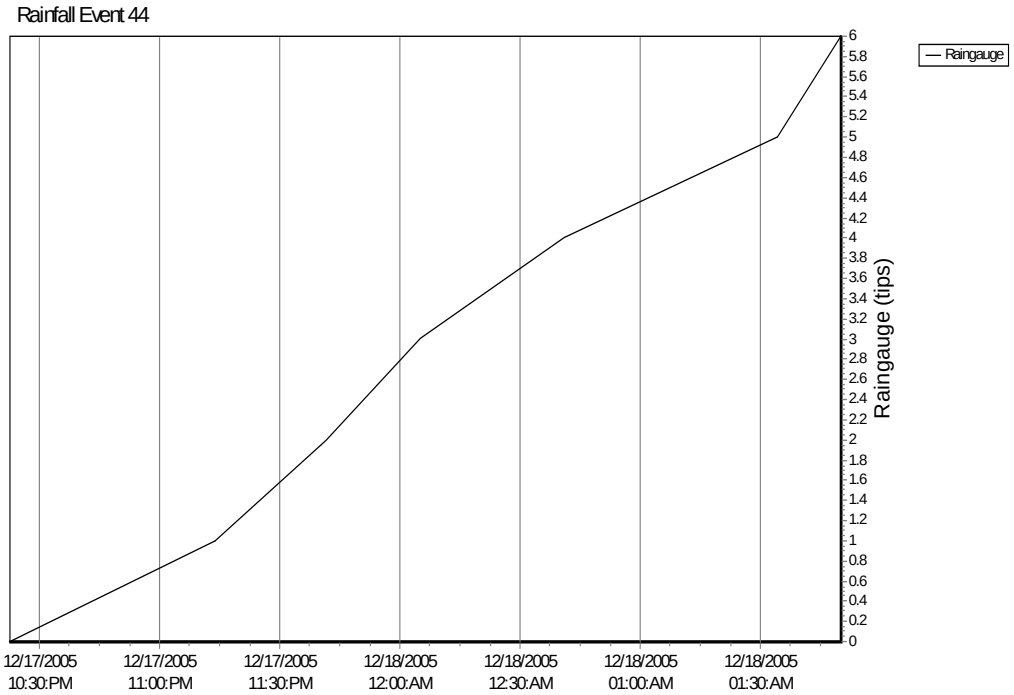

Figure 83: Rainfall Event 44 (Dec. 17-18, 2005)

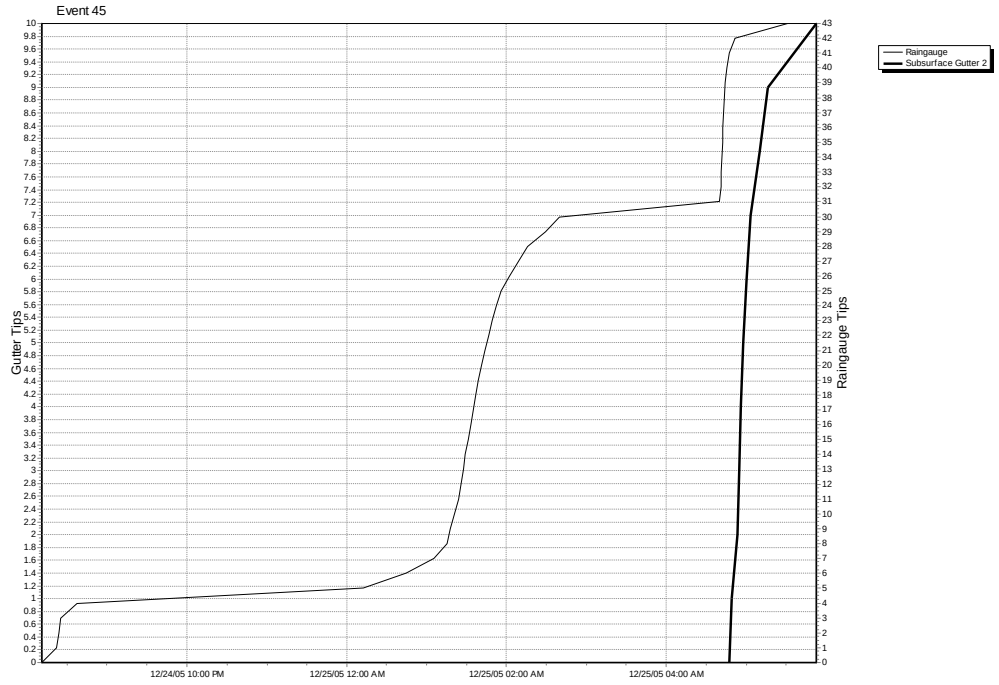

Figure 84: Rainfall Event 45 (Dec. 24-25, 2005)

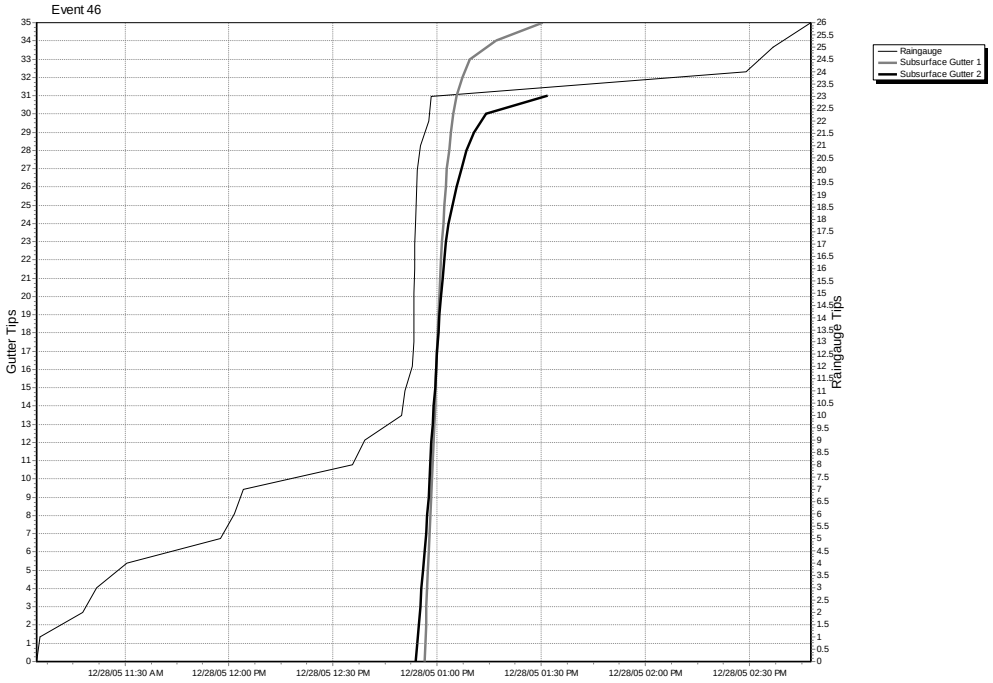

Figure 85: Rainfall Event 46 (Dec. 28, 2005)

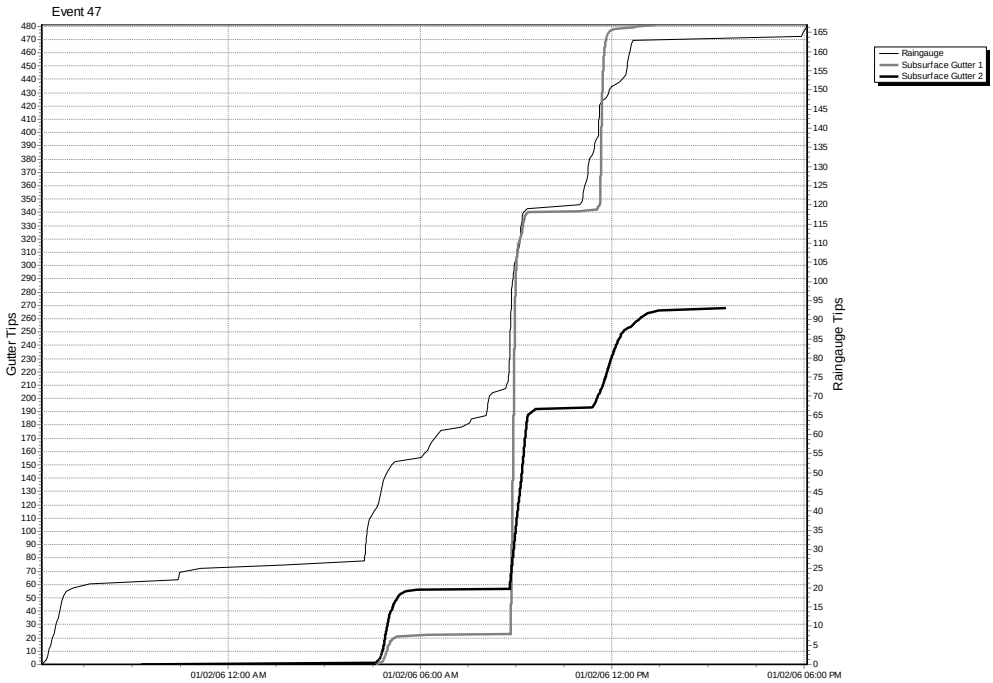

Figure 86: Rainfall Event 47 (Jan. 1-2, 2005)

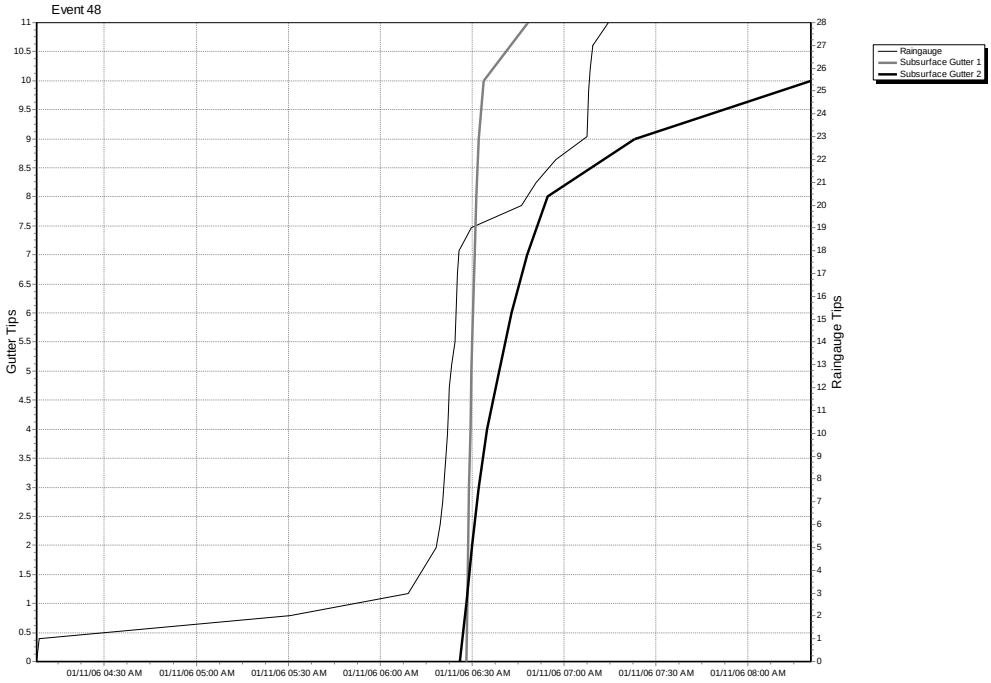

Figure 87: Rainfall Event 48 (Jan. 11, 2005)

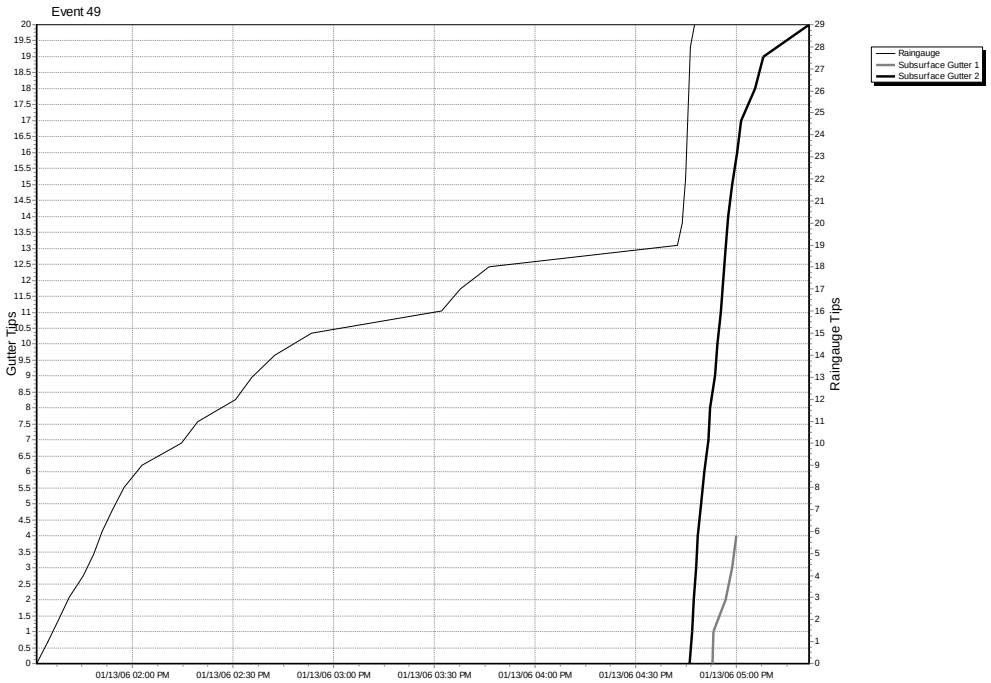

Figure 88: Rainfall Event 49 (Jan. 13, 2005)

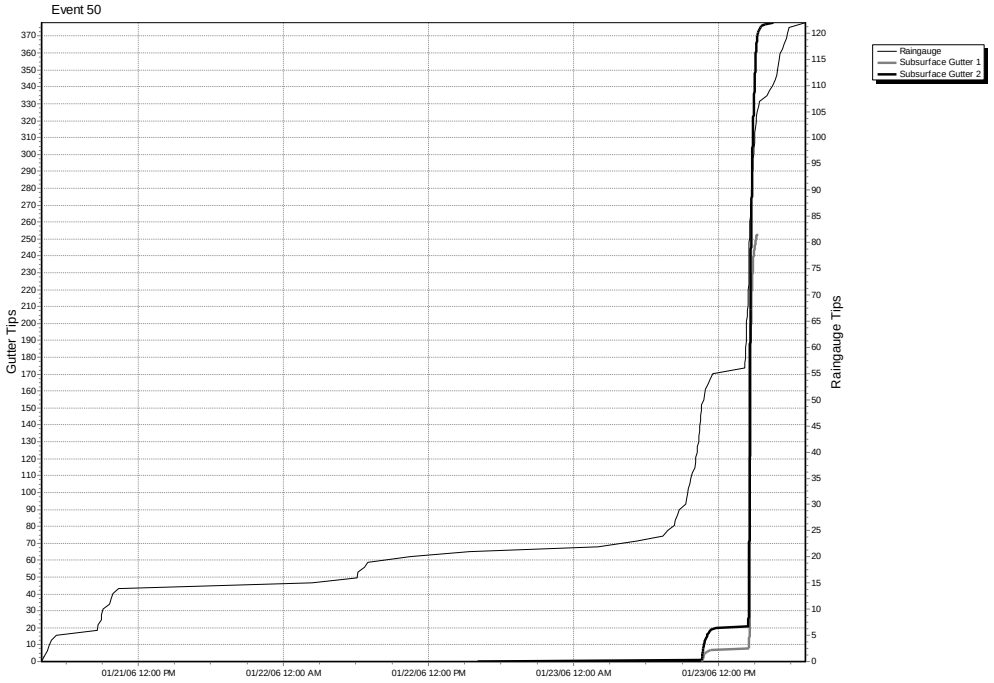

Figure 89: Rainfall Event 50 (Jan. 21-24, 2005)

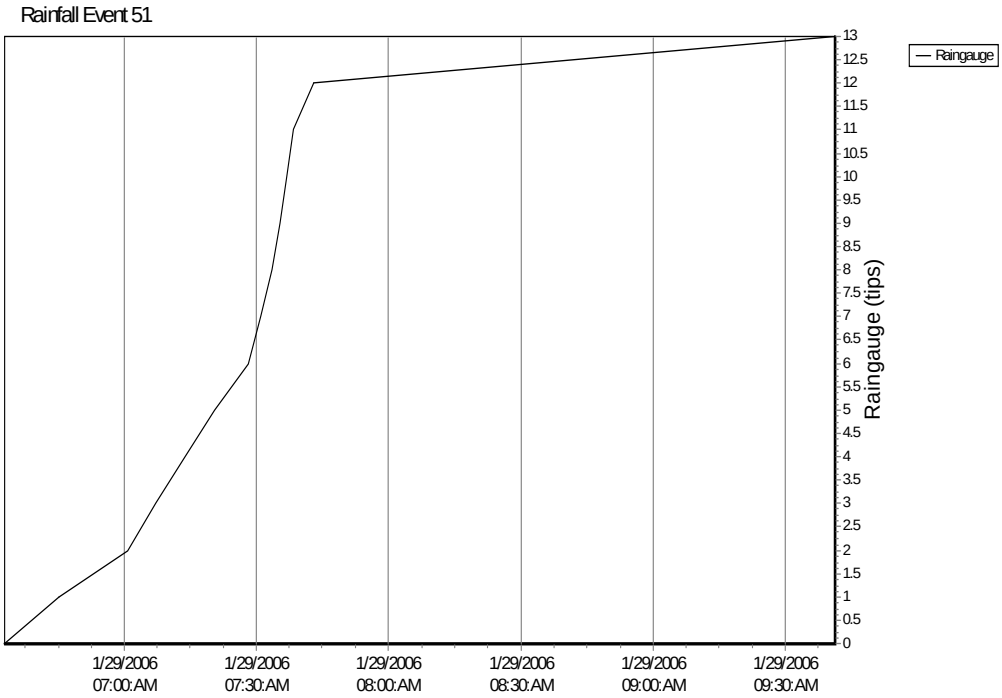

Figure 90: Rainfall Event 51 (Jan. 29, 2005)

APPENDIX D: DEUTERIUM ANALYSIS RESULTS

Run Date	Run #	Sample ID	Event Date	Log#	uL sample	Inlet V	delta mean	delta stdev	delta D	accepted dD	corrected dD
4/5/2005	1	ATWS		H286	2	4.913	251.871	0.262	-29.8	-26	-26.00
4/5/2005	2	GISP		H287	2	4.994	43.762	0.253	-191.09	-190	-190.00
4/5/2005	3	L3		H288	2	5.014	247.502	0.204	-33.186		-29.44
4/5/2005	4	P-W		H291	2	4.996	251.286	0.24	-30.253		-26.46
4/5/2005	5	P-W		H290	2	5.004	252.024	0.239	-29.682		-25.88
4/5/2005	6	L3		H289	2	4.873	247.09	0.318	-33.505		-29.77
4/5/2005	7	ATWS		H292	2	4.94	251.465	0.501	-30.115		-26.32
4/5/2005	8	ATWS		H293	2	4.8	250.643	0.341	-30.751		-26.97
4/5/2005	9	ATWS		H294	2	4.978	251.642	0.497	-29.977		-26.18
4/5/2005	10	ATWS		H295	2	4.894	251.427	0.23	-30.144		-26.35
4/5/2005	11	ATWS		H296	2	4.895	251.08	0.077	-30.413		-26.62
4/5/2005	12	ATWS		H297	2	4.889	250.547	0.414	-30.826		-27.04
4/8/2005	1	ATWS		H298	2	4.975	249.529	0.369	-31.615	-26	-26.00
4/8/2005	2	GISP		H299	2	4.953	44.5	0.118	-190.51	-190	-190.00
4/8/2005	3	L1	3/8/2005	H300	2	4.974	244.278	0.237	-35.685		-30.20
4/8/2005	4	P--R	3/8/2005	H302	2	4.967	228.448	0.355	-47.953		-42.86
4/8/2005	5	L1	3/8/2005	H301	2	4.993	244.761	0.198	-35.31		-29.81
4/8/2005	6	P--R	3/8/2005	H303	2	5.022	228.231	0.349	-48.121		-43.04
4/20/2005	1	ATWS		H304	2	5.03	249.364	0.216	-31.743	-26	-26.00
4/20/2005	2	GISP		H305	2	4.99	44.15	0.169	-190.78	-190	-190.00
4/20/2005	3	SS—W	4/8/2005	H306	2	4.961	232.103	0.339	-45.12		-39.79
4/20/2005	4	SS—R	4/8/2005	H308	2	4.93	234.956	0.335	-42.909		-37.51
4/20/2005	5	SS—W	4/8/2005	H307	2	4.9	231.852	0.391	-45.314		-39.99
4/20/2005	6	SS—R	4/8/2005	H309	2	4.967	234.291	0.437	-43.424		-38.05
5/11/2005	2	ATWS		H314	2	4.974	250.474	0.388	-30.883	-26	-26.00

5/11/2005	3	GISP		H315	2	4.932	45.529	0.328	-191.27	-190	-190.00
5/11/2005	1	SS—W	3/25/2005	H310	2	4.914	263.049	0.132	-21.137		-16.03
5/11/2005	4	SS—R	3/25/2005	H312	2	4.932	261.767	0.149	-22.13		-17.05
5/11/2005	5	SS—W	3/25/2005	H311	2	4.934	263.239	0.157	-20.99		-15.88
5/11/2005	6	SS—R	3/25/2005	H312	2	4.932	261.279	0.199	-22.509		-17.44
5/11/2005	12	P—R	3/25/2005	H320	2	4.946	261.177	0.484	-22.588		-17.52
5/11/2005	13	P—W	3/25/2005	H319	2	4.942	259.948	0.289	-23.541		-18.49
5/11/2005	14	P—R	3/25/2005	H321	2	4.999	259.886	0.292	-23.589		-18.54
5/13/2005	10	VSMOW		H327	2	4.934	275.545	0.386	-11.453	0	0.00
		SLAP(avg)							-421.54	-428	-428.00
5/13/2005	9	SLAP		H331	2	4.849	-252.12	0.26	-420.39		-426.80
5/13/2005	6	SLAP		H332	2	4.985	-254.47	0.284	-422.22		-428.70
5/13/2005	2	SLAP		H333	2	4.849	-254.22	0.46	-422.02		-428.49
5/13/2005	4	ATWS		H323	2	4.966	247.889	0.48	-32.886		-22.37
5/13/2005	5	ATWS		H329	2	4.727	247.215	0.321	-33.852		-23.38
5/13/2005	7	ATWS		H330	2	4.98	247.536	0.262	-33.16		-22.66
5/13/2005	8	ATWS		H324	2	4.938	248.236	0.249	-32.617		-22.09
5/13/2005	3	ATWS		H328	2	4.951	247.983	0.249	-32.813		-22.29
5/13/2005	11	ATWS		H322	2	3.466	246.338	0.529	-34.088		-23.62
5/17/2005		VSMOW(avg)							-8.37	0	0.00
5/17/2005		SLAP(avg)							424.214	-428	-428.00
5/17/2005	5	VSMOW		H338	2	4.982	280.896	0.438	-7.305		-1.05
5/17/2005	6	VSMOW		H339	2	4.94	277.706	0.34	-9.778		1.39
5/17/2005	10	VSMOW		H343	2	4.958	279.933	0.143	-8.052		-0.31
5/17/2005	11	SLAP		H344	2	4.974	-257.42	0.431	-424.5		411.72
5/17/2005	12	SLAP		H345	2	4.924	-256.68	0.242	-423.93		411.15
5/17/2005	2	ATWS		H335	2	5.065	252.962	0.381	-28.954		20.37
5/17/2005	3	ATWS		H336	2	5.031	250.89	0.33	-30.56		21.95
5/17/2005	1	ATWS		H334	2	5.084	253.597	0.277	-28.462		19.88
5/17/2005	7	ATWS		H340	2	5.01	249.994	0.212	-31.852		23.23
5/17/2005	8	ATWS		H341	2	4.967	249.528	0.422	-31.616		23.00
5/17/2005	9	ATWS		H342	2	4.967	249.984	0.426	-31.262		22.65

5/18/2005	1	ATWS		H346	2	5.084	249.93	0.346	-31.305	-26	-26.00
5/18/2005	2	GISP		H347	2	5.086	44.414	0.172	-190.58	-190	-190.00
5/18/2005	3	P--W	4/11/2005	H348	2	4.914	210.085	0.361	-62.852		-58.48
5/18/2005	5	P--R	4/11/2005	H350	2	5.039	205.903	0.403	-65.425		-61.13
5/18/2005	6	P--R	4/11/2005	H351	2	4.956	205.727	0.464	-65.562		-61.27
5/18/2005	7	L1	4/12/2005	H352	2	5.05	248.114	0.387	-32.712		-27.45
5/18/2005	8	L1	4/12/2005	H353	2	5.022	247.903	0.415	-32.875		-27.62
5/18/2005	9	SS--R	4/11/2005	H354	2	5.047	205.792	0.284	-65.511		-61.22
5/18/2005	10	SS--R	4/11/2005	H355	2	4.913	205.206	0.283	-65.965		-61.69
5/18/2005	11	L3	4/12/2005	H356	2	5.028	241.896	0.221	-37.53		-32.41
5/18/2005	12	L3	4/12/2005	H357	2	4.95	241.64	0.296	-37.729		-32.61
5/23/2005	1	ATWS		H358	2	5.409	250.179	0.219	-31.112	-26	-26.00
5/23/2005	2	GISP		H359	2	5.43	44.693	0.459	-190.36	-190	-190.00
5/23/2005	3	P--W	3/22/2005	H360	2	5.404	237.315	0.443	-41.081		-36.27
5/23/2005	4	P--R	3/22/2005	H362	2	5.346	233.969	0.33	-43.674		-38.94
5/23/2005	5	SS--R	3/22/2005	H364	2	5.398	254.165	0.314	-28.022		-22.82
5/23/2005	7	L3	3/23/2005	H368	2	5.23	235.79	0.391	-42.263		-37.48
5/23/2005	8	P--W	3/22/2005	H361	2	5.494	235.46	0.488	-42.518		-37.75
5/23/2005	9	P--R	3/22/2005	H363	2	5.116	233.802	0.298	-43.803		-39.07
5/23/2005	10	SS--R	3/22/2005	H365	2	5.298	253.048	0.199	-28.888		-23.71
5/23/2005	11	L1	3/23/2005	H367	2	5.348	240.883	0.42	-38.316		-33.42
5/23/2005	12	L3	3/23/2005	H369	2	5.45	234.438	0.111	-43.311		-38.56
5/25/2005	1	ATWS		H370	2	5.396	249.551	0.352	-31.598	-26	-26.00
5/25/2005	2	GISP		H371	2	5.406	44.183	0.28	-190.76	-190	-190.00
5/25/2005	3	P--W	2/22/2005	H372	2	5.263	250.333	0.374	-30.992		-25.38
5/25/2005	4	P--R	2/22/2005	H373	2	5.337	250.807	0.342	-30.625		-25.00
5/25/2005	5	SS--W	2/22/2005	H376	2	5.361	243.145	0.324	-36.681		-31.24
5/25/2005	6	SS--R	2/22/2005	H377	2	5.346	252.546	0.113	-29.277		-23.61
5/25/2005	7	P--W	2/22/2005	H374	2	5.367	248.587	0.389	-32.345		-26.77
5/25/2005	8	SS--R	2/22/2005	H381	2	5.295	250.783	0.188	-30.643		-25.02
5/25/2005	9	SS--R	4/8/2005	H379	2	5.38	232.786	0.168	-44.591		-39.39
5/25/2005	10	P--R	2/22/2005	H375	2	5.292	248.176	0.471	-32.664		-27.10
5/25/2005	11	SS--W	2/22/2005	H380	2	5.295	241.194	0.288	-38.075		-32.67

6/16/2005	1	ATWS		H382	2	5.35	249.907	0.339	-31.322	-26	-26.00
6/16/2005	2	GISP		H383	2	5.31	44.23	0.283	-190.72	-190	-190.00
6/16/2005	3	L1	4/25/2005	H384	2	5.35	242.946	0.355	-36.717		-31.55
6/16/2005	4	L3	4/25/2005	H385	2	5.33	246.695	0.151	-33.811		-28.56
6/16/2005	5	P--W	4/25/2005	H388	2	5.399	253.146	0.193	-28.812		-23.42
6/16/2005	6	P--R	4/25/2005	H390	2	5.29	252.637	0.232	-29.206		-23.82
6/16/2005	7	P--R	4/8/2005	H392	2	5.342	234.22	0.202	-43.48		-38.51
6/16/2005	8	L1	4/25/2005	H386	2	5.346	242.026	0.378	-37.429		-32.28
6/16/2005	9	L3	4/25/2005	H387	2	5.25	244.704	0.222	-35.354		-30.15
6/16/2005	10	P--W	4/25/2005	H389	2	5.161	251.146	0.845	-30.362		-25.01
6/16/2005	12	P--R	4/8/2005	H393	2	5.258	229.197	0.727	-47.372		-42.51
6/23/2005	1	ATWS		H394	2	5.172	246.621	0.311	-33.869	-26	-26.00
6/23/2005	3	GISP		H395	2	5.166	44.36	0.138	-190.62	-190	-190.00
6/23/2005	2	P--W	6/13/2005	H396	2	5.198	243.633	0.271	-36.184		-28.42
6/23/2005	4	SS--W	6/13/2005	H397	2	5.161	232.033	0.211	-45.174		-37.83
6/23/2005	5	L1	6/16/2005	H398	2	5.106	238.6	0.312	-40.085		-32.50
6/23/2005	6	L3	6/16/2005	H399	2	4.93	238.643	0.188	-40.052		-32.47
6/23/2005	7	P--W	6/8/2005	H400	2	5.038	268.339	0.291	-17.037		-8.39
6/23/2005	8	SS--W	6/8/2005	H401	2	5.111	266.798	0.406	-18.232		-9.64
6/23/2005	9	L1	6/16/2005	H402	2	5.122	238.334	0.361	-40.292		-32.72
6/23/2005	10	L3	6/16/2005	H403	2	5.094	240.385	0.474	-38.701		-31.06
6/23/2005	11	P--W	6/13/2005	H404	2	5.116	242.566	0.22	-37.012		-29.29
6/23/2005	12	SS--W	6/13/2005	H405	2	5.089	229.663	0.289	-47.011		-39.75
7/22/2005	1	ATWS		H406	2	5.11	251.178	0.299	-30.337	-26	-26.00
7/22/2005	2	GISP		H412	2	5.27	45.017	0.257	-190.11	-190	-190.00
7/22/2005	3	P--W	6/28/2005	H407	2	5.15	238.49	0.319	-40.17		-36.09
7/22/2005	4	L1	6/10/2005	H408	2	5.1	240.469	0.324	-38.637		-34.52
7/22/2005	5	SS--W	7/7/2005	H409	2	5.15	240.461	0.131	-38.642		-34.52
7/22/2005	6	L1	7/8/2005	H410	2	5.13	249.237	0.228	-31.842		-27.54
7/22/2005	7	P--W	7/7/2005	H412	2	5.13					
7/22/2005	8	L1	6/28/2005	H413	2	5.12	243.464	0.284	-36.315		-32.14
7/22/2005	9	SS--W	6/28/2005	H414	2	5.79	239.525	0.284	-39.368		-35.27

7/22/2005	10	SS--R	5/1/2005	H415	2	5.94	238.001	0.184	-40.549		-36.48
7/22/2005	11	P--R	5/1/2005	H416	2	5.71	218.83	0.496	-55.407		-51.73
7/22/2005	12	SS--W	5/1/2005	H417	2	5.71	255.712	0.406	-26.823		-22.39
8/3/2005	1	ATWS		H446	2	5.034	247.165	0.14	-33.447	-26	-26.00
8/3/2005	2	GISP		H447	2	5.127	43.26	0.359	-191.47	-190	-190.00
8/3/2005	3	P--R	4/6/2005	H448	2	5.122	203.903	0.179	-66.975		-60.80
8/3/2005	4	SS--R	4/6/2005	H449	2	5.135	247.035	0.186	-33.548		-26.10
8/3/2005	5	L3	4/6/2005	H450	2	5.082	247.475	0.216	-33.207		-25.75
8/3/2005	6	L4	4/6/2005	H451	2	5.082	244.706	0.472	-35.353		-27.98
8/3/2005	7	P--W	3/8/2005	H452	2	5.177	229.826	0.426	-46.885		-39.95
8/3/2005	8	SS--W	3/8/2005	H453	2	5.079	241.251	0.313	-38.031		-30.76
8/3/2005	9	SS--R	3/8/2005	H454	2	5.113	240.074	0.36	-38.942		-31.70
8/3/2005	10	L3	3/8/2005	H455	2	5.121	225.598	0.257	-50.162		-43.35
8/3/2005	11	L4	3/8/2005	H456	2	5.066	243.074	0.256	-36.618		-29.29
8/3/2005	12	L2	4/12/2005	H457	2	5.095	243.908	0.153	-35.971		-28.62
11/1/2005	13	ATWS		H470	0.5	1.063	238.325	0.395	-40.298	-26	-26.00
11/1/2005	2	GISP		H459	0.5	1.07	46.829	0.373	-188.71	-190	-190.00
11/1/2005	3	L1	10/11/2005	H460	0.5	1.084	225.334	0.692	-50.366		-37.13
11/1/2005	4	L2	10/11/2005	H461	0.5	1.066	228.233	0.485	-48.119		-34.64
11/1/2005	5	L3	10/11/2005	H462	0.5	1.049	218.915	0.264	-55.341		-42.62
11/1/2005	6	L4	10/11/2005	H463	0.5	1.062	221.628	0.288	-53.238		-40.30
11/1/2005	7	PRECIP	10/9/2005	H464	0.5	1.073	209.793	0.203	-62.41		-50.43
11/1/2005	8	SS--W	10/9/2005	H465	0.5	1.081	217.039	0.401	-56.886		-44.33
11/1/2005	9	SS--R	10/9/2005	H466	0.5	1.062	208.054	0.665	-63.758		-51.92
11/1/2005	10	L2	3/23/2005	H467	0.5	1.068	232.161	0.296	-45.075		-31.28
11/1/2005	11	PRECIP	10/9/2005	H468	0.5	1.068	209.984	0.297	-62.262		-50.27
11/1/2005	12	SS--W	10/9/2005	H469	0.5	1.074	218.19	0.475	-55.903		-43.24
11/9/2005	1	ATWS		H471	2	4.999	244.691	0.306	-35.365	-26	-26.00
11/9/2005	2	GISP		H472	2	4.961	45.048	0.384	-190.09	-190	-190.00
11/9/2005	3	P--W	8/6/2005	H473	2	4.996	264.802	0.435	-19.778		-9.48
11/9/2005	4	SS--W	8/6/2005	H474	2	4.999	244.195	0.369	-35.749		-26.41
11/9/2005	5	L4	3/23/2005	H475	2	4.999	241.135	0.388	-38.12		-28.92

11/9/2005	6	SS--R	3/31/2005	H476	2	4.975	249.248	0.506	-31.833		-22.26
11/9/2005	7	P--R	3/31/2005	H477	2	4.999	243.122	0.363	-36.581		-27.29
11/9/2005	8	SS--W	3/31/2005	H478	2	4.994	251.036	0.278	-30.447		-20.79
11/9/2005	9	L1	4/1/2005	H479	2	5.02	243.474	0.258	-36.308		-27.00
11/9/2005	10	L2	4/1/2005	H480	2	5.004	242.668	0.463	-36.932		-27.66
11/9/2005	11	SS--R	3/31/2005	H481	2	5.017	250.019	0.458	-31.235		-21.62
11/9/2005	12	SS--W	4/25/2005	H482	2	4.95	240.916	0.228	-38.29		-29.10
12/21/2005	1	ATWS		H483	2	4.918	242.704	0.277	-36.904	-26	-26.00
12/21/2005	2	GISP		H484	2	4.951	44.297	0.141	-190.67	-190	-190.00
12/21/2005	3	PRECIP	12/16/2005	H485	2	4.966	225.331	0.23	-50.368		-40.36
12/21/2005	4	PRECIP	11/21/2005	H486	2	4.983	199.898	0.291	-70.079		-61.38
12/21/2005	5	SS--W	11/21/2005	H487	2	4.99	255.979	0.192	-26.616		-15.03
12/21/2005	6	SS--R	11/21/2005	H488	2	4.921	256.458	0.253	-26.245		-14.63
12/21/2005	7	PRECIP	12/16/2005	H489	2	4.946	224.874	0.24	-50.722		-40.74
12/21/2005	8	SS--W	12/16/2005	H490	2	4.946	239.014	0.377	-39.886		-29.18
12/21/2005	9	SS--R	12/16/2005	H491	2	4.922	231.474	0.348	-45.607		-35.28
12/21/2005	10	L2	12/19/2005	H492	2	4.942	237.131	0.212	-41.224		-30.61
12/21/2005	11	L3	12/19/2005	H493	2	4.937	240.763	0.382	-38.409		-27.61
12/21/2005	12	L4	12/19/2005	H494	2	4.943	233.029	0.351	-44.402		-34.00
2/22/2006	1	ATWS		H513	2	4.994	244.907	0.325	-35.197	-26	-26.00
2/22/2006	2	GISP		H514	2	5.073	47.947	0.462	-187.84	-190	-190.00
2/22/2006	3	P--R	6/19/2005	H515	2	4.993	247.491	0.186	-33.195		-23.85
2/22/2006	4	SS--W	6/19/2005	H516	2	4.994	250.086	0.268	-31.184		-21.69
2/22/2006	5	P--W	8/17/2005	H517	2	4.999	264.71	0.336	-19.85		-9.51
2/22/2006	6	SS--W	8/17/2005	H518	2	4.962	268.13	0.106	-17.199		-6.66
2/22/2006	7	PRECIP	1/25/2006	H519	2	5.002	250.743	0.339	-30.674		-21.14
2/22/2006	8	SS--W	1/25/2006	H520	2	5.034	257.269	0.248	-25.617		-15.71
2/22/2006	9	SS--R	1/25/2006	H521	2	5.02	255.715	0.449	-26.821		-17.00
2/22/2006	10	L2	1/25/2006	H522	2	4.974	245.045	0.273	-35.09		-25.89
2/22/2006	11	L4	1/25/2006	H523	2	4.966	247.107	0.2	-33.492		-24.17
2/22/2006	12	PRECIP	1/25/2006	H524	2	4.942	249.428	0.427	-31.693		-22.24

APPENDIX E: SOIL PROPERTIES

Figure 43 displays the results of the particle size distribution analyses for the study plot soils. An additional soil core (SC9) was taken at the University of Georgia Horticulture Farm. The results of a particle size distribution analysis on the additional core were as follows:

- % sand= 70.3
- % clay= 3.16
- % silt= 26.54

Using a textural triangle (Hillel, 1980), the textural class of the soil samples was determined to be a sandy loam.

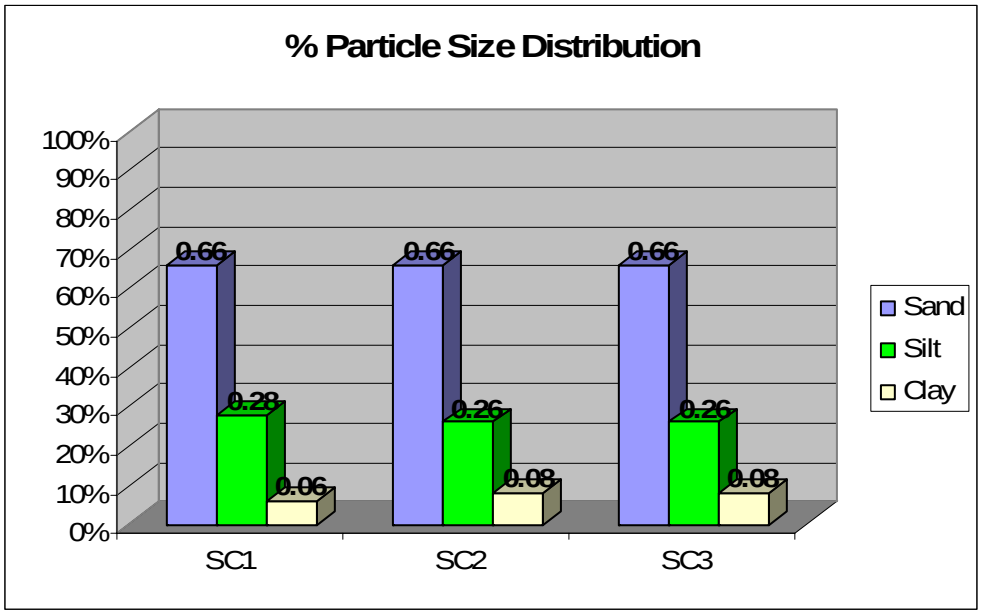

Figure 91: Study plot particle size distribution

Shown in Table 4 are the results of bulk density and water content analyses on three soil cores taken within the study plot. Bulk density measurements were averaged to

0.0960 g/cm^3. The bulk density and gravimetric water content (averaging 1.39 cm^3/cm^3) were used to derive volumetric water content (average= 0.134 cm^3/cm^3), relative water content (average= 0.284 cm^3/cm^3), and porosity (average= 0.476 cm^3/cm^3). Soil Core 7 was extracted from the UGA Horticulture Farm and yielded results that fell within the range of values produced from the soil cores taken within the study plot.

Table 4: Ap soil horizon hydrological characteristics

Soil Core	Wet wt. (g)	Dry wt. (g)	Bulk Density (g/cm^3)	Gravimetric Water Content	Volumetric Water Content	Porosity	Relative Water Content
1	517.77	480.75	0.095	1.41	0.14	0.48	0.29
2	475.96	447.60	0.080	1.32	0.11	0.50	0.21
3	533.71	488.88	0.11	1.44	0.16	0.46	0.36
7	587.13	550.80	0.079	1.35	0.107	0.49	0.27

Three intact soil cores were extracted from the study plot to determine saturated hydraulic conductivity; results are shown in Figure 44. Soil Core 4 was slightly higher in

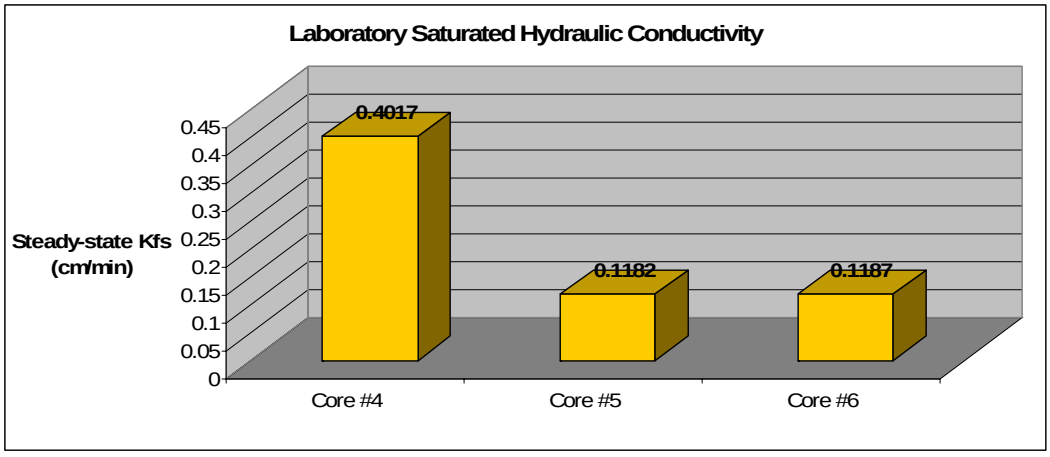

Figure 92: Study plot laboratory saturated hydraulic conductivity

conductivity than the other cores, which can be attributed to spatial variability of the soil structure on the hillslope. An additional core (SC8), from the University of Georgia Horticulture Farm, was analyzed and had a saturated hydraulic conductivity of 0.13 cm/min.

Using the saturated hydraulic conductivity, the volumetric flow rate of water per unit crossectional area, or water flux, was determined for the soil core samples using Darcy's Law (Table 5). For vertical movement, the negative values indicate downward flow.

Table 5: Water flux

Soil Core	Water Flux (cm/min)
4	-0.541
5	-0.155
6	-0.153
8	-0.237

Three boreholes were dug in the upslope area within the study plot to determine in situ saturated hydraulic conductivity, in the Ap soil horizon, using a compact constant head permeameter. The boreholes were 18 cm in depth. Figure 45 gives the results of the experiment. An additional borehole (Borehole 4) was dug at the Horticulture Farm, approximately one mile from the study area. Borehole 4 had a field saturated hydraulic conductivity of 0.00199 cm/min, which falls within the range of conductivities exhibited by study plot boreholes. Borehole 2 exhibited a slightly higher conductivity than the other boreholes; this is likely due to the fact that it was dug at a point where the microtopography of the hillslope leveled off, while the other boreholes were located on a mid-slope incline.

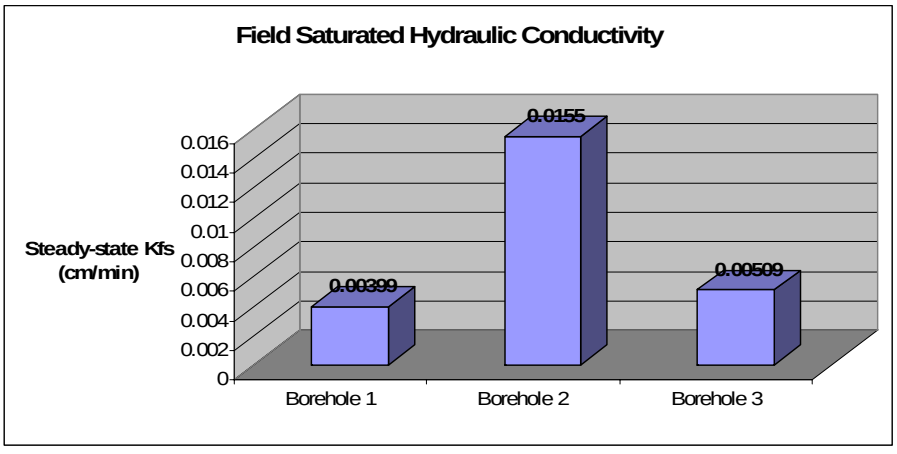

Figure 93: Study plot field (in-situ) saturated hydraulic conductivity